The Effect of Specimen Preparation on Degree of Conversion and Hardness of Dental Resin Composites

UNIVERSITY OF BIRMINGHAM

By

Babatunde Adelowo Adedayo

A thesis submitted for the degree of

Master of Science by Research

Biomaterials Units

School of Dentistry

University of Birmingham

December 2020

DEDICATION

I dedicate this research work to my family for their sacrifices during the time of my studies.

'If an iron axe head is blunt and a workman does not shapen its edge, he must exert a great deal of effort; so, wisdom has the advantage of giving success' Ecclesiastes. 10:10 (New English Version of the Bible).

CONTENT

ACKNOWLEDGEMENT

I would like to thank my Creator (Rom. 1:25 KJV), who is the Omnipotent (Rev. 19:6 KJV), the Merciful one (Ex.34:6 KJV), the Alpha and the Omega; the Beginning and the Last (Rev.1:8 KJV), the Almighty God (Gen. 17:1 KJV) for his protection over my life and my family during the time of Covid-19 pandemic.

I would like to express my appreciation and respect to the Course Lead and Supervisor, Prof. William M. Palin, for his encouragement, timely advice, and positive criticism. Also, my appreciation and respect go to the lead supervisor, Dr. Mohammed A. Hadis for his brilliant guidance, continuous support, and understanding.

I would like to express my appreciation to my University Mentor, Dr. Emma Frew, for the encouragement, and support during my studies. Also, I would like to express my appreciation to my referees, Dr. K. M. Oluwasegun and Mr. Moses Bhebhe.

My appreciation goes to all the research laboratory team, led by Gay Smith for their contributions and special thanks to Dr Jianguo Liu (MDS Infrastructure and facilities) for his continuous supply of liquid nitrogen and general laboratory guidance and training. Also, I thank all my fellow post graduate students at the dentistry post-graduate research laboratory.

I wish to express my appreciation to all other non-academic and support staff of the School of Dentistry, University of Birmingham for their assistance. My sincere appreciation, also, goes to the leadership and members of Foursquare Gospel Church Erdington, Birmingham for spiritual upliftment.

Lastly, but not the least, I want to thank my lovely wife and beautiful children for their assistance, encouragement, prayers, and moral support. They all assisted me to proof-read my thesis.

ABBREVIATIONS

RBC	Resin Based Composite
DC	Degree of Conversion
NSNP	Non-Sliced & Non-Polished Specimen
NSP	Non-sliced & Polished Specimen
DSPS	Dry-Sliced & Polished Specimen
WSPS	Wet-Sliced & Polished Specimen
Bis-GMA	Bisphenol A-glycidyl methacrylate
UDMA	Urethane di-methacrylate
AFM	Addition Fragmentation Monomers
MSDS	Material Safety Data Sheet
PMMA	Poly Methyl Methacrylate
MMA	Methyl Methacrylate
ATR	Attenuated Total Reflectance
DTA	Differential Thermal Analysis
DSC	Differential Scanning Calorimetry
CQ	Camphorquinone
PPD	1-phenyl-1 2-propanedione
TPO	2, 4, 6-Trimethylbenzoyldiphenylphosphine oxide
SEM	Scanning Electron Microscope
i.e.	That is
e.g.	Example
h	Hour
mm	millimetre

10K	10,000
&	And
η	Viscosity
CCD	Charged Coupled Device
CC-3-DA	Cosine Corrector

LIST OF FIGURES

Figure 3.32b: SEM images comparing non-sliced &non-polished and non-sliced & polished specimens at 3-4 mm depth of Filtek^{TM} one bulk fill restorative composites, processed within 6 h after curing and viewed at 10K magnification, revealing the exposed fillers.

LIST OF TABLES

ABSTRACT

Purpose: Material characterisation of dental resin-based composites in research laboratories involves cutting and slicing procedures which may impact the reliability and reproducibility of data. The purpose of this research is to study the effect of wet- and dry-slicing and polishing procedures on degree of conversion (DC) and surface microhardness (VHN) of resin-based composite (RBC) materials.

Materials and Methods: 3M Filtek^{TM} One bulk fill restorative material was prepared in white nylon mould 13 mm inner & 24 mm external diameter and 1 - 5 mm thickness increment of 1 mm, were light activated using the 3M ESPE Elipar^{TM} Deepcure-S curing unit (2.468 W/cm^2; 20 s; 49.4 J/cm^2; radiant exposure). A total of 72 specimens were prepared and divided into two main groups (Figure 2.1). Lower surfaces of specimens were characterised using surface microhardness meaurements (Vickers Hardness; Duramin Struers, ver. 0.04; 9.807 N, 15 s), and by two methods of attenuated total reflectance Fourier transform infrared spectroscopy (ATR-FTIR): 1) centrally located single point measurements over a 3mm diameter; and 2) multiple mapped measurements at 500µm increments over 13mm diameter. Polymer surface was further characterised by surface reflection measurements and scanning electron microscopy (SEM). Data generated were analysed using one-way ANOVA and post-hoc Turkey comparison (p=0.05).

Results/Discussion*:* The dry-sliced & polished specimens (DSPS) and wet-sliced & polished specimens (WSPS) revealed: for *single point DC*, DSPS was 40 ± 13 % higher than WSPS for 6 h specimens and DSPS was 41 ± 14 % higher WSPS for 24 h specimens; for *mapped DC*, DSPS was 54 ± 6 % higher than WSPS for 6 h specimens and DSPS was 25 ± 11 % higher than WSPS for 24 h specimens; for *hardness values*, DSPS was 19 ± 3 % higher than WSPS for 6 h specimens and DSPS was 21 ± 5 % higher than WSPS for 24 h specimens.

The WSPS and non-sliced & non-polished specimens (NSNP) revealed: for *single point DC*, WSPS was 33 ± 11 % lower than NSNP for 6 h specimens and WSPS was 50 ± 17 % lower than NSPS for 24 h specimens; *for mapped DC*, WSPS was 50 ± 17 % lower than NSPS for 6 h specimens and WSPS was 26 ± 9 % lower than 24 h specimens; for *hardness values*, WSPS was 5 ± 2 % lower than NSPS for 6 h specimens and no significant difference between both 24 h specimen groups. The DSPS and NSNP revealed: for *single point DC*, DSPS increased by 19 ± 2 % than NSNP for 6 h specimens and DSPS increased by 5 ± 2 % than NSNP for 24 h specimens; for *hardness values*, DSPS increased by 13 ± 4 % than NSNP for 6 h specimens and DSPS increased by 27 ± 5 % than NSNP for 24 h specimens, and for *mapped DC*, no significant difference between the groups ($p>0.05$) for both (6 h & 24 h). The reasons for the above results may be due to heat generated due to friction which resulted to increase diffusion and cross-linking. Wu, et al 2016 & Peng, et al 2019, explained that the interfacial friction heat generation instantaneous increase of temperature to the flow temperature of the composite matrix, which confirmed the observed bonded surface of SEM images of dry sliced specimens and washing away of loosed particles on the surface of the specimens by ionized water, during slicing and polishing processes.

Conclusions: Experimental procedures during specimen preparations have a significant effect on study outcomes. This research demonstrated the effect of wet / dry slicing and polishing where dry-sliced specimens exhibited significantly higher DC and hardness compared to wet-sliced & non-sliced specimens. Researchers should note the limitations of their study design and implement appropriate control measures to minimise experimental artefacts. Better designed, controlled experiments that simulate clinical conditions will minimise these experimental artefacts and will improve reliability and reproducibilty to improve consistency between both studies and practice, which may lead, ultimately, to a better understanding of RBC cure characteristics, and performance.

CHAPTER ONE

INTRODUCTION AND LITERATURE REVIEW

1.0 Introduction

In dentistry, there are many dental materials and devices that dentists can use for direct and indirect restorative purposes. Amongst these dental materials are range of photo-cured resin–based composite (RBC) restorative materials, dental adhesives/cements, glass ionomer materials (GIC), and dental amalgams. The dental devices include array of light curing units which allow for rapid setting of light activated materials and spatial and temporal control during the process of producing restoration.

Resin-based composites are synthetic resins which are used as restorative materials or adhesives in dentistry. They are mostly composed of bisphenol A-glycidyl methacrylate (Bis-GMA) and: tri-ethylene-glycol-dimethacrylate (TEGMA), urethane dimethacrylate (UDMA), 1, 6-hexanediol dimethacrylate (1-, 6-HDDMA) (Peutzfeldt, 1997). RBC also contains filler materials, such as: silica, zirconia, ytterbium trifluoride, which are used to provide mechanical strength (3M, 2016), to decrease the viscosity of monomers in order, to improve handling, and in most applications, photoinitiator are added to RBC for light irradiation, such as: camphorquinone (CQ), 1-phenyl-1 2-propanedione (PPD), Lucirin®, 2,4,6-tri-methyl-benzoyl-diphenyl-phosphine oxide (TPO). Mainly, there are two types of RBC materials namely conventional and bulk-fill. The micro-mechanical retention properties of RBC when compared to amalgam make them more effective for filling small cavities on like amalgam that requires undercuts for the macro-mechanical retention (Foreest, 1998). In addition, resin-based composites have good tooth-like appearance, they are easy to manipulate, insoluble in water,

insensitive to dehydration, and reasonably inexpensive when compared to amalgam. (Sharma, 2018).

Previous studies on resin chemistry have shown optimization which enhanced post cure reactions with studies demonstrating a significant level of 'dark' cure in modern bulk fill materials (Palin, et al., 2018). However, this property of RBC bulk fill materials is poorly understood, and the use of these materials have not been fully investigated.

Consequently, there exists inconsistencies in data that has been reported in terms of degree of conversion (DC), micro hardness (VHN), the extent of postcure and other important material characteristics (Collares, et al., 2013; Voyiadjis and Yaghoobi, 2017). The variation in data that has been reported is likely to be a result of experimental conditions which have not previously been considered or thought to affect study outcomes. These include sample preparation and handling prior to measurements.

More specifically, post-cure measurements of RBC materials are often conducted using attenuated fourier transform infrared spectroscopy (ATR-FTIR) which requires intimate contact between disc-shaped flat specimens and the ATR crystal. Whilst intimate contact between the crystal and specimen can be achieved when the material is unpolymerized, postcure measurements require further preparations such as slicing or polishing to achieve intimate contact. These procedures may affect degree of conversion and post-cure measurements due to several reasons which include heat generation by friction to accelerate post-cure processes, or the removal of free radicals by slicing, polishing or simply washing away. Thus, understanding the effects of specimen preparation is essential to understand the cure characteristics of RBC materials.

Therefore, the current research seeks to study the effect of specimen preparation on the DC and VHN of a commercial bulk fill RBC material. The DC and VHN values through the depth of the material specimen were assessed by taking slices through the cross section of the cured,

thick cylindrical specimens and prepared the various surfaces at (1 - 4 mm) thicknesses, then assessing the DC and VHN values at the surfaces.

1.1 Free Radical Polymerization

The free radical polymerization mechanism involves three main stages -initiation, propagation, and termination. These three stages co-exist to one another but are not successive steps during the polymerization process. Each of these stages varies during the reaction depending on the mobility of the active species of the system.

1.1.1 Initiation

The first step of polymerization initiation stage creates active centre from which a polymer chain is generated, and the second step involves the transfer of the radicals from the initiator molecules to the monomer units. There are three types of initiation systems available; 1) thermal decomposition: heat induced homolytic bond cleavage, which produces radicals from organic peroxides or azo compounds (Hageman, 1985); 2) photolysis: light induced homolytic bond cleavage which produces radicals metal iodides, metal alkyls, ketones, and azo compounds (Hageman, 1985); 3) chemical initiators: chemical induced homolytic bond cleavage to commence polymerization process. However, direct restorative materials are activated through blue light (400-500nm) absorption, typically by the photoinitiator/co-initiator system such as the camphorquinone (CQ)/amine). The absorption of light leads to an excited triplet state which extracts hydrogens from amine co-initiators to subsequently generate free radicals (Figure 1.1). It is these molecules with unpaired electrons which start the polymerization process as an active centre is created (Hadis, et al., 2012). The radical formation rate that initiates photopolymerization is localised to photons penetration depth.

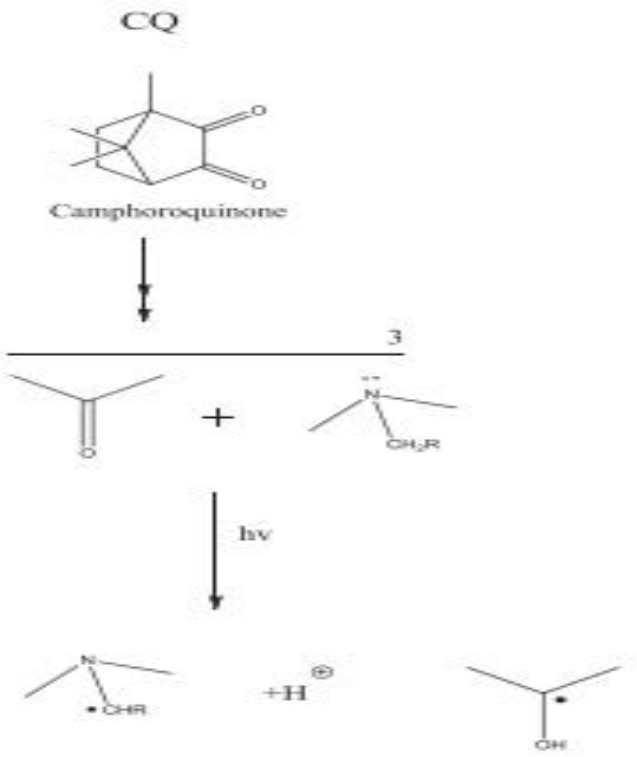

Figure 1.1 Hydrogen extraction from amine co-initiators which subsequently generate free radicals (Hadis, et al., 2012)

For conventional RBC materials, incremental thickness during restoration placement is limited to <2 mm due to poor depth of photon penetration compared with modern bulk fill materials where up to 6 mm increments are possible (Moore, et al., 2008). Curing light transmission is significantly reduced through depth due to surface reflection, photo initiator and pigment absorption (Hadis., et al., 2012), type of fillers, filler morphology and the interfacial refraction between the resin and the filler as well as scattering of light at the interfaces of resin matrix and filler particles (Shortall, et al., 2008). However, it has been demonstrated that these properties change dynamically during photopolymerization. They are governed by the relative refractive index of fillers, the resin matrix (Shorthall, et al., 2008; Hadis, et al., 2010), concentration and the type of the photo initiator (Hadis, et al., 2012) amongst other factors, which points to the complex optical interactions intrinsically. Extrinsically, the penetration of the light into the

depth of the materials depends upon the optical properties of the light, including wavelength, irradiance, and power distribution and perhaps the exposure time, indirectly (Palin, et al., 2018).

1.1.2 Propagation

The propagation reaction is the second stage of polymerization process which involves the growing of the polymer chain by rapid sequential polymerization addition mechanism. This process proceeds until termination and is governed by a few factors which include material viscosity and reaction rate. The process involves radicals that are generated from initiation attacking positively charged centres on carbon double bonds on the functional group e.g methacrylate group. This then opens the **π**-bonds and forms a new **σ**-bond between the methacrylate group and initiating radical (situated on the photoinitiator). Due to the imbalance in the number of electrons this creates on the methacrylate group (i.e., a radical carbonyl), the radical carbonyl becomes the free-radical centre which can go onto attach another positive centre (un-reacted methacrylate). This is known as propagation which leads to a spiral of radical generation and attacks on positive centres. Thus, a multitude of polymer chains start to grow, which can also attack each other to produce a highly cross-linked network prior to termination.

1.1.3 Termination

The third step is called termination and it occurs via two main mechanisms. The first involves radical-radical annihilation where two radicals will randomly collide together to balance the valance by the formation of a bond between to molecules carrying radicals. This process is governed by a number of factors which include material viscosity, mobility and concentrations of active species such as radicals and monomers. The second mechanism of termination involves radical entrapment within the highly cross-linked polymer network. As the reaction proceeds, cross-linking between monomers leads to gelations which restricts mobility of both

monomers and radicals, radical entrapment within cross-linked networks removes radicals from circulation in the system and therefore suppresses radical activity. The presence of these trapped radicals has been detected using electron paramagnetic resonnce even months after photopolymerization (Leprince et al., 2011). In addition, termination may also occur when two or more active chain ends combined.

1.2 Monomer Matrix

Monomers are molecules which react together in the process called polymerization to form a larger macro-molecule (Clayden, et al., 2001). Methacrylic acid in Figure 1.1 was synthesised in 1900 which led to the discovery of methyl methacrylate ester (MMA) (Knock and Glenn, 1952). Polymerization of MMA results in poly-methyl-methacrylate (PMMA) in Figure 1.1 which has been used for the manufacturing of denture base resin and indirect filling resin. Poly-methyl-methacrylate has many defects and shortcomings, which include large polymerization shrinkage 20 - 25% by volume, high incidence of secondary caries due to ingress of bacteria through marginal gap, severe pulp damage, high coefficient of thermal expansion, and serious discoloration (Peutzfeldt, 1997). The shortcomings and defects led to many studies and research to find solutions to these problems to develop materials with better properties.

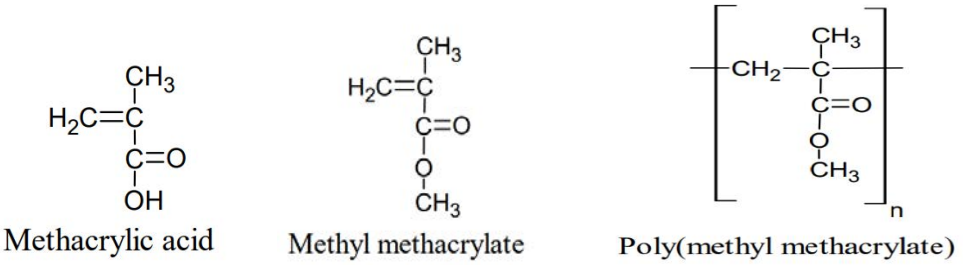

Figure 1.2: The structure of methacrylic acid, methyl methacrylate and poly (methyl methacrylate (Peutzfeldt, 1997).

1.2.1 Bisphenol A-glycidyl methacrylate

In 1956, another important monomer known as BisGMA (2,2-bis(4-(2-hydrooxy-3-methacrylyoxypropoxy) phenyl) propane, also called Bowen's Resin was developed. This monomer in Figure 1.2 was produced from the reaction of bisphenol A, MW=228.29g/mol and glycidyl methacrylate, MW=142.15g/mol. BisGMA is a viscous hygroscopic monomer and its polymerization led to a lot of the development of RBC, that are now extensively used

inrestoration in dentistry as a restorative material, sealants and adhesives, and dental cements. When methyl methacrylate (MMA), MW=100.12 g/mol was compared with Bis-GMA, MW= 512 g/mol, it revealed that Bis-GMA was superior, because to its large molecular weight and chemical structure difunctional, which gives the good mechanical characteristics of its polymer (Peutzfeldt, 1997). The importance of the two functional methacrylate groups at each ends of the carbon-carbon double bonds is to aid crosslinking process which is a significant factor that contributed to the good mechanical and physical characteristics BisGMA based polymers. Another important physical characteristic of Bis-GMA is its high viscosity, 5 x10^5 – 8 x 10^5 mPa.s, 23^{0}C which is a direct result of the hydroxy groups bonding interactions of the BisGMA molecules. Thus, provides superior mechanical properties, and reduced polymerization shrinkage than other monomers (Peutzfeldt, 1997). Nevertheless, BisGMA must be diluted with other lower viscosity monomer like tri-ethylene-glycol-di-methacrylate (TEGDMA) in Figure 1.3 or ethylene-glycol- di-methyl-acrylate (EGDMA) when in use (Peutzfeldt, 1997).

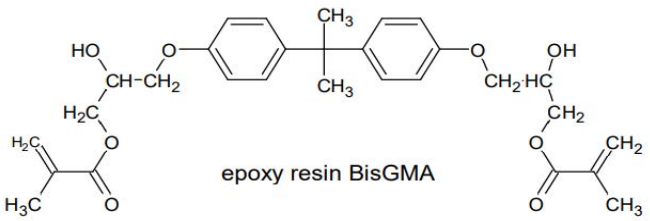

Figure 1.: 3 The structure of bisphenol A-glycidyl methacrylate (BisGMA) (Peutzfeldt, 1997**)**

1.2.2 Tri-ethylene glycol di-methacrylate

TEGDMA, MW=286 g/mol, viscosity (η)=0.01 Pa; (Gajewski, et al.,2012) is a difunctional methacrylic monomer with low viscosity that has been employed as a co-polymer agent. It exhibited relatively high degrees of conversion due to its stereochemistry due to the length of its chain and flexibility of di-methacrylates (Asmussen and Peutzfeldt, 1998). With an increase

in the content of BisGMA in copolymer BisGMA/TEGDMA, degree of conversion (DC) was found to decrease (Peutzfeldt, 1997). Other diluents of importance in this regard include ethylene glycol, hexamethylene-glycol-di-methacrylate, and benzyl-methacrylate, a mono functional monomer was added to enhance polymer chain elongation and degree of cure (Ferracane, 1995). Study have shown that the addition of TEGDMA generally, decreases mechanical properties hinders colour stability, and. increases water sorption (Gajewski, et al.,2012).

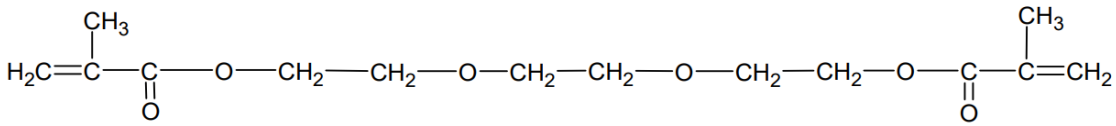

Figure 1.4: The structure of tri-ethylene glycol di-methacrylate (TEGDMA) (Peutzfeldt, 1997)

1.2.3 Urethane di-methacrylate

Urethane di(meth)acrylates (UDMAs) (1,6-bis-(methacryloyloxy-2-ethoxycarbonyamino)-2,4,4-trimethyhexane) in Figure 1.4 are monomers with dual methacrylate groups at both ends like BisGMA, which serves as an advantage because it can be cured either by using light or thermal processes (Atai, 2007). Urethane is more hydrophobic than BisGMA because its viscosity decreases with increasing length of alkyl urethane chain substituent (Fink, 2018). It has been an alternative dental formulation for Bis-GMA either partly or totally, because its chemical structures can be tailored easily, resulting in different kind of monomers with corresponding polymers having a wide range of chemical, physical, and mechanical properties (Barszczewska-Rybarek, 2014). The advantage of UDMA, MW=470 g/mol; η=23 Pa; (Gajewski, et al., 2012) over Bis-GMA is its lower viscosity. Photopolymerization of UDMAs monomers when compared to Bis-GMA produces polymers with lower polymerization shrinkage and higher degrees of conversion due to its lower viscosity than Bis-GMA (Fink,

2018). Moreover, the hydroxyl bonding associated with UDMA functionality is weaker than that on BisGMA because OH groups bond is stronger than NH groups bond to the extent that urethane-containing di-methacrylate monomers have greatly reduced viscosities (Stansbury, 2012). However, the use of Bis-GMA as resin-matrix has remained largely unchanged for a period of ~6 decades.

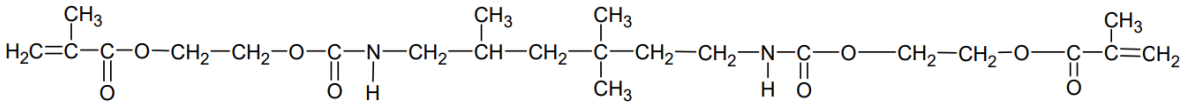

Figure 1.5: The Structure of urethane di-methacrylate (UDMA): [l,6-bis(methacrylyloxy-2-ethoxycarbonlamino)-2,4,4-trimethylhexane] (Peutzfeldt, 1997)

1.2.4 Cyclic Monomer

Cyclic monomers generally exhibited less shrinkage because the polymerization process of these monomers involve ring opening reactions. as compared to the vinyl monomers, which involves essentially, the opening of the double bond membered ring. For example, α-methylene-γ-butyrolactone does not show shrinkage of the material during polymerization (Fink, 2018). The di-methacrylate has both aliphatic and aromatic monomers. When the di-methacrylate composite involving aromatic groups are compared with that involving aliphatic groups, it revealed that aromatic monomers produced rigid polymers, while aliphatic groups produced flexible polymers (Peutzfeldt, 1997). However, the di-methacrylate composite containg both the aromatic and aliphatic groups in the same composite produced polymers exhibiting increased toughness (Peutzfeldt, 1997). Some examples of cyclic monomers are Spiro-orthocarbonates (SOC)s, spiro-orthoesters, bicyclic orthoesters (Fink, 2018) and Silorane (Palin, et al., 2018).

1.2.5 Ring-Opening Polymerization

The common feature of ring open polymerization (ROP) is that the monomers involved in the process are cyclic monomers rings and the mechanisms of ring open polymerization are grouped into radical ROP (RROP), cationic ROP (CROP), anionic ROP (AROP) and ring-opening metathesis polymerization (ROMP). Different groups of cyclic monomers whichcan be polymerized by ROP process are amines, anhydrides, carbonates, disulfides, ethers, lactams, lactones, olefins, phosphazenes, phosphonites, silicones, thioethers, and thiolactones (Kubisa and Vairon, 2012). The driving force behind chain polymerization has been the conversion of multiple bonds to single bond reaction., while the driving force behind most ring-opening polymerization is ring strain and associated steric factors (Duda and Kowalski 2009). Enthalpy difference between C-C and C=C bond does not affect ring open polymerization, which counteracts the entropy loss experience due to polymerization via chain polymerization, whereas composite comprising of 3-8 atoms rings may polymerize because of enthalpy loss associated with the loss of ring strain (Nuyken, et al., 2013). One problem with ROP is that the reactions are relatively slow, thus catalysts or co-catalyst are developed and used to enable the increase the rate of polymerization reaction of ROP. However, more developmental knowledge has been discovered which resulted in the increase of the application of these reactions to commercially viable systems e.g., the discovery that metathesis catalysts can be used to open the rings with exo funtional groups, resulted in a novel polymer structure (Nuyken, et al., 2013). Some of the areas where ring-opening polymerization have proved to be very useful in the process route to produce polymers with specific, and controllable properties like refractive index, production of synthetic of variants to naturally occurred polymers like chitin, and optimizing biodegradable polymers for pharmaceutical, agricultural, and medical applications (Nuyken, et al., 2013). Another area of its usefulness is to produce well-defined hyper-branched polymers by contolling the backbiting reactions and controlling ring/chain equilibria as well to

produce well defined polymers (Voit, 2000). Backbiting reaction occurs when intermolecular chain transfer occurs within a poymer for example from the terminal group to a location on the polymer backbone by hydrogen abstraction. This reaction result in the branching of the backbone like olycyclooctene, polynorbornene, polyethylene oxide, polysiloxane and polysiloxane produced via ROP (Nuyken, 2013).

1.2.6 Silorane

Silorane-based resin composites used silorane monomer as the matrix which is formed by (CROP) process unlike polymerization of methacrylates which is occurs through linear chain reaction via free radicals. Silorane-based composite has minimal polymerization shrinkage among other unique polymerization characteristics. The change in the chemistry of the composite and the polymerization reaction resulted in a significant reduction in the polymerization shrinkage to less than 1.0 % of the total volumetric shrinkage of the composite (Weinmann, et al., 2005) as compared to the 2.6 % to 7.1% assosiated with methacrylate-based resin composites (Feilzer, et al., 1988). Literature revealed that the silorane molecule in silorane based resin composite which contains siloxane core with attached four oxygen and rings called oxirane (Maghaireh, et al., 2017). During polymerization, the oxirane rings opened and form bond with other monomers. The physical properties and the reduced polymerization shrinkage in silorane-based composites are attributed to the oxirane rings, while the siloxane molecules are responsible for the hydrophobic properties of the material (Maghaireh, et al., 2017). Furthermore, water absorption and discoloration properties of the composites are minimized (Lee and Park, 2006). Previous research by Boaro, et al.2010, compared elastic modulus, and volumetric shrinkage of silorane-based composites to a methacrylate-based composites and found that the silorane-based resin composites had high polymerization stress value of 4.3MPa despite low volumetric shrinkage of 1.4 %.

1.2.7 Thio-lene Chemistry

Alkene hydrothiolation is a reaction between a thiol and an alkene which results in a thioether. A thiol is an organosulfur compound of the form R-SH, where R is an alkyl or other organic substituent. This reaction is also known as thio-lene reaction and its an example of a chemistry reaction called 'click'. The word 'click' can be explained to be a process of combining molecular building blocks just like two pieces of a seat belt buckle are joined, thus thiol–ene-based resins exhibit a step growth radical polymerization mechanism in contrast to the chain growth polymerization mechanism of (meth)acrylate systems (Boulden, et al 2011) and it produces substances by joining small modular, but it is a process of generating products which follow the examples in nature (Kolb, et al., 2001). Click chemistry is a group of reactions which are wide in scope, given high yields and generating only by-products that can be removed by non-chromatographic methods but not necessarily by enantioselective synthesis or stereospecific reaction. (Hein, et al., 2008).

Click reactions sometimes proceed without the elimination of by-product and therefore the reaction is classified as a polyaddition polymerization (Zhang, et al 2012). Thiol–ene photopolymerization exhibits a relatively numerous kinetic advantages over the common dimethacrylate-based materials, which results from delayed gelation point conversion, reduced volume shrinkage per double bond, delayed vitrification process, delayed auto deceleration and ultimately lead to higher functional group conversions (Boulden, et al 2011). An important characteristic of click reaction is that it produces high conversions at relatively low temperatures in virtually any solvent, including aqueous solvent systems (Nilsson, et al., 2008). The following combined advantages can be derived from click reactions; specific reactants, other functional groups tolerance, and high conversion which makes the reactions suitable for step-growth polymerization (polytriazoles) of various types (linear, graft, hyper-branched, and

dendritic polymers) (Lowe, 2010). Other attributes of thiol-ene reactions includes insensitivity to oxygen inhibition, high conversions with fast kinetics and mild reaction conditions (Podgorski, 2015). Thiol–ene photopolymerization has, therefore, gained significant attention as a process for producing dental restorative materials in the past decade (Reinelt, et al 2014).

1.2.8 Kinetics of Polymerization

Polymers are formed through the process of polymerisation by the conversion of monomers, in two distinctly different mechanisms. The first mechanism is chain-growth polymerization, also known as addition polymerization and the second mechanism is called step-growth polymerization. Chain-growth polymerization is mostly used for monomers containing C=C bonds (vinyl monomers) and certain types of monomers in which the C=C bonds is contained in ring-shaped molecules (cyclic monomers). The second mechanism involves the build-up of molecular weight in a stepwise pattern by the random combination of reactive functional groups with the monomer molecules (Kroschwitz, 1985-90). The complexity of polymerization depends largely on the functional groups which are present in the reactants and their inherent steric effects, which are the interactions that influences the conformation, and which are not related to bonding and the reactivity of ions and molecules in the process (Clayden, et al., 2000). Other literature revealed that the kinetic profile of polymerization process of RBC is affected by variations of the nature of monomer (mono-or di-methacrylate molecule stiffness and molecular weight) and the mixture proportions of monomers e.g., BisGMA and TEGMA (Leprince, 2010).

The kinetic processes of chain polymerization reaction involve three phases: pre-gel, gel, and post-gel. At the beginning of the process of polymerization, resin-based composite exhibits significant viscous behaviour at the *pre-gel phase* and the stresses generated at this point can be easily relieved by material flow relaxation processes (Santos, 2007). Both the crosslinking

density and degree of conversion are low, according to the steady state approximation; assuming that the concentration of free radical was stable, rate of radicals created by initiation (R_i) and radicals consumed by termination (R_t) are equal and the rate of propagation (R_p) was constant (Leprince, 2010).

The next stage is the *gel phase*, at this point, the system viscosity increases due to increase of both the crosslinking density and degree of conversion, which then result in the decrease of the mobility of the chemical species. This is the stage when the system loses its fluidity, and its viscosity becomes very large. Gelation (the process of forming a gel or solification by freezing) can occur either by physical linking, which involves physical bonds or by chemical crosslinking and it involves covalent bonds. As a result, the mobility of active species is restricted. Also, at gel phase, the growing of polymer is affected because free radicals located on the large molecules are restricted too, allowing only the small molecules to diffuse through the network and the resultant effect of that is a significant decrease in termination rate despite that fact that the rate of propagation remain constant because new active growth centre is being created by initiation process. Thus, giving rise to increase in the rate of propagation because of the rise in the concentration of new radicals and this is called *auto-acceleration.*

The studies by Anseth, et al., 1996, revealed that a higher cross-linking density and a higher concentration of double bonds both lead to an early onset of auto-acceleration. Termination occurs via reaction-diffusion at this stage, which depends on the rate of propagation.

The last process stage is called *post-gelation phase*, at this point, the diffusion process of the species becomes very difficult to the extent that the small monomer molecules find it difficult to reach the radical or to be added to the chain because the high viscosity of the system. Thus, the opposite phenomenon to *gel-phase* set in called *auto-deceratration* which is decrese in the rate of propagation (Leprince, 2010)

1.2.9 Polymerrization Shrinkage / Stress

Polymerization shrinkage is one of the major problems of RBC restorative materials. It is an inherent problem associated with the resin matrix and its magnitude depends on the composition and volume of the composites (Schneider et al., 2010). Polymerization shrinkage occurs in composites when the monomer inter-atomic distance is reduced i.e., the weak van der Waals bond are converted to covalent bonds, thus resulting in loss / decrease in volume of the composite from 2.6% to 7.1% Maghaireh, et al., 2017).

The free-radical photo polymerization of di-methacrylate exhibits chain-growth propagation mechanism which leads to very rapid curing under mild conditions, results in significant shrinkage and stress (Kleverlaan, and Feilzer, 2005). The shrinkage is due to bulk contraction as the resin transforms from pre-gel phase to solid phase as the viscosity of resin matrix gradual increase during the conversion phase (Stansbury, 2012). Hadis et al, 2012 stated that the amount of C=C double bonds present in the reaction environment determined the magnitude of polymerization and as a result, the concentration of C=C double bond are increased by increasing the proportion of low molecular weight monomers and thus the DC increases with and increase volumetric shrinkage.

When the material is bonded to tooth surfaces, the resulting stress associated shrinkage cannot be dissipated by viscous flow and therefore stress builds up. This stress is transferred to the tooth-restoration interfaces and leading to de-bonding or other deterious effects such as tooth fracture. Debonding occurs when shrinkage stress is greater than the bond strength, it leads to other problems such as postoperative hyper-sensitivity, pulpal inflammation, and secondary caries due to the penetration of saliva, bacteria, and other irritating substances into the interface (Kim, 2015). However, if there is adequate bond strength and there is substantial shrinkage stress, inherent flaws within the tooth or restoration itself can lead to fractures and restoration failures.

In the study by Braga et al, they discovered that shrinkage stress and microleakage is proportional to the diameters and the depth of the cavity but not its C-factor, which is the ratio of the bonded surface area to unbonded surface area of the restoration, that is the shrinkage stress and microleakage were higher in restorations with larger diameters and depths. (Braga et al., 2006). The literature revealed that the shrinkage forces in high C-factor cavities cannot be relieved by resin flow during light induced polymerization of resin composite which resulted in the debonding of one or more walls. However, the level of stress varies according to the clinical situation e.g., cavity restoration, and cementation of indirect restorations (Braga et al., 2012). Many methods have been proposed to reduce polymerization shrinkage, which includes curing light irradiance control (Feilzer, et al., 1995), increase in filler load, incremental layering techniques and flowable resin liner application (Schneider, 2010) and in addition, modern methods such as the use of addition fragmentation chemistry have proved effective in reducing polymerization shrinkage. Other methods used to reduce polymerisation shrinkage include the control of curing is in form such as soft start, ramp curing, pulse delay high irradiance/short exposure time and low irradiance/ long exposure time.

1.2.10 Viscosity

Viscosity can be defined as the property of a material which reveals the degree of molecular mobility of a material (Ayub, et al.,2014) and it also expresses the magnitude of internal friction in the fluid-like material and it is measured as the force per unit area resisting in uniform flow (Bayne et al., 2019). The viscosity of resin-based composites has played an important role in RBC's formulations, the addition of filler particles has been found to increase the viscosity of material (Bayne et al., 2019). Conventional resin-based compsites and bulk-fill resin-based composites may be classed generally into two groups: high-viscosity or sculptable composites and low-viscosity or flowable composites. Sculptable composites contain a higheramount of

inorganic fillers and are much more resistant to slumping while flowable composites contain reduced filler contents and adapt better on the cavity, especially in irregular surfaces, and shows greater polymerization shrinkage and lower mechanical properties. The viscosity of silylated monomer was discovered to be fifty times lower than that of the parent monomer (Rivera-Torres & Vera-Graziano, 2008).

Previous research by Leprince et al revealed that viscosity can be controlled in two ways: 1) by modification of filler contents; 2) by modification of resin matrix monomers. The modifications of both will also produce significant effects (Leprince et al.,2011). Beun et al., suggested that the significant local increase in viscosity in RBC materials may be due to large contact area between fillers and resin (Beun et al.,2009). Voigt et al pointed out that the presence of filler particles, modifies mechanical properties such as tensile strength, toughness, and resistance to fracture of resin-based restoration materials (Voigt et al., 2019). Also, viscosity is affected by the length of the chain because the longer the chain the more entangle the chain will be in a polymer, like in Bis-GMA. The effect of viscosity on resin-based composite has been explored extensively. Dos Santos reported that superior marginal adaptation is achieved when low viscosity composites are used because better contact with prepared tooth surfaces resulted from greater fluidity and capacity. (Dos Santos, et al,.2011). In a research conducted by Ayub, et al., 2014, the viscosity of RBC affects the degree of polymerization of bull-fill RBC material because previous research study has shown that UDMAs monomers with lower viscosity revealed significant high DC of the vinyl groups when compared to Bis-GMA with higher viscosity (Gajewski, et al., 2012).

1.2.11 Water Sorption

Dental polymer compsites are prone to water sorption (both hygroscopic and hydrolytic effects) to some extent depending on their chemical structure. Water up-take weakens resin matrix and

causes debonding of interface between fillers and matrix interface, thereby causing hydrolytic degradation of the fillers, which resulted in a significant mechanical properties and wear resistance reduction. ISO standard indicated that the dental restorative resins water sorption should be less than 50 $\mu g/mm^3$ (Sideridou, et al 2003) and the linear expansions caused by water sorption vary between 0.02 – 0.6 % (Peutzfeldt, 1997). The importance of solvent sorption and elution of component, which is of great concern, are the leaching of unreacted components in the short-term and the elution of degradation products in the oral cavity in the long-term (Fink, 2018). Apart from the above, water absorption also produces swelling in the resin-based material and makes the composite softer (lower elastic modulus and lower viscosity) which leads to reduced strength of the restoration material (Darvell, 2018). Water sorption decreased when esters or urethanes, Fluorocarbon-containing polymers, and non-hydroxylated homologues of Bis-GMA were used as monomer matrix (Peutzfeldt, 1997). Furthermore, to solve the problem of water sorption in Bis-GMA based polymer, silylation was used. Silylation is the introduction of a silyl group (R_3Si) to a molecule, this process is the basis of organosilicon chemistry. When dimethyl isopropyl siloxane is introduced to Bis-GMA, the water sorption and desorption of such a polymer is completely different from the original Bis GMA polymer without silylation as the silane modified polymer is stable in water (Fink (2018).

1.2.12 Discolouration

Discolouration is another problem associated with resin materials and one of the primary reasons resin-composite restorations are being replaced is because of colour change (Barutcigil, 2012), Resin restoration discolouration has been attributed to structural change which occur due to aging, development of coloured degradation products, and surface structure changes with extrinsic staining presence. The intrinsic factor which causes discoloration is due to changes in interface of matrix and fillers the interface of matrix and fillers and alteration of the resin matrix.

Also, discolouration occurs due to chemical reaction for example because of unreacted pendant methacrylate groups, oxidation of the amine accelerator and oxidation in the structure of the polymer matrix (Barutcigil, 2012). Another intrinsic factor which has been identified which affect colour change is the size and distribution of filler particles; larger particles composites are more susceptible to colour change due to hydrolysis than smaller filler particles composites. Valizadeh, et al (2020). Extrinsic factor like polishing may also induce discolouration which means the polishing technique used for composite resins should be carefully applied to prevent inducing of color change (Heshmat, et al 2013).

One method of solving the problem of discolouration involve the synthesis and purification by recrystallization of the following aromatic diesters, the bis-(2-methacrylyloxyethyl) esters of phthalic, isophthalic, and terephthalic acids that were used instead of BisGMA monomer (Peutzfeldt, 1997). The purification of BisGMA cannot be achievedby crystallization or by distillation because its a mixture of high molecular-weight optical isomers (Peutzfeldt, 1997).

1.3 Filler Particles

In the late 1960s, when the earliest resin based composite materials was introduced, they were simple and unfilled materials with numerous shortcomings. Thereafter, the development of inorganic filler particles commenced and has undergone tremendous improvement in the aspect of increasing the quantity of filler particles in the monomer and modifications in the size of particle of the fillers in the matrix from large particles size term 'micro' to 'nano' over the years. Generally, enhanced composite's physical and mechanical properties have been directly attributed to the quantity, the size and the type of filler particles added to the dental composite restoration materials. For example, fillers provide radiopacity in composites, reduced dimensional changes when heated and cooled (Yamaguchi et al, 1989), increase strength, increase stiffness (Kim et al, 1994), lower thermal coefficient of expansion (Stevens, 2001), higher mechanical properties generally (Palin et al., 2003) and higher resistance to abrasion (Turssi et al., 2005). There are wide range of fillers available for dental composite materials and these include glass particle fillers, made of silicone dioxide, lithium or barium-aluminium glass, and borosilicate glass containing zinc/strontium/lithium and fiberglass which are commonly used to improve mechanical and physical properties and reinforcement of the composite material. Previously, quartz was used because it was available, stable, and achieved better mechanical properties in the composites, when compared to other fillers like ceramic filler materials; zirconia-silica, or zirconium oxide. Filler particles can be classified based on their particle size and shapes such as: Micro fillers (0.4 μm, 40-45% by weight); Hybrid fillers (0.04-0.1 μm, 75-85% by weight; Nano fillers (0.005-0.01 μm; 2 - 20 nm); and Bulk fillers (Nano + Hybrid particles) 77% by weight (Bonsor, 2013; Chesterman, et al 2017). The most often seen morphologies of inorganic fillers are spherical or irregular and hybrid fillers (Randolph, et al 2016). Some studies have shown the influence of filler shape on the properties of dental composites. The studies carried out by Scatterthwaite et al, revealed that the

composites with spherical fillers had lower values of shrinkage stress and strain when compared to composites containing fillers with irregular shapes (Satterthwaite et al., 2012). Filler particle size and distribution are important parameter in the selection of composite materials. Research has shown that reducing the surface area of filler particles by increasing the particle size of the filler particles improved light penetration into the lower part of a composite and concentration of the filler particles also affect light penetration of a composite material which is the reason the loading level in polymer must exceed certain level or else it imparts the desired properties in the composite.

1.4 Photoinitiators

Photoinitiators are molecules which generates active species when they are exposed to electromagnetic radiation such as light, and ultraviolet radiation. They are classed based on the mode of radical generation into Norish Type I or Type II. The free radicals which initiate polymerization process are generated by either cleavage (Type I) or by transfer of hydrogen atom (H) from a co-initiator (Type II). Furthermore, photoinitiators can be grouped into single initiator system or dual initiator system.

1.4.1 Norish Type I Initiators

Norish type I initiators typically undergo homolytic cleavage of the excited α-carbon bond to produce two radical fragments. Example is the cleavage of 2,2-dimethoxy-1,2-diphenyl-ethaan-1-one which yields methoxybenzl and benzoyl radicals. The benzoyl radical intiate free radical polymerization while the methoxybenzyl radical further decomposes to give stable methyl and methyl benzoate. Other photoinitiators e.g., Lucirin® TPO (2,4,6-Trimethylbenzoyldiphenylphosphine oxide) have also been utilised in RBC materials (Moszner, et al., 2008). These initiators having high molar extinction coeficients and efficient quantum yields, and they have been available since the mid-1990's. These types of initiators generate radicals through homolytic cleavage of C-P bonds and have absorbance peak values below 420 nm (Scientific documentation, 2014). As a result of their absorbance peaks, they may not be activated efficiently by monowave LED-based LCUs which deliver light mostly in the 445 nm to 480 nm spectral range (Jandt, and Mills, 2013). *Ivocerin® (a dibenzoyl germanium derivative*) is another example of alternative photoinitiator developed to provide broader spectrum of shortwave absorption. Some of the factors aiding light attenuation along the radiation path are filler particle size and increased Rayleigh scattering of the lower

wavelengths of light. This is what prevents many photons from reaching the bottom of the RBC even though the alternative photoinitiators are more reactive than CQ. (Price, et al., 2014).

1.4.2 Norish type II initiators

Norish type II initiators absorb electromagnetic radiation to excite molecules which abstract electron or hydrogen atom from a donor molecule called co-initiator. It is the donor molecule that reacts with the monomer to initiate polymerization process. Example of type II photoinitiators systems includes benzophenone and its derivative and isopropyl thioxanthone in combination with a synergist such as tertiary amines.

The result was that the amines donated an active hydrogen to excited photoinitiators, then the abstraction of hydrogen produces alkyl-amino radical which is known to be very reactive to initiate polymerization. (Schwalm, 2001). The most widely used photo initiator for commercial RBC materials camphorquinone (CQ) / amine initiator system involves radical generation through hydrogen abstraction donated by tertiary amine molecule, to CQ at its exited state, then the amine forms free radical polymerization with the methacrylate resin system and not the CQ. This system produces free radicals when exposed to 400 – 500 nm radiation (Jandt, and Mills, 2013). Thus, CQ / amine photo initiation system is less photon efficient than the Type I systems because of the free radical generation mechanism (Hadis, et al., 2012). However, it is important for the Type II photo initiator to remain in its excited state otherwise hydrogen abstraction will not proceed. The excited state lifetime is short, and the radical generation quantum yield is also low. One of the ways to reduce the probability of this 'back electron transfer process' is by using iodonium salts. Other problems of using CQ initiation system include production of yellow colour stain, low reactivity, slow rates compared to other initiators and the use of amine co-initiators which can be cytotoxic (Neumann, et al., 2005). Another example of Type II photoinitiators is 1-phenyl-1 2-propanedione (PPD), it has more absorption values in the blue

spectral region, and often time combined with CQ, to create a synergy, thus the yield enhanced resin polymerization process. Although, it has an overall slow rate of reaction, but reduces the yellowish residual of the restorative material.

1.4.3 Dual-Initiator Systems

This type of system incorporates more than one different molecule to generate free radicals in the monomer for example having light-initiator and self-curing system combined in the monomer or light and heat-initiated system combined in a monomer. The initiators in dual-initiator systems cannot all operate at the same efficiency. The combination of light and self-cure initiators enables polymerization process to proceed further even when the curing light has been removed or after the completion of restoration process and this will further make the restoration secure (Yin, 2004).

1.5 Resin-Based Composites

1.5.1 Packable Materials

Packable composites are common dental resin materials which were introduced to dentistry in the late 1990s. The forming process of these composites begins with the fillers which are mainly made up of either silicone dioxide or barium aluninum slicate or strontium glasses and aluminium oxide. Filler alteration can take various forms including change of level or volume contents, shape of particles and size of filler contents (Zhou, et al., 2019). Packable composite forming process design was aimed at eliminating stickiness property of the composite by altering filler contents slightly above the conventional composite which has maximum filler contents approximately greater than 60% by volume, other manufacturers have used fused agglomerate particles or fibrous additions and fillers with better close parking particles and reduce matrix viscosity by changing the percentage composition of the monomer matrix. The resultant effect of the two alterations mentioned above ensured sufficient flow of the composite into the cavity during restoration.

The packable composites are tightly packed resin materials because of its higher filling particle content with greater viscosity more than other hybrid composites, but their physical properties are as good as other hybrid composites. The mechanical and physical properties of parkable resin composites are like natural tooth (Adiguzel and Cangul, 2017).

Furthermore, improvement to control the handling characteristics such as viscosity, resistance to flow, reduced stickiness and condensability is achieved when ultra-fine collodial silica particles are used. (Yeli, et al., 2010).

1.5.2 Flowable Materials

Flowable composite dental materials have been in the use in dentistry since 1995, they are composite materials obtained by increasing the particle size in the composite and reducing the quantity or number of fillers in the composites. Generally, it is observed that the reduction of the amount of particles fillers in the composite or the increase in the ratio of diluent monomers such as tri-ethylene glycol dimethacrylate (TEGDMA) in the composite composition, produced a reduction in the viscosity of the flowable composite material (Baroudi, et al., 2007). Flowable RBC have some tangible adventages and disadvantages, depending on the application at hand. For example, the use of flowable composites in high stress-bearing areas should be with caution because of its poor mechanical properties. the increased resin content due to reduce filler particule content in the composite, result to higher polymerization shrinkage, lower elastic moduli and high fracture toughness. However, its favourable wetting properties make it adaptable to enamel and dentine surfaces but difficult to manipulate because of stickiness (Yeli, et al., 2010).

1.5.3 Bulk-Fill Materials

The bulk- fill- resin-based restorative material can be classified according to method used in curing the restorative material (light or dual cured) and their viscosity. Division according to viscosity, divided bulk filled RBC materials into high viscosity and low viscosity materials (Tauböck, et al., 2017). Since the time it was introduced, it has undergone various modifications in filler, matrix, and initiator technology (Zorzin, 2015) in view to enhance its clinical longevity and ease of use. Research, by Boaro, (2019) suggested that the bulk filled restorative materials should be completely capped with a conventional resin-based restorative composite. The purpose of this was to enhance the aesthetic and build strong physical characteristics of the

restoration (Boaro, et al., 2019). The bulk-fill resin-based composite was designed for large 'layer placement' of greater than 2 mm in cavity as compared to conventional resin-based "composite" which has the maximum 'layer placement' of 2 mm in cavity (Abouelnaga, 2014). Thus, this material can be cast-off more proficiently to restore large mostly posterior cavities, such as in cases following the accomplishment of root canal treatment. Bulk fill resin-based composite restoration has strong mechanical properties, and these properties make them available for use as a base in the restoration (Maghaire, et al., 2019). There is some clinical evidence emerging to demonstrate that bulk-fill (RBCs) are more appropriately used as an alternative to amalgam. A recent randomized clinical trial concluded comparing the conventional layering technique of composite with the bulk-fill resin-based composite, revealed, bulk filled material attained a high success rate (Kojic, 2018). Modern bulk fill resin-based composite (RBC) material is one of the many dental materials available now for restorative purposes, especially posterior restoration which required materials with strong adhesive bonding to the tooth and lack restoration voids (Chesterman, et al (2017). Bulk-fill resin-based composite are modified dental materials, as compared to conventional resin-based materials, with lower quantity of fillers and enlarged filler size particle contents which allows better light penetration into the deeper layers. One of the ways light penetrates the deeper layers of a composite is by incorporating a nano-filler with the desired properties (Pulickel, et al., 2004). Research have shown that filler particle size below 40 nm are adequate not to interrupt the pathway of light through a composite and it allows good light penetration to the lower part of the material. However, handling of particle of that size pose a big problem because nanoparticles often agglomerate and/or form stable suspensions as colloids, which is the reason for pre-polymer treatments instead of melting process, but it is an expensive process and pose environmental and safety hazards (Tsai, et al., 2012). Another method to achieve light penetration in the lower part of a composite is by matching the refractive indices of the filler

materials and matrix materials and it allows for the use of microscale particles, which may not require special handling during processing and may be less expensive (Keaney, 2018). Also, the new sets of bulk-fill composite materials currently being produced differ considerably from their predecessors because they contain alternative photoinitiators, improved monomer resins matrix, special modulators, unique fillers, and filler distribution system (Hamama 2019).

1.5.4 Depth of Cure of Photo Cure Composites

Recently in the market, the bulk-fill resin composite can be solely cured by the light cure mechanism. Manufacturers have planned and tried to increase the depth, by enhancing the use of additional photo-initiators. Highly reactive photo-initiator namely, Ivocerin allowed polymerization in superior increments as compared to the standard photo-initiators (Eltayeb, 2017). Some previous literature reported that some of the manufacturers also claimed that the success of some photo cure composites is based on high intensity LED light-curing units (Daugherty, et al., 2018). When there is a considerably distance (greater than 8 mm) between restoration and the light tip used to cure the material, it will delay the process of setting the material (Sartori, et al., 2019). Some authors advised for cautious when attempting to cure an increment of 4 mm or more (Ferracane, and Hilton, 2016). They explained that the recommended time for light-cure bulk-fill resin materials may not be sufficient enough and it might require longer time to cure especially at lower part of the materials than conventional resin materials (Ferracane, and Hilton, 2016). However, recent studies supported the fact that with optimal conditions the bulk-fill resin-filled composite materials can easily be cured by light and achieve adequate hardness (Chesterman, et al., 2017).

1.5.5 Polymerization Characteristics of Modern Bulk Fill Materials

The bulk-fill resin-filled composite has presented with similar volumetric shrinkage to traditional resin-based composite restorative materials. It makes it controversial to use it in various conditions of cavities (Nikolaidis et al., 2019). Though, considering the in vitro- studies the shrinkage stress the bulk fill RBC exhibit less shrinkage than the normal conventional resin-based composite (Boaro, et al 2019). Lins et al, suggested that polymerization shrinkage predominantly considers as resin matrix property. The DC is one of the contributing factors in causing polymerization shrinkage (Lins et al., 2019). Equally, the increase of the filler fraction in the matrix of composite resin contributes to minimise polymerization shrinkage and reduced the overall matrix content. The restoration techniques used with bulk-fill composites are more user-friendly than meticulous incremental layering techniques and it speed up the restorative procedures (Hall, 2017). It is the most significant reason that most of the clinicians preferred this technique over the conventional method. There are few clinical trials that reported the evaluation of restoration with the bulk-fill resin composite and conventional composite which clearly showed encouraging results (Ilie, 2017).

1.5.6 Optical Matching of Filler (Refractive index)

The direct optimal matching of filler is a necessary component while using the light-curing method. The filler particles showed perceptible colour changes during and after the process of polymerization. Optimal matching of fillers along with incremental filling is highly preferred for light-activated resin composites. In bulk-fill resin-based composite, the photoactivation and formation of a refractive index can be achieved in a thicker increment. The additional filler particles present in a matrix might develop a discoloration due to having non – parallel edges. Hence, with increased concentration of filler, the discoloration might increase, and it could decrease the transmission of filler particles causing a mismatch with the tooth colour (Keaney,

et al., 2018). A successful direct composite resin restoration demonstrates high strength and durability; however, it should be aesthetically good. The colour change of bulk-fill resin is still a problem despite having advance resin monomer and filler particle technology. The colour constancy and optimal matching of fillers can be related to material properties such as compositematrix, filler-matrix interface, filler composition, and refractive index can be managed and maintained by adopting restorative techniques. Literature elaborated that the refractive index optimal matching of shaded fillers in resin composite were related to restoration size (Darvell, 2018). It was stated that the refractive index of the filling increased with reduction of restoration size and this enhances the translucency of filling materials (Thomas, 2019). Furthermore, it was revealed that optimal shading increased when the colour difference between the restoration and all surrounding walls decreased.

1.5.7 Resin for Better Control of Translucency

The translucency is a significant optical property, which can be measured in terms of the translucency parameter (TP) or contrast ratio (CR). TP is the colour difference between uniform thicknesses of the material over a white background as compared to a black background (Algarni, 2019). The CR is the percentage of spectral reflectance of a specimen over a black background when compared with a white background. Therefore, a material having high CR would be relatively lower translucency (Algarni, 2019). Although, various studies have been carried out on the translucency of conventional resin composite, no direct study has been carried out on the bulk-fill resin composite material used with thick layers. Bulk-fill resin composites was introduced to shorten the restoration procedure by allowing 4-mm-thick increments to be light-polymerized, but to achieve a deeper light penetration needed for curing, higher translucency is paramount. Studies have found out that the overall translucency of the restorations has linear correlations with the number of filler particles (Piccoli et al., 2019).

Recent study on translucency elaborated that the translucency of resin composites has direct relationship on the difference between the refractive indices of the filler particles and the monomers. The lesser the mismatch, the higher will be the translucency of the cured material. Other studies revealed that, in the composition of bulk-fill resin-based composite materials, Bis-GMA and silica filler particles are used to improve the translucency of the material (Dieckmann et al., 2019).

1.6 Polymer Properties

Polymer may be grouped according to thermodynamics properties e.g, thermoset, thermoplastic, or bulk properties thus the properties such as mechanical properties e.g., tensile strength and Young's modulus of elasticity; transport properties, e.g., diffusivity and reptation; chemical properties, e.g., reactivity, and stability; electrical properties, e.g., insulation, and semiconductivity; optical properties e.g., light transmission, and refractive index (Duarte, 1999). Stresses within the molecules and polymer chain affect the polymer's response to external forces. The intermolecular stress affects the dipoles in monomer units in a similar way that, the different functional group affects the type of bonding operating within the polymer structure, whether ionic or hydrogen bonding between its chains (Kiriy and Stamm, 2012). The type of bonding within a polymer is directly related to tensile strength and crystalline melting point (Duarte, 1999).

1.6.1 Effect of Temperature on Polymer Properties

Epoxy based resin, e.g., bisphenol A diglycidyl ethers is an example of a polymer. The properties of epoxy-based resin are sensitive to elevated temperatures especially the mechanical and physical properties (Khotbehsara et al, 2019). Study conducted by Polansky et al 2009, revealed that exposure of epoxy-based fibre reinforced laminates polymer to temperature ranging from 170^0 to 200^0C for a duration of 10 – 480 h decrease the material's glass transition temperature (T_g) because of decrease in thermal related stress reaction. The above study was based on construction industry. However, in dentistry many composites are based on epoxy-based resin (bisphenol A diglycidyl ethers) and the mouth's temperature is not as high as that in the construction industry but, what is the long-time effect of fluctuating temperature on these composites. Khotbehsara et al, 2019 studied the flexural and viscoelastic properties' response

to post cured temperature changes in epoxy/alumina polymer nano composite, revealed that there was significant enhancement of the flexural and viscoelastic properties at 80^0C for the polymer composite which was a temperature below the glass transition temperature of the epoxy/alumina polymer nano composite, but at temperature (e.g.,120^0C and 150^0C) above the glass transition temperature of the epoxy/alumina polymer resulted in adverse effect on the polymer composite properties.

1.6.2 Effect of Hydration Post-Curing on Polymer Properties

Hydration in science is the process by which water is absorbed by a substance or ingested into the body. Polymer composites used for restorative materials are exposed to oral environment, thus the knowledge of the effect of hydration on post cured polymer properties is vital. Some of the adverse effects of hydration on composite include softening of resin matrix (Martos, et al 2003) and leakage of filler particles (Xu, 2003). Generally, an improvement in the flexural strength, tensile strength, hardness, and fracture toughness properties was expected when a composite post-cured (Shah, et al, 2009). However, research revealed a lowered flexural strength by ≈32% in micro-hybrid and ≈50% in nano-filled composites due to hydration and a lowered peak toughness by ≈18% due to hydration (Shah, et al, 2009

1.6.3 Effect of Sample Preparation Methods on Polymer Properties

Experimental specimen preparation techniques for resin composite samples may involve slicing or cutting, grinding, and polishing of composite materials depending on the nature of analyses required for the specimens. Similarly, *in vivo* restorative placement methods, some clinical composite sample placement methods finish with grinding and polishing of the surfaces of restorative composite materials. There has been a careful consideration of the effect of stress

due to polymerization which some of the clinical placement methods have tried to minimise. It was reported that the incremental placement techniques reduce the cavity configuration factor (C factor). which is directly related to the stress developed at the interface of the bonding area (Van Dijken, 2010).

Likewise experimental specimens where prepared by subjecting them to cutting or slicing, grinding, and polishing for the analyser to be able to measure the desired parameters from some of the specimens. The process of these experimental preparation methods subjects these specimens to further stresses due to friction and wear & tear due to vibration of the tools being used to prepare these specimens. The aim of this reseach was to link these effects of sample preparation methods to degree of conversion and surface hardness obtained from the the analysers.

1.7 Hardness Properties of Resin Composites

Hardness is one of the mechanical properties of a material. Fundamental mechanical properties of a material are related to the response of the material to the amount of deformation caused by external force. In the case of hardness property, the material responds to compression force. Thus, surface hardness test measures the resistance of material to an indenter or cutting or abrasion. Hardness properties of resin composite are affected by types/amount of filler particles, resin compositions, polymerization kinetics and flatness/ homogeneity of the test surface (Chang, et al 2013).

The principle of measurement of hardness involves dimensional measurement of indentation made on the surface of the test material by an indenter e.g., Vickers and Knoop make a pyramid shape, Brinell makes a ball shape and Rockwell makes a cone shape on surface of the test samples (Noort, 2007). A specimen having varing filler content across the surface of the material will show varing surface hardness values across the specimen. Chang, et al 2013, compared the Vickers and Knoop indentation obtained during the measurement of hardness of polymeric materials and came to the conclusion that elastic recovery after removal of the load could affect both Vickers and Knoop measurement of Vickers indentation.

The Vickers hardness number (VHN) is computed from the following equation Instron-Corporation, (2006):

$$VHN = (1000P)/A \qquad \text{Equation 1.1}$$

where P = test force in kg and A = surface area of indent in mm^2.

Another method of hardness measurement involves the use of depth sensing devices without the indentation imaging Doerner, & Nix, (1986) The principle involves the measurement of depth created by indentation by both elastic and plastic displacements of the material, after which the elastic displacement is subtracted. This method provide time saving and repetitive improvement when compared to other methods of hardness measurement Doerner, & Nix,

(1986). Another method is nano hardness testing method which uses the same principles as the conventional hardness tester, but the indentation obtained on the surface of the material is of submicron in size produced by a fixed quantity of force ≈ 0.1mg to 5g. Nano indentation has been useful in the study of material with varing hardness across the surface area such as tooth (Mahoney et al 2000).

1.8 Aims and Hypotheses

Experimental procedures during sample measurements may have a significant effect on the study outcomes due to experimental arefacts which may affect post-cure polymerisation kinetics, DC, and other material properties such as surface micro-hardness.

Researchers used specimen preparation techniques such as sectioning or slicing, grinding, and polishing to prepare specimens for micro-hardness and DC measurements / analysis. Take the example of the research conducted by Venturini, et al., 2006, in which the experimental specimens used for the research were prepared teeth. These specimens were sliced at 5 mm above and below the cemento-enamel junction using a low speed diamond saw disk, and cooling water as lubricant, in order, to have access to the inner surface, emphasis is on the word 'slicing' and the buccal surface of each of the sliced teeth, was grinded with 180 grit silicon carbide paper under running water, emphasis on the word 'grinding', and then subjected to various methods of polishing before measurement / analysis were carried out on the specimens, also, emphasis is on word 'polishing' (Venturini, et al., 2006). This example showed the various methods used to prepare experimental specimens when there is the need to access the internal part or sections of the specimens. The purpose of the current research is to demonstrate the effect that slicing and polishing procedures conducted under wet and dry conditions will have on the DC and VHN values of experimental specimens. Therefore, the hypothesis is specimen preparation will affect the degree of conversion and hardness of dental resin composite samples and the hypothesis was tested through the following objectives:

a) The difference in the DC and VHN obtained depends on the depth at which measurements are taken.

b) The DC and VHN values for non-sliced & non-polished specimens (NSNP) will depend on time between curing and measurement.

c) The dry-slicing and polishing within 6 hours after curing will lead to higher DC and VHN values due to heat generated by friction.

d) The result of slicing and polishing process carried out at 24 h after curing will lead to non-significant differences in DC and VHN values obtained when compared with non-sliced and non-polished samples regardless of wet or dry conditions.

e) The slicing and polishing process carried out under wet conditions, within 6 h of curing will result in the lowest DC and VHN, which may be due to removal of free radicals.

f) The difference observed in DC and VHN values for specimens that are sliced (both wet & dry) and polished depend on process time between curing and preperation.

CHAPTER TWO

MATERIALS AND METHODS

2.1 Materials

The material used for this research is 3M™ Filtek™ One bulk fill restorative material (A2 shade; 3M ESPE Dental Products, USA), which was selected to assess the effect of specimen preparation of a modern bulk fill material. In order, to determine the effect of specimen preparation on material, the degree of conversion (DC) and hardness (VHN) values of the cured materials were determined at (1 - 4 mm) depths. Table 2.1 contains technical details about the 3M™ Filtek™ One bulk fill restorative material supplied by the manufacturer in the MSDS.

Monomers	The resin matrix used for this composite are aromatic urethane di-methacrylate (AUDMA), 1,12-Dodecanediol di-methacrylate and addition-fragmentation monomer (AFM).
Fillers	Total inorganic filler loading is about 76.6 % by weight or 58.5 % by volume comprising of acombination of non-agglomerated / non-aggregated 20 nm silica filler; a non-agglommerated / non-aggregated 4 – 11 nm zirconia particles and ytterbium trifluoride fillers consisting of agglomerate 100nm particles.

Table 2.1: Technical information of 3M™ FiltekTM One bulk fill restorative material which shows the monomer combinations and fillers used in the composite materials (3M, 2016).

2.2 Sample Preparation

The sampling arrangement which includes, type of process, time of process, and arrangement of specimens are shown in Figure 2.1. 3M^{TM} Filtek^{TM} One bulk fill restorative material was dispensed and packed into white nylon moulds with 13 mm inner diameter and 24 mm external diameter and (1 - 5 mm) thickness in increment of 1 mm in Figure 2.2. The packed samples were sandwiched between two acetate cover slips which was positioned under a manual hand press and compressed for about 3 s using firm pressure. Following that, the specimens were placed on the laboratory work bench directly below the tip (10 mm diameter) of the Deepcure-S unit (3M ESPE, USA) and delivering an average irradiance of 2468 ± 120 mW/cm^{2}at the surface of specimen. A fibre-based UV – Visible spectrometer (model USB 4000; Ocean Optics, UK) was used to measure the light curing unit (LCU) at the surface of the specimen.

The LCU was fixed at 2 mm distance away by a universal clamp facing the specimen, and perpendicular to the upper surface of the specimen. Concentric and repeatable alignment were ensured for the LCU, thereby ensuring each specimen receiving equal irradiance. The materials were subsequently light activated for 20 s to deliver a radiant exposure of 49.4 ± 2.4 J/cm^2. Subsequently, the specimens were carefully ejected from the nylon moulds by applying firm pressure to the upper surface of the cured specimen and ensuring minimal contact with the lower surface. All the group of specimens prepared in 5 mm thickness mould were protected from ambient light in light proof container and stored for 24 h at 23^0 C (Figure 2.2).

2.3 Slicing and Polishing Process

For sliced specimens, the following procedure was adopted. The sliced specimens were either dry-sliced or wet-sliced. Prior to slicing, specimens were fixed to a plastic stub using impression compound (Green Stick, Kerr) to ensure a rigid fixture onto the saw anvil and the calibrated micrometre was used to control the blade of the saw against the outer surface of the samples by setting it to the desired thickness 1 mm, 2 mm 3 mm, or 4 mm, (Figure2.1). For wet sliced speciemns, the blade of the slicing machine was lubricated with deionized water. Specimens were sliced into 1 mm, 2 mm, 3 mm, and 4 mm thicknesses and polished before they were subjected to other processes. Two main groups of non-sliced and sliced specimens were prepared. The first non-sliced & non-polished specimens were processed within 6 h after the LCU was timed out. The second non-sliced & non-polished specimens were kept for 24 h before they processed. Similarly, the sliced specimens were divided into wet-sliced & polished 6 h & 24 h and dry-sliced & polished 6 h & 24 h and for all the different groups of specimens (n=3). All the sliced specimens were polished before carrying out any tests. First, hand polishing was used on the specimens to flatten the surface of the specimens on silicon carbide abrasive paper P800 for 20 s. Subsequently, specimens were then machine polished using a Phoenix Beta Grinder/Polisher machine (Buehler, UK, at 300 rpm) with sequential grades of silicon carbide abrasive papers (P1000 for 20 s, P1200 for 30 s and P2500 for 30 s) were used to surface grind the specimen and lastly, silicon carbide abrasive cloth was used with the polishing discs (Buehler, UK) for the specimens for 60 s until a lustrous surface was obtained. All specimens were polished wet, using deionized water. In addition, a set of specimens that were prepared in moulds with different thickness 1 - 4 mm were polished as described above.

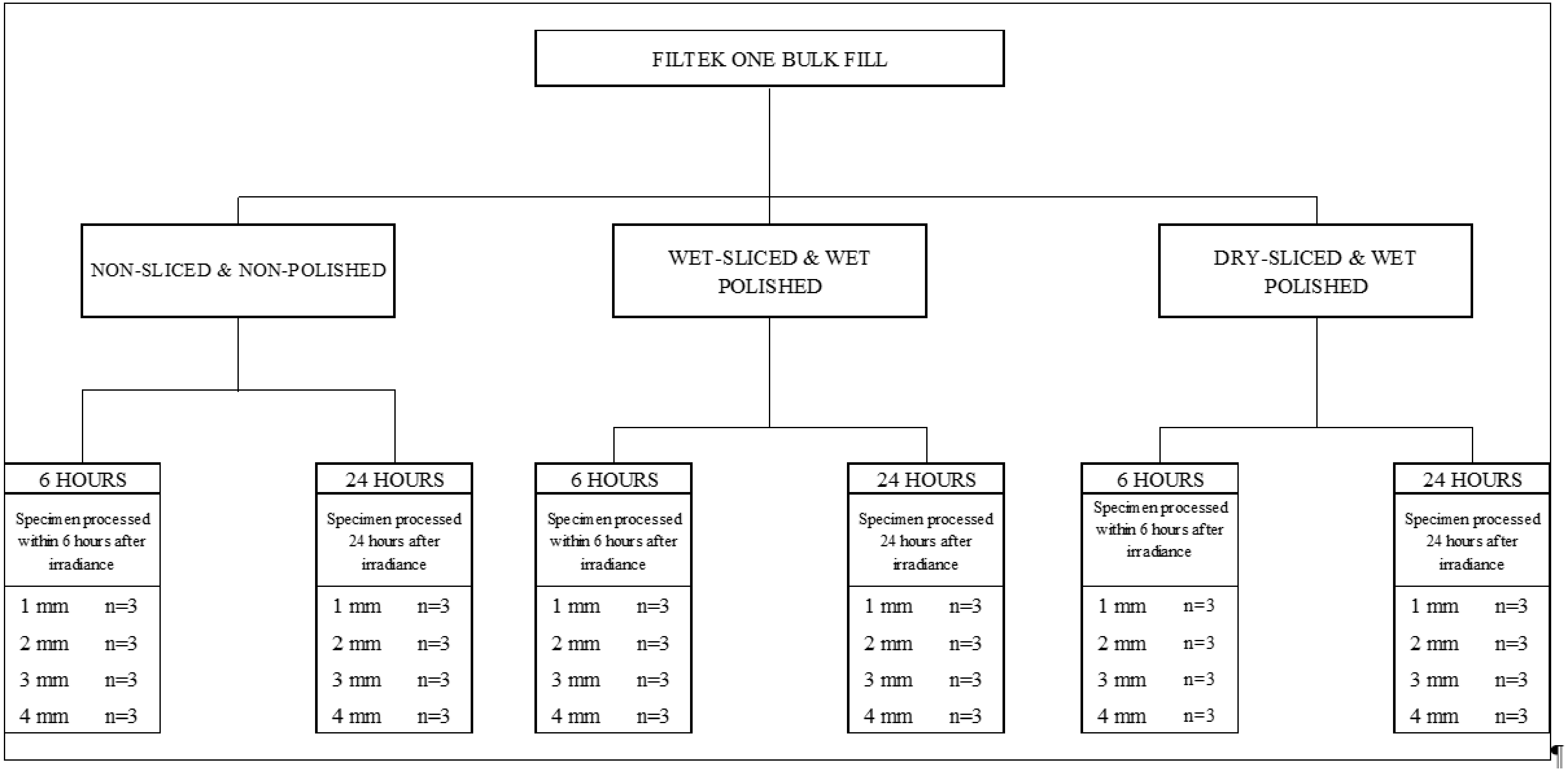

Figure 2.1: The specimen preparation plan for the current research study. The non-sliced &non-polished specimens were prepared in different mould sizes 1 – 4 mm thicknesses. While the sliced (wet & dry) specimens were prepared in 5-mm thickness moulds before they were sliced at 1 – 4 mm thicknesses. The two-process time zones were applied, that is, one set of specimens were process within 6 hours and the other after 24 hours.

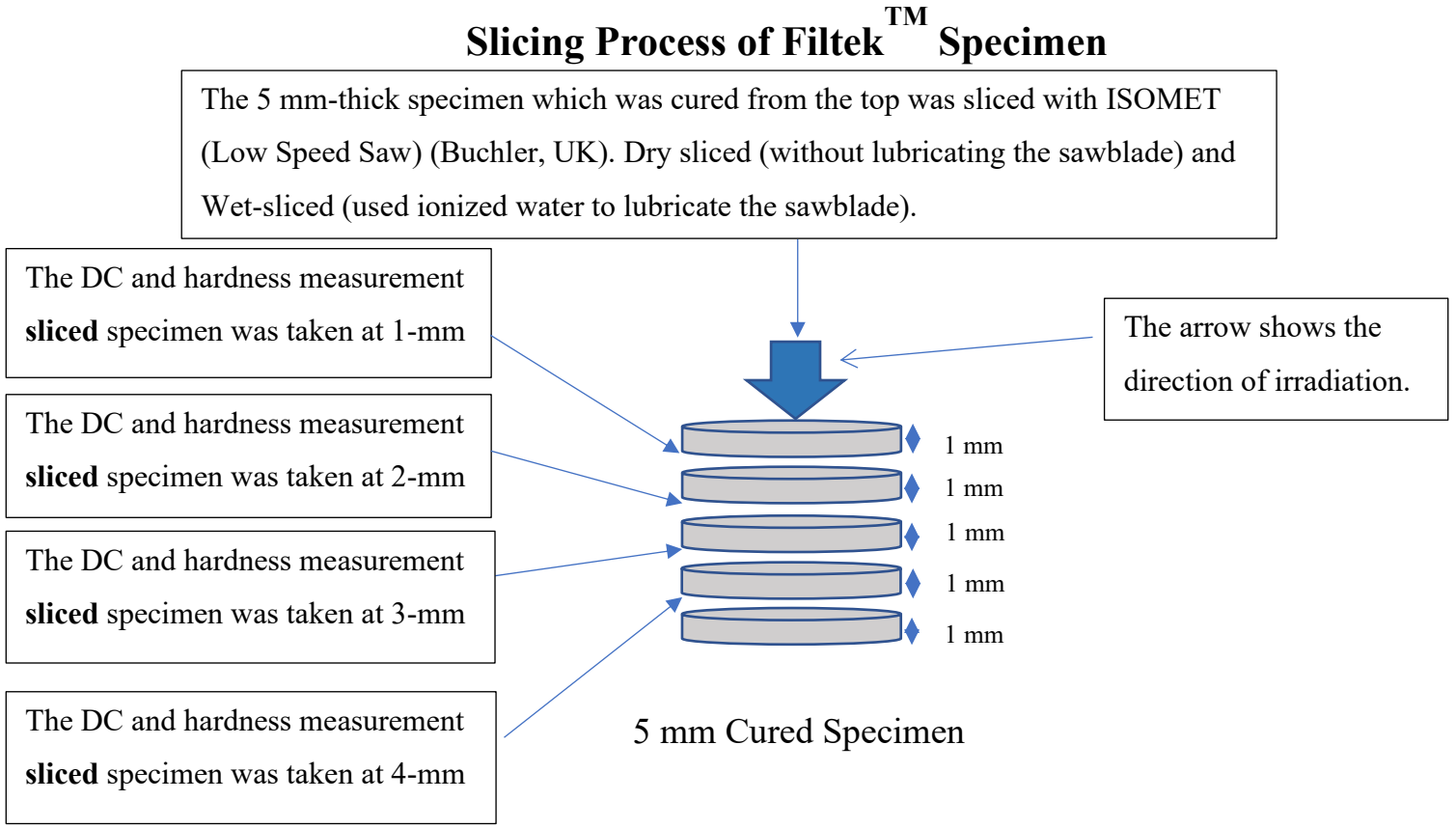

Figure 2.2: The slicing process involves slicing cured 5 mm specimens using the ISOMET low speed saw. The specimen is sliced into 1 - 4 mm sizes. The slicing process was carried out with / without using lubricant for the blade wet-sliced and dry-sliced operation.

2.4 Characterisation of Light Curing Unit

2.4.1 Spectral irradiance

A spectrometer; STS-UV-RAD, Ocean Optics, UK having spectralon cosine corrector; CC-3-DA; Ocean Optics, UK, attached to it was used to measure the spectral irradiance of Deepcure-S curing unit;3M ESPE, USA. OceanView software; Ocean Optics, UK was used to measure the spectral irradiance (n=3), from the cosine corrector which was positioned at 0 cm parallel to the light-emitting surface. The absolute irradiance within the LED emission region was calculated which is the total area under the spectral irradiance curve

2.4.2 Beam Profile

Beam Gage Software (Ophir, UK) was used to measure thhe beam profile. A charged-coupled device (CCD) camera beam profiler (SP620, Ophir, UK) was used to record the beam profile images in order, to prevent sensor saturation for each measurement and a combination of neutral-density filters (Ophir, UK) was used. Calibration of the linear scaling was performed to enable the calibration of of pixel dimension in the plane of the targets. Thus, the diameter of the active light beam was calculated based on the linear calibration and the pre-determined power values ontained using photodiode sensor (Diameter=10 mm; PD300; Ophir, UK) held at 0 cm distance.

2.5 Infrared Spectroscopy

Fourier transform infra-red (FT-IR) spectroscopy is a technique which by measuring the interaction of infrared radiation with the specimen can be used to calculate the DC of the specimen. This interaction may be in form of absorption, transmission, or reflection of the

infrared radiation by the sample. Thus, the various analytical techniques are based on these interaction methods.

Transmission Technique: this technique was developed at the begining for specimen with limited thickness of approximately 25 m of unfilled resins due to the strong absorptivity over the mid-IR frequency range. The unfilled transmission technique is based on the measurement of the decrease in the intensity of the methacrylate C=C stretching mode absorption at 1637 cm-1 in the process of conversion of methacrylate monmer to polymer. This procedure required the avalability of a stable absorption band which remain constant during polymerization reaction which can be used as a reference to normalise the monomer and polymer spectra in BisGMA based composites (Stansbury, 2001) The stable band could be aromatic absorption at 1608 cm-1 or 1583 cm -1 in BisGMA and N-H or C=O absorption as internal standard in urethane di-methrylate-based resins (Gureea, et al 2010)

Reflection technique: This technique involves the use of detector to measure the reflected infrered radiation reflected by specimen. There are different types of reflectance techniques which includes attenuated total reflectance (ATR) technique, diffuse reflectance technique, specular reflectance technique and multiple internal reflection technique. The multiple internal reflection technique is like the transmission technique mentioned above for metaccrylate monomer and urethane monomer.

The conversion formular used to calculate the intensity at each band for a Bis-GMA/TEGDMA system is shown in equation 1.2:

$$\text{Degree Conversion \%} = \frac{\text{1638 cm-1/1608cm-1 [Cured]}}{\text{1638 cm-1/1608cm-1 [Uncured]}} \times 100 \quad \ldots\ldots \text{ Equation 1.2}$$

Absorption Technique: This type of Infra-red (IR) spectroscopy technique is based on the absorption of infrared radiation of the electromagnetic spectrum by the specimen. The chemical

structure of molecules can be revealed by the characteristic absorption at specific frequencies and can be used to identify and quantify the specific functional group of of the molecule. This technique is used to measures the direct conversion as a function of the un-reacted metacrylate group in RBC. There are three spectral parts in within the region, i.e., the near-IR 4,000 -approx. 14,000 cm-1, the mid-IR 400 – 4,000 cm-1 and the far-IR aprox.25 - 400 cm-1 (Moraes, 2008). The unit of IR frequencies are presented in 'mm', but for comparison and clarity-sake, all vibrational frequenceies are given in 'wavenumbers':1 wavenumber (cm 1) = 10,000 / λ μm.

2.6 Fourier-Transform Infrared Spectroscopy

DC for each prepared specimen was calculated from the measured data using Fourier transform infrared (FTIR) spectrometer aith ATR spectroscopy technique. Single central measurements were made on the lower surface of each specimen using FTIR spectrometer (model: Nicolet 6700; Thermo Scientific, Madison, USA). Spectral absorbance was measured statically using ATR between wavenumber range: 600 - 4000 cm^{-1}, resolution: 16 pixels per cm; data spacing: 1.928 cm^{-1}. Specimens were placed centrally onto a diamond crystal plate and intimate contact between the crystal and sample was achieved using the attached pressure anvil. The data were analysed to determine degree of conversion using the following formula in Equation 1.2:

1608 cm^{-1} corresponds to the peak aromatic C=C double bond of One bulk restorative Filtek™ material used while 1638 cm^{-1} corresponds to aliphatic C=C double bond peak. The aromatic peak 1608 cm^{-1} is the reference peak in the calculation of the DC because it is the stable C=C peak bond of the materials used in Figure 3.1. Then, the generated data was used to calculate the DC based on the decrease observed in the absorbance of the aliphatic peak at 1638 cm^{1}.

2.7 Fourier-Transform Infrared Microscopy

Specimens were further analysed to assess spatial degree of conversion using FTIR spectrometer with an ATR accessory and equipped with a microscope (Nicolet, iN10 Mx, Thermo-Scientific, Madison, WI, USA). The spectral format used, was absorbance detection set at cooled (using liquid nitrogen) mode and the collection mode was set at ATR with spectral range set at 1570 cm^{-1} to 1670 cm^{-1}. Spectral resolution was set at 16 scans at 3 s intervals and the mapping step was set at 500 μm intervals for both the background and actual measurement. Each data set collected from the IR microscope were auto-baseline corrected in the region 1570 cm^{-1} to 1670 cm^{-1} and a conversion map was generated on the peak area ratio between the aliphatic group, 1635 cm^{-1} and an isosbestic point, aromatic 1596cm^{-1}. The collected data: 28 x 28 = 784 data on each specimen, was processed and analysed using a Macro prepared on Microsoft Excel to calculate the DC for each of the 784 generated data (See Appendix 1). Thereafter, the generated data representing the X, Y, Z coordinates were plotted as contour plots on Sigma plot to obtain maps showing the distribution of DC calculated using the equation 2.1 across the surfaces of the specimens of the resin material.

2.8 Reflection Test

Novo-Curve small area glossmeter Instrument (Rhopoint, United Kingdom) was used to measure reflection by focusing a light beam on the test surface at an angle of 60^0 to the normal line and measure the reflected angle which a measurement of specular reflection.

The measurement obtained from a glossmeter relates to the amount of reflected light from a black glass used as a standard with a known refractive index, and not the amount of incident light. The measured value for this known standard is equal to 100 gloss units (GU). The standard was calibrated using a white tile on the instrument, aligning the arrows with the

gridlines on the plate, before the reading was taken and compared to the value assigned to the while tile (93.6 GU) for the matching measurement angle. The necessary adjustment needed during calibration was made accordingly and the equipment was used to test the gloss of the specimens (both the non-sliced and sliced) and the results were recorded and analysed.

2.9 Scanning Electron Microscope

Specimens were made electrically conductive by attaching a two-sided carbon tape (Agar Scientific, UK) to connect the surface of specimen to aluminium sample stubs and by applying a plasma coating (gold-like sputter) (K550X; Emitech, UK) twice to reduce the charging effect on the surface of the specimens ≈50 Å thickness in a vacuum. The specimens were mounted on a stage in the chamber area of a ZEISS SEM (EVO 10 | MA, UK) and was positioned below the column where a focused beam of electrons would be able to hit the surface of the specimen. Both the column through which the electron passes to the sample and chamber evacuated by a combination of pumps. The scanning of the specimen enables information from a specific area on the specimen to be collected. Thus, due to the electron-specimen interaction, some signals, such as secondary electrons, backscattered electrons, and characteristic X-rays, are produced. These signals are collected by one or more detectors to form the images which are displayed on the computer display screen. The images obtained from the specimens at 10k magnification and at accelerating voltages of 5-20 kV were captured and collated.

2.10 Hardness Test

The surface hardness characteristics of non-sliced and sliced specimens was measured directly at 1 mm, 2 mm, 3 mm, and 4 mm depth, assessing the spatial differences in micro hardness at those depths. The micro-hardness was measured in North-South & East-West directions in a

cross shape at increments of 1mm. A Duramin Ver 0.04 with electric revolver (Rotherham, United Kingdom) was set at (indentation load: 9.807 N; dwell time: 15 s) to make indentations at 1 mm intervals across two perpendicular directions, i.e., longitudinal, and latitudinal of the surface area. Twenty-one (21) indentations were formed on the surface of each specimen and the data generated were analysed for all sample groups within 6 h and 24 h after irradiation.

2.11 Statistical Analysis

Statistical analyses were performed on all the data collected, which include data collected from roughness test, reflection test, DC data, and Micro-hardness test using Minitab 19 (Coventry, United Kingdom). The one-way ANOVA and post hoc Tukey Comparison were used, at 95 % significance level ($p=0.05$), to analyse and compare the significant difference of the means of the specimens. Likewise, regression analysis was performed on the DC values versus the depths of the specimens.

CHAPTER THREE

RESULTS

3.1 Characterisation of Light Curing Unit

3.1.1 Spectral Irradiance

Spectral irradiance of 3M Deepcure-S light curing unit is shown in Figure3.1. It is a single peak λ_{max} = 449 nm: ~410 nm - 500 nm delivering an average irradiance of 2468 ± 120 mW/cm^2. The radiant exposure = irradiance × time (2468 ± 120 mW/cm^2 x 20 s) which was the radiant energy applied to the surface area of the specimen over time 49.4 ± 2.4 J/cm^2.

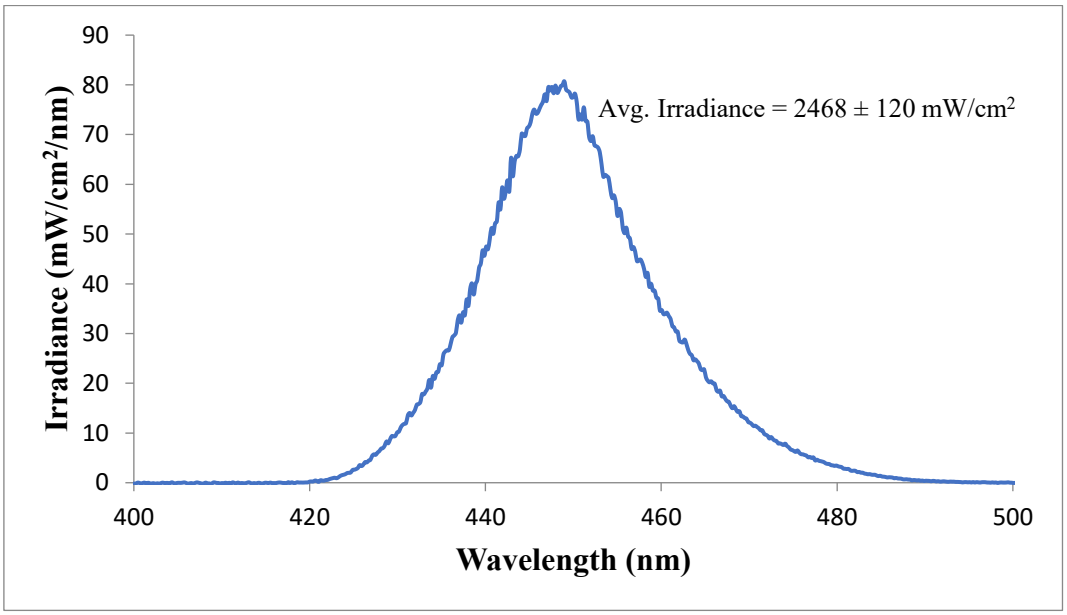

Figure3.1: Spectral Irradiance of Deepcure-S light curing unit showing the peak output (λ_{max} = 449 nm) and the spectral range. The absolute irradiance of the light as given by the area under the curve was 2468 ± 120 mW/cm^2.

3.1.2 Beam Profile

The beam profile of Deepcure-S light curing unit is shown in Figure3.2. It shows the distribution of light across the face of the curing tip. The tip exhibits homogeneous irradiance distribution across the 10 mm tip diameter.

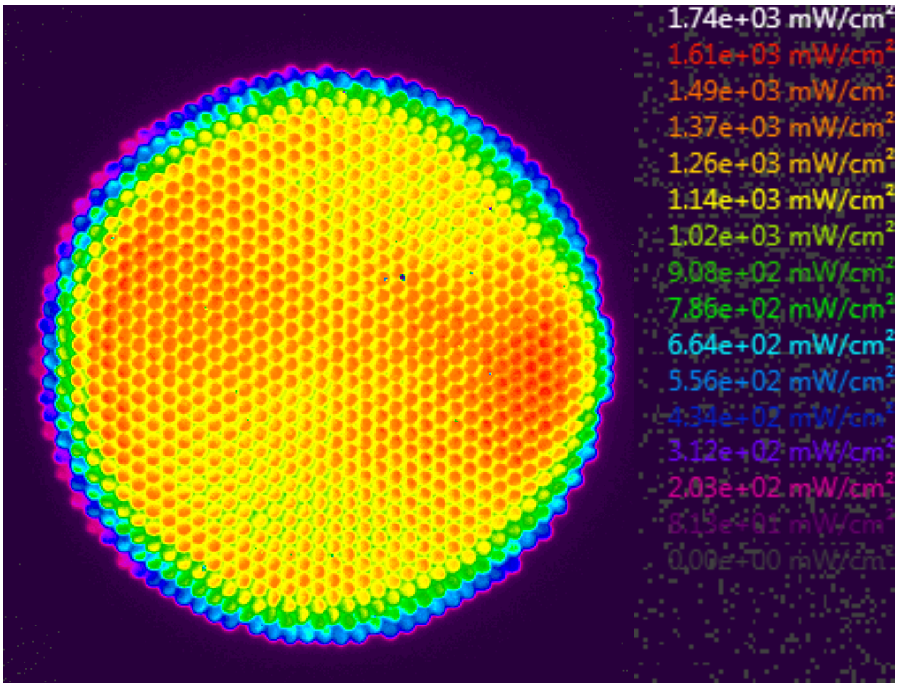

Figure 3.2: The beam profile of Deepcure-S light curing unit showing thedistribution of light across the face of the curing tip. It exhibits homogeneous irradiance distribution. The colour scales from red to purple represent high to low radiant exitance.

3.2 Central Single Point Degree of Conversion

The results of the single point DC measured at the centre of the specimens using FT-IR spectroscopy is shown in Figure 3.3. The plot compared the result of the specimens' irradiance against thickness of the specimens, measured within 6 h and 24 h after irradiation. The post-hoc Tukey (upper case letters) clearly revealed that the DC values were deceasing against the specimen thickness 1 - 4 mm for all group categories. Also, the plot compares the different categories of specimens with each other within the same processing time. For specimens processed within 6 h after irradiation, the post-hoc Tukey, lower case letters revealed no significant difference between the mean of DC for dry-sliced and polished specimen (DSPS) and non-sliced and non-polished (NSNP) specimens at 1 - 2 mm depths, also there was no significant difference between the meansof DC for NSNP specimens and DSPS at 3 – 4 mm depths and wet sliced & polished specimens 1 – 2 mm depths but there was significant difference between the means DC for wet sliced & polished specimens at 3 – 4 mm depths. On the other hand, for specimens processed at 24 h after the irradiance, the post-hoc Tukey (lower case letters) revealed there was no significant difference between the means of DC for NSNP specimens at 1 - 4 mm depths; DSPS at 1 - 3 mm depths and wet sliced & polished specimen at 1 mm depth. Also, there was no significant difference between the means of DC, for NSNP specimen at 4 mm depth and wet-sliced and polished specimen (WSPS) at 2 - 3 mm depths but there was significant difference between the means for WSPS at 4 mm depth. Lastly, the specimens were compared by process time zone per group category i.e., 6 h vs 24 h specimens of group categories i.e., NSNP, WSPS, and DSPS. The result revealed there was significant difference between the means of DC values and 24 h specimens showing higher values than 6 h specimens.

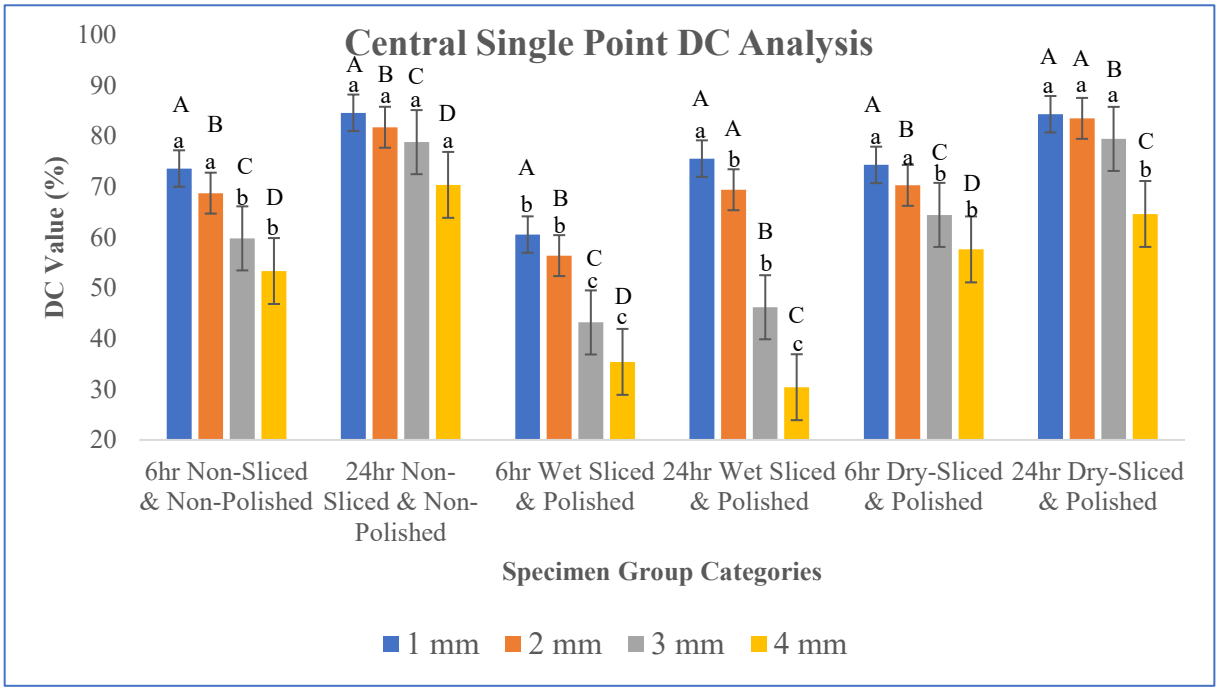

Figure 3.3: Central Single Point DC values plot of Filtek™ One bulk fill restorative material measured within 6 h and 24 h after irradition. The plot shows clear trends of decreasing DC as the depth increases from1 mm to 4 mm. The post-hoc Tukey represented by upper case letters compares the data within each category against different thickness 1 mm vs 2 mm vs 3 mm vs 4 mm while the lower case compared the data among the group category i.e., NSNP vs. WSPS vs. DSPS at both process time zones. Significant difference determined by one way ANOVA and post hoc Tukey comparisons ($p<0.05$) are representedin ascending alphaphetical order from high to low within each group.

3.3 Degree of Conversion by FTIR Microscopy

Figure 3.4 and Figure 3.5 show the result of FTIR DC mapping at 6 h and 24 h respectively. The average DC data in Figure 3.6 and Table 3.1 there was significant difference ($p<0.05$) between the average DC through depth with 1 mm specimens having the highest DC and 4 mm having the lowest. When the average DC of specimens tested at 6 h were compared with specimens tested at 24 h revealed significant differences within all groups with NSPS having highest DC followed by DSPS and WSPS having the lowest DC. This trend was less apparent for 24 h specimens. At 1 mm depth, dry-sliced & polished specimen showed significant difference when compared to NSNP specimens and WSPS, both have no significant difference. At 2 mm depth, there was no significant difference between the group categories. At 3 mm depth, DSPS and NSNP specimens showed no significant difference, but both showed significant difference when compared to WSPS. At 4 mm depth, NSNP specimens showed significant difference when compared to dry-sliced & polished and wet-sliced & polished specimens while there was no significant difference between DSPS and WSPS. Lastly, there was significant difference between the means of mapped DC values in Table 3.1 for WSPS and DSPS, with 24 h specimens showing higher values when compared 6 h specimens. Whereas with NSNP specimens, 6 h showed higher values than 24 h at 1 mm & 3 mm depths and the reverse at 2 mm & 4 mm depths.

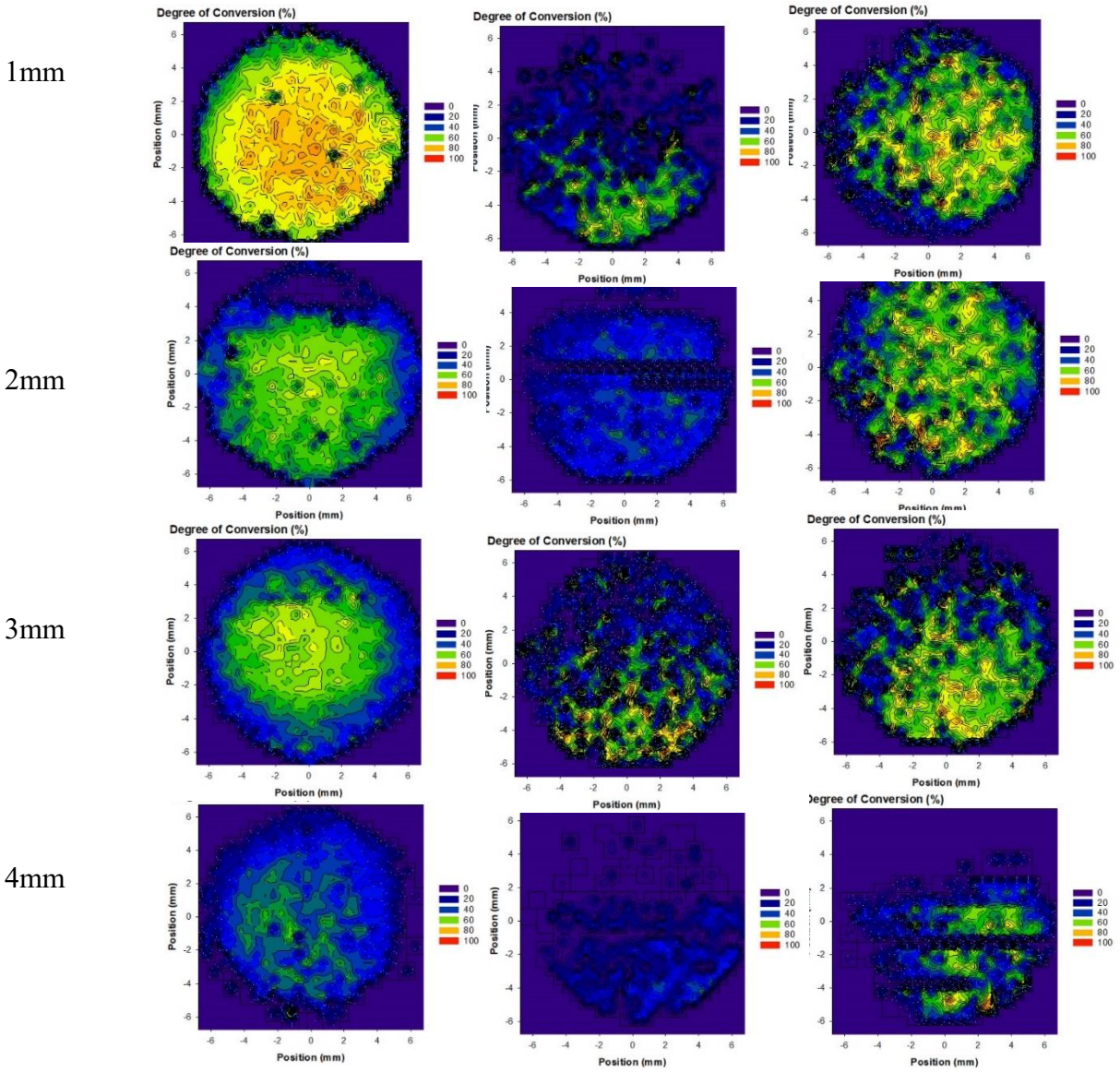

Figure 3.4: The mapped DC images of 6 h, NSNP, WSPS and DSPS of Filtek One bulk fill restorative (A2) material. The maps show the spread of DC on the surface of specimens at 1 – 4 mm depths. NSNP and DSPS mapped DC shows a trend of reduction in DC values and in the distribution of the DC across the surface of the specimens as the depth of specimen increases. The colour scales represent DC.

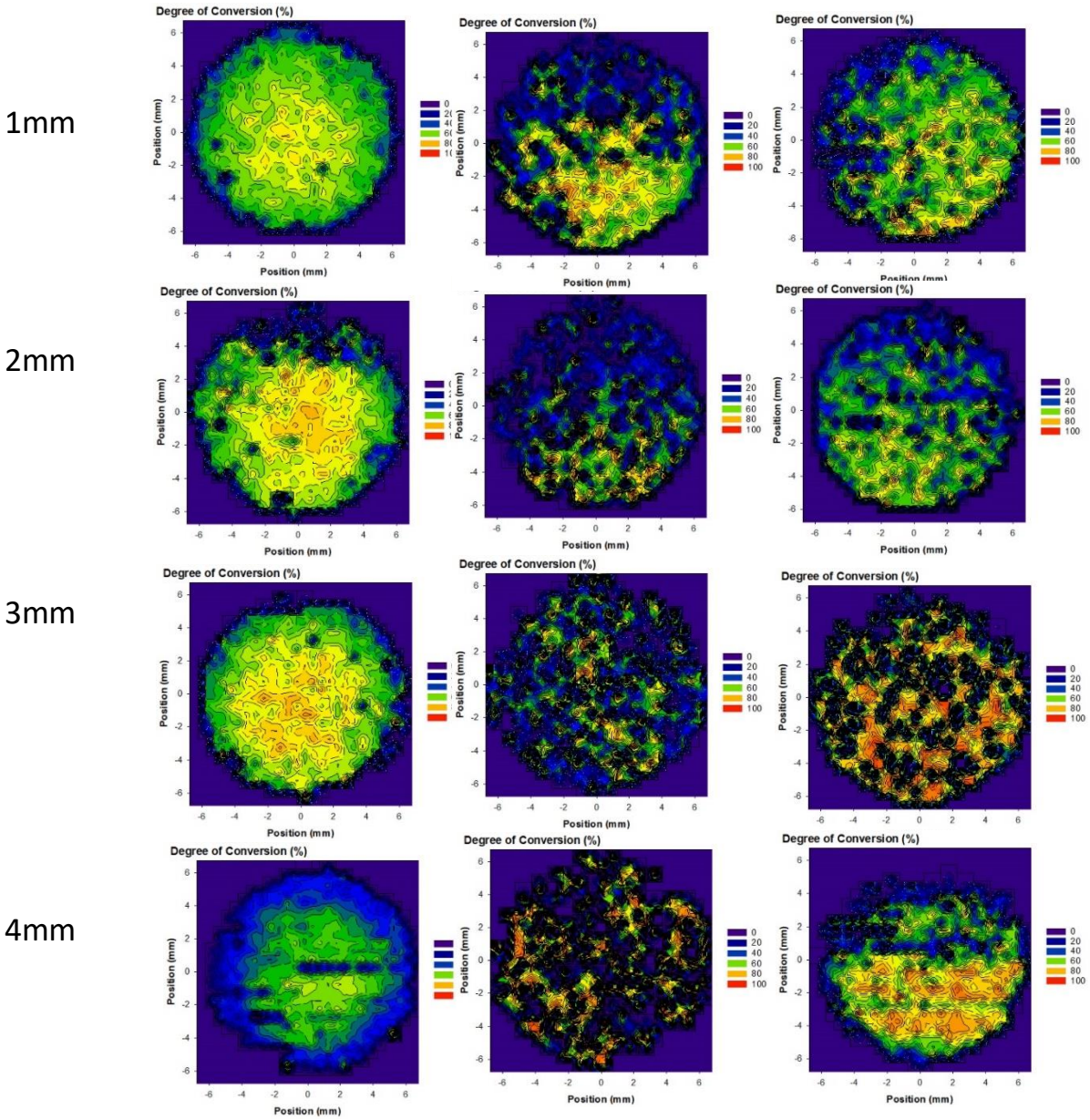

Figure 3.5: DC distribution on the surface of specimens processed at 24 h after curing shows no clear trend of DC values. The values of the DC were significant and shows more spread over the surface of the specimen. The colour scales represent DC.

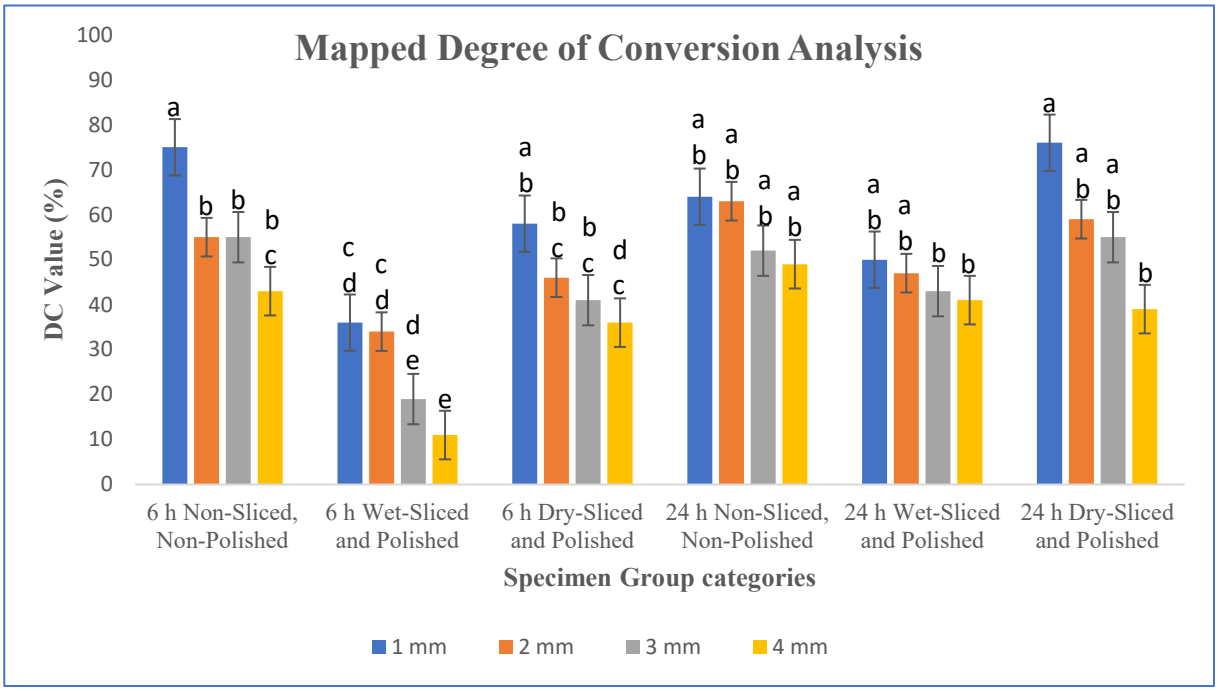

Figure 3.6: Average mapped DC values plot of Filtek^{TM} One bulk fill restorative (A2) shade material, measured within 6 h and 24 h after irradiation. The plot shows clear trends of decreasing DC as the depth increases 1 - 4 mm. The post-hoc Tukey also compares data within each time zone i.e., 6 h and 24 h respectively. Significant difference determined by one-way ANOVA and post hoc Tukey comparisons ($p<0.05$) are represented in ascending alphaphetical order from high to low within each group.

Mapped Degree of Conversion Analysis						
	6 h Non-Sliced, Non-Polished	**6 h Wet-Sliced and Polished**	**6 h Dry-Sliced and Polished**	**24 h Non-Sliced, Non-Polished**	**24 h Wet-Sliced and Polished**	**24 h Dry-Sliced and Polished**
1 mm	**75 (1.9)^{a}**	**36 (10.8)^{cd}**	**58 (9.6)^{ab}**	**64 (6.7)^{ab}**	**50 (8.4)^{ab}**	**76 (9.5)^{a}**
2 mm	**55 (4.0)^{b}**	**34 (9.3)^{cd}**	**46 (1.5)^{bc}**	**63 (11.3)^{ab}**	**47 (7.6)^{ab}**	**59 (6.4)^{ab}**
3 mm	**55 (6.5)^{b}**	**19 (3.4)^{de}**	**41 (3.3)^{bc}**	**52 (6.8)^{ab}**	**43 (16.4)^{b}**	**55 (5.5)^{ab}**
4 mm	**43 (5.5)^{bc}**	**11 (2.2)^{e}**	**36 (6.3)^{cd}**	**49 (3.8)^{ab}**	**41 (14.1)^{b}**	**39 (16.2)^{b}**

Table 3.1: The average values of measured 16 points at the central part of the mapped DC of NSNP, WSPS and DSPS at 1 - 4 mm depths. The numbers in bracket are the standard deviation and the letters are the post-hoc Tukey comparison ofaverage DC results. Significant difference determined by one-way ANOVA and post hoc Tukey comparisons ($p<0.05$) are represented in ascending alphaphetical order from high to low within each group.

3.4 Longitudinal and Latitudinal Micro-Hardness Analysis

Figure 3.7-3.10 compared the results of micro-hardness test for 1 - 4 mm depths of the group category (i.e., NSNP, WSPS and DSPS) analysed within 6 h and 24 h after irradiance. Table 3.2 compared the average hardness values of all the group categories of the specimens processed against 1 – 4 mm depths. The average hardness when compared against depth revealed a significant difference between the means of various group categories, with 1 mm having the highest value and 4 mm having the lowest ($p<0.05$). The average hardness values when compared against group categories for 6 h specimens showed significant difference, with DSPS having highest values hardness values. While NSNP VHN values were in the middle VHN values and WSPS having the lowest VHN values ($p<0.05$). Meanwhile, the results of 24 h specimens revealed there was significant difference at 1-, 3- & 4-mm depths with DSPS having the highest values, WSPS, VHN values in the middle and NSNP specimens having the lowest hardness but there was significant difference between the average VHN values at 2 mm depth. DSPS had the highest value while NSNP specimens' value was in the middle VHN values and WSPS had the least VHN value ($p<0.05$). Lastly, the comparison of the group categories processed at different time intervals i.e 6 h versus 24 h revealed significantly higher VHN values at 24 h compared with 6 h ($p<0.05$).

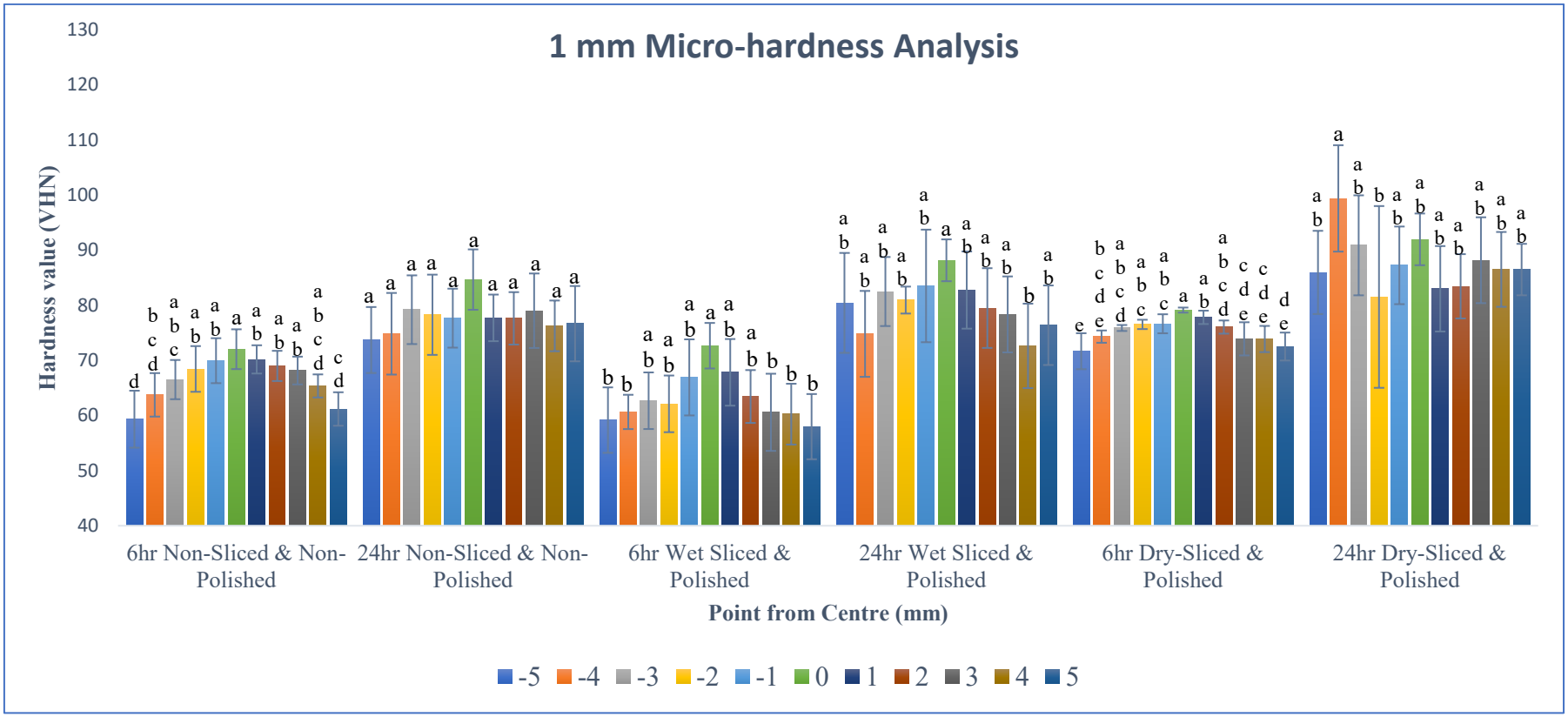

Figure 3.7 Micro-hardness plot of non-sliced & non-polished and sliced & polished specimens under both wet and dry conditions for 1 mm depth. VHN values within the category of specimens measured within 6 h after curing and among the group category ($p<0.05$). while, for specimens measured at 24 h after curing, there was no significant difference between the means for non-sliced & non-polished specimens ($p>0.05$) but there was significant difference between the means of hardness for sliced & polished specimens both wet and dry ($p<0.05$. Significant difference determined by one-way ANOVA and post hoc Tukey comparisons ($p<0.05$) are represented in ascending alphaphetical order from high to low within each group.

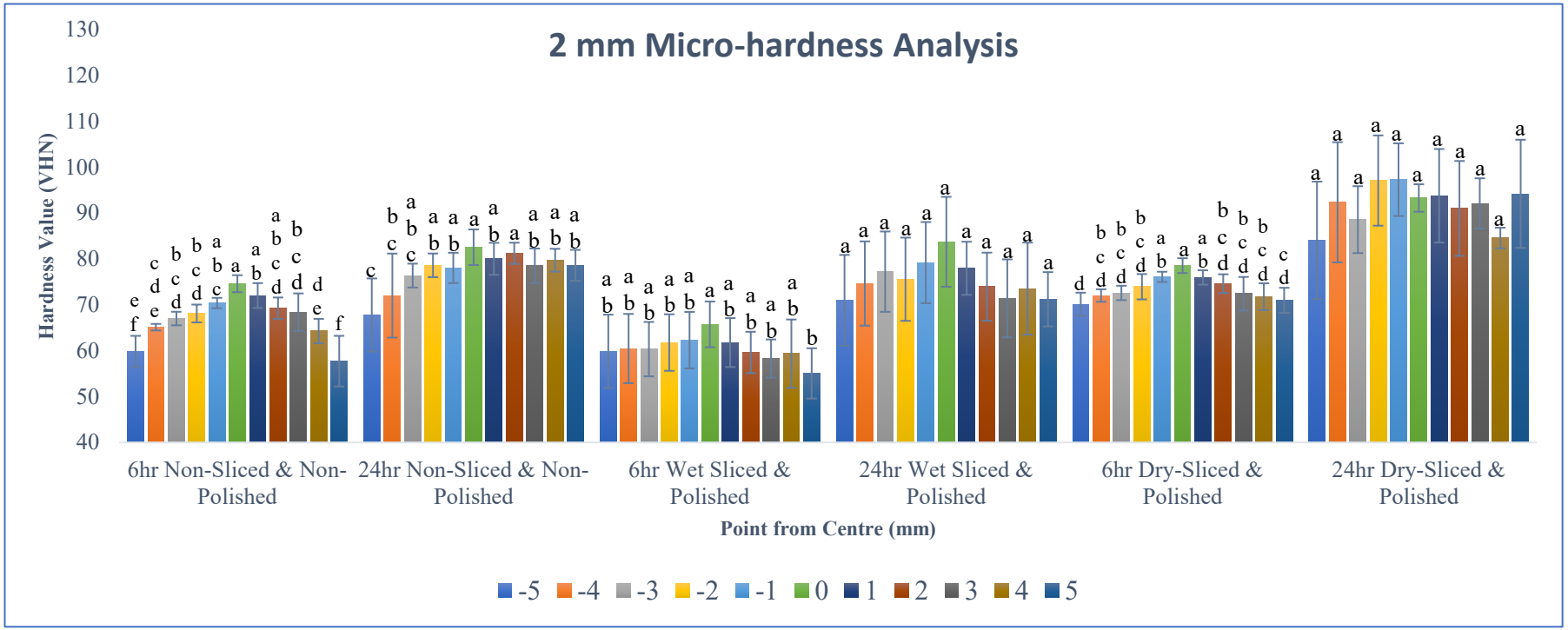

Figure 3.8 Micro-hardness plot of NSNP and sliced & polished specimens under both wet and dry conditions at 2 mm depth. There was significant difference between the means of VHN values within the category of specimens ($p<0.05$) for specimens measured within 6 h after curing. On the other hand, for specimens measured at 24 h after curing, there was significant difference between the means for NSNP ($p<0.05$), while there was no significant difference between the means for the group category of WSPS and DSPS ($p > 0.05$). Significant difference determined by one-way ANOVA and post hoc Tukey comparisons ($p<0.05$) are represented in ascending alphaphetical order from high to low within each group.

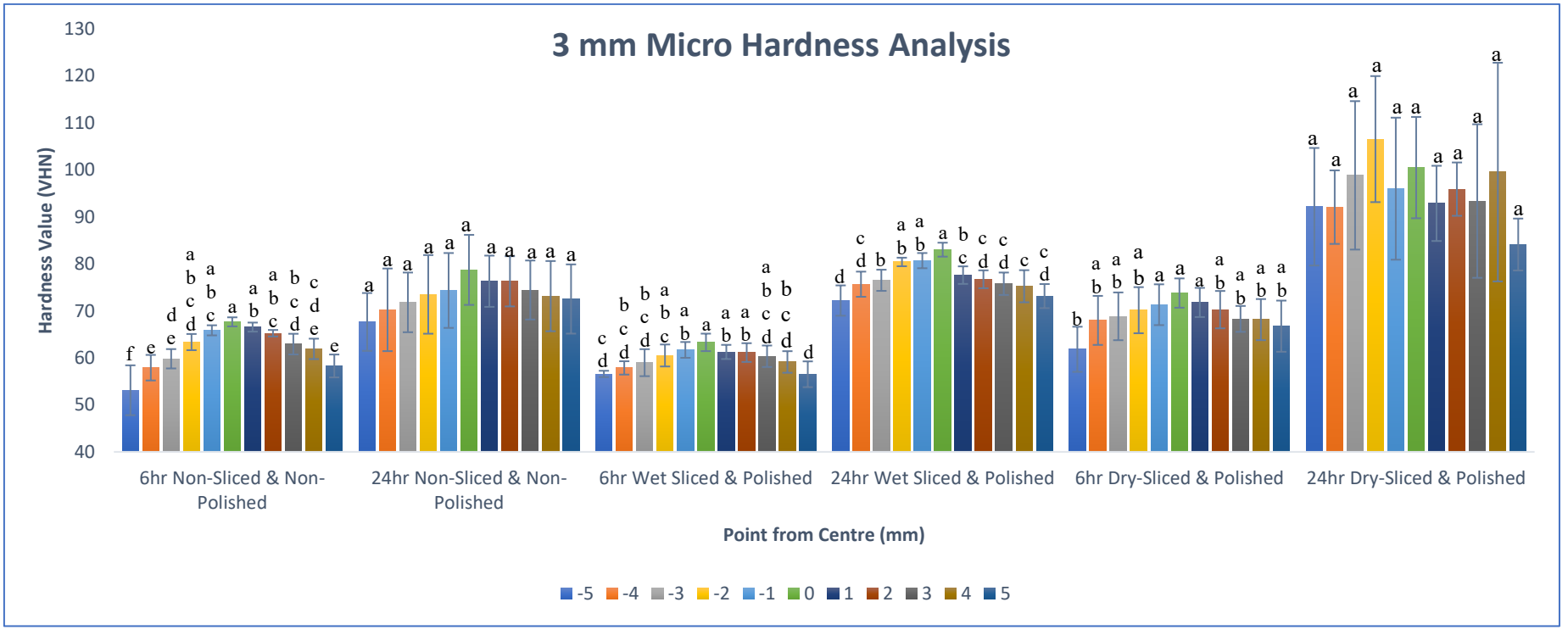

Figure 3.9 Micro-hardness plot of NSNP and sliced & polished specimens under both wet and dry conditions at 3 mm depth. There was significant difference between the means of the VHN values within the category specimens ($p<0.05$) for specimens measured within 6 h after curing. However, for specimens measured 24 h after curing, there was significant difference between the means for WSPS ($p<0.05$), while there was no significant difference between the means for the group category of non-sliced & non-polished and dry sliced & polished specimens ($p > 0.05$). Significant difference determined by one-way ANOVA and post hoc Tukey comparisons ($p<0.05$) are represented in ascending alphaphetical order from high to low within each group.

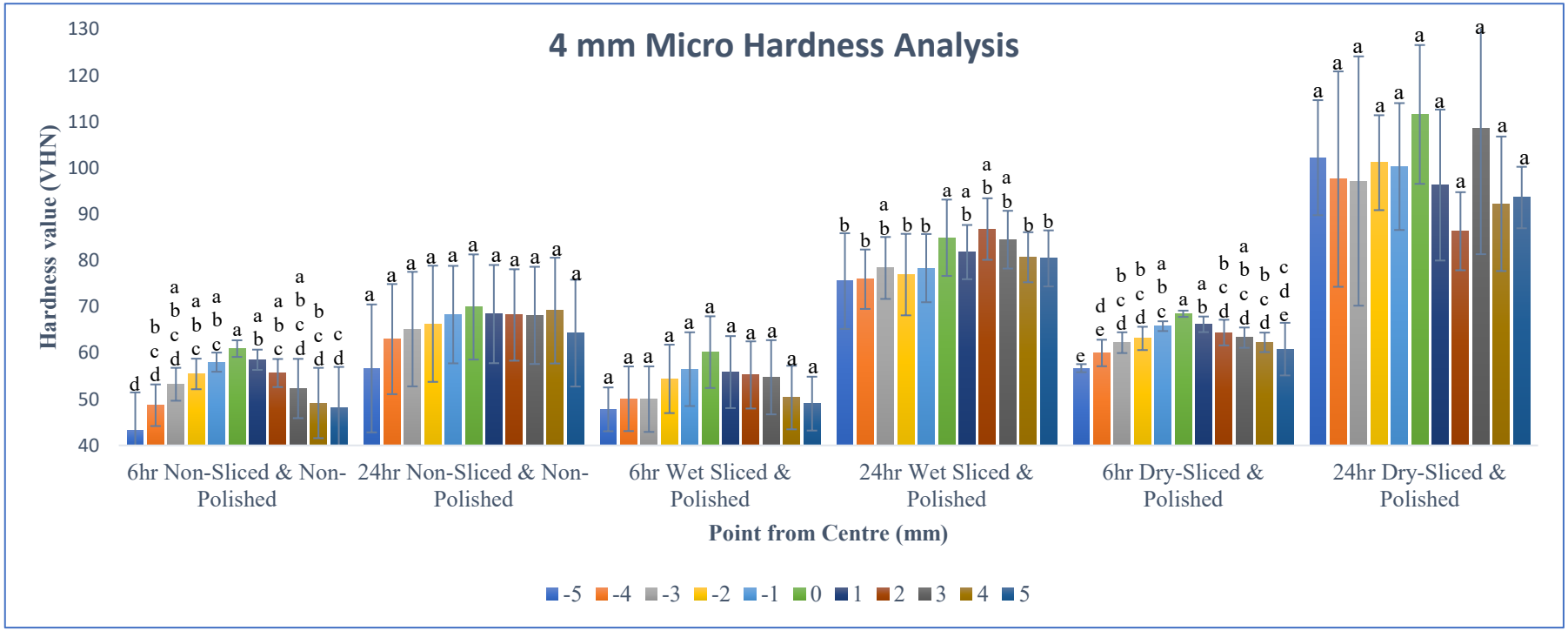

Figure 3.10: Micro-hardness plot of non-sliced & non-polished and sliced & polished specimens under both wet and dry conditions at 4 mm depth. There was significant difference between the means of NSNP and DSPS ($p<0.05$) and no significant difference between the means of WSPS ($p>0.05$) measured within 6 h after curing. Meanwhile, for specimens measured at 24 h after curing, there was significant difference between the means for WSPS ($p < 0.05$) and there was no significant difference between the means for the remaining groupcategory ($p>0.05$). Significant difference determined by one-way ANOVA and post hoc Tukey comparisons ($p<0.05$) are represented in ascending alphaphetical order from high to low within each group.

Average Hardness Analysis						
	6 h Non-Sliced, Non-Polished	**24 h Non-Sliced, Non-Polished**	**6 h Wet-Sliced and Polished**	**24 h Wet-Sliced and Polished**	**6 h Dry-Sliced and Polished**	**24 h Dry-Sliced and Polished**
1 mm	**67 (4.0)^{b}**	**78 (2.8)^{b}**	**63 (4.4)^{b}**	**80 4.4)^{b}**	**75 (2.3)^{a}**	**88 (5.0)^{a}**
2 mm	**67 (5.0)^{b}**	**78 (4.3)^{b}**	**60 (2.7)^{c}**	**72 (3.9)^{b}**	**74 (2.5)^{a}**	**92 (4.4)^{a}**
3 mm	**62 (4.4)^{b}**	**74 (3.1)^{b}**	**60 (2.2)^{b}**	**77 (3.3)^{b}**	**69 (3.1)^{a}**	**95 (5.8)^{a}**
4 mm	**53 (5.3)^{b}**	**66 (3.8)^{c}**	**53 (3.9)^{b}**	**80 (3.8)^{b}**	**63 (3.2)^{a}**	**98 (7.2)^{a}**

Table 3.2: Average of all micro-hardness measurements North-South & East-West for non-sliced & non-polished and sliced & polished specimen under wet and dry conditions. There was significant difference between the means of WSPS (6 h) and NSNP (24 h) while for all the remaining group categories, there was no significant difference between the means of the VHN values ($p>0.05$). The numbers in bracket are the standard deviation, and significant difference determined by one-wayANOVA and post hoc Tukey comparisons are represented in ascending alphaphetical order from high to low within each group.

3.5 Surface Reflection Analysis

Figure 3.11 shows the result of surface reflection (Rt) analysis for all group categories of specimens measured within 6 h and 24 h after irradiance. The surface reflection results when compared among the specimen revealed no significant difference between the means of the Rt values for NSNP at 1 – 4 mm depths, and for WSPS at 1-, 2- & 4-mm depths and DSPS at 1-, 2- & 4-mm depths ($p<0.05$) but showed significant difference for the sliced (wet & dry) specimens measured within 6 h after irradiance at 3 mm depth ($p<0.05$). On the other hand, for 24 h specimens, the result revealed significant difference of Rt values for sliced & polished specimens both wet and dry at 1 – 4 mm depths ($p<0.05$), while there was significant difference for NSNP specimens at 2 - 3 mm depths ($p<0.05$) but no significant difference at 1, 4 mm depths ($p>0.05$). Furthermore, when the group categories were compared with each other within the same process period, 6 h NSNP specimens showed significant difference Rt values when compared to sliced specimens (wet and dry) and for both there was no significant difference ($p>0.05$). For 24 h group categories, there was significant difference between the groups ($p<0.05$). Lastly, comparison of specimens measured at 6 h compared with specimens measured at 24 revealed no significant difference in Rt value in all the groups except, WSPS and DSPS.

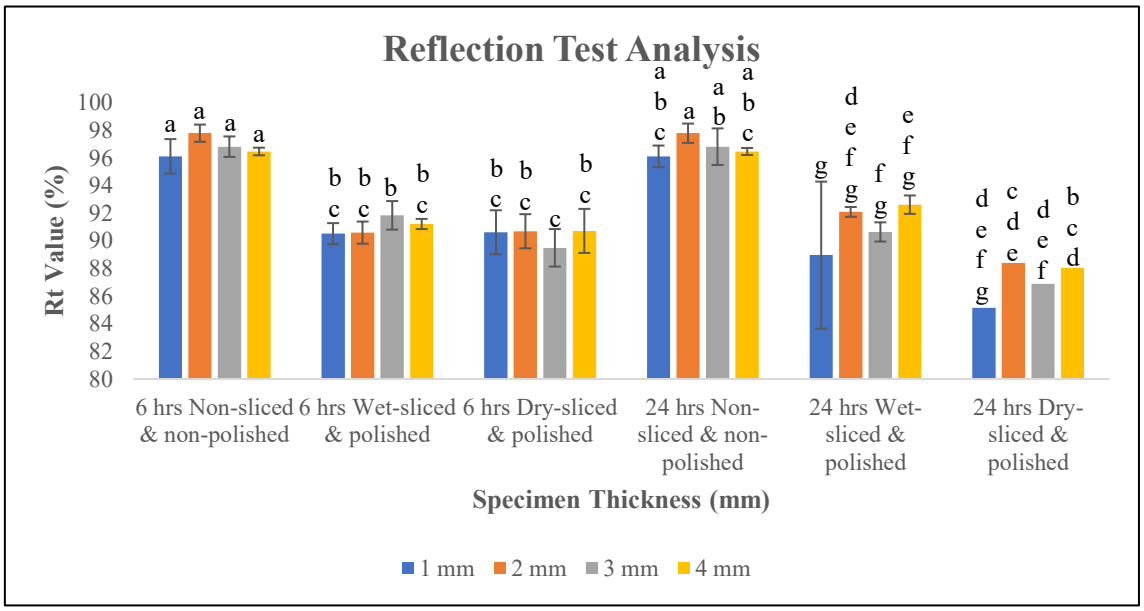

Figure 3.11: The plot compared the lustrous surfaces of wet-sliced & polished, dry-sliced & polished specimen and non-sliced & non-polished specimens prepared using acetate as a cover for the mould measured for 1 - 4 mm thicknesses within 6 h and 24 h after curing. Significant difference determined by one-way ANOVA and post hoc Tukey comparisons ($p<0.05$) are represented in ascending alphaphetical order from high to low within each group.

3.6 Surface Analysis by Scanning Electron Microscopy

Figure 3.12 compared SEM images of NSNP, WSPS and DSPS at 1 - 4 mm depths, viewed at 10K magnification. NSNP specimens showed the homogeneous mixture of resin monomer and clusters of the inorganic fillers evenly distributed throughout the body of the composites. WSPS revealed the exposed filler particles due to slicing and polishing processes and the varied in sizes which imply that the particles are hybrid particles. Also, the wet-sliced specimens, the boundary between the particles and resin matrix is clearly visible and the resin matrix appeared to have been removed on the surface allowing the inorganic particles to stand out. On the other hand, the DSPS reveal the surface which clearly bonded the resin matrix and the inorganic particles together. For 1 mm and 2 mm dry sliced specimen, it appears that the boundary lines are becoming hard to trace.

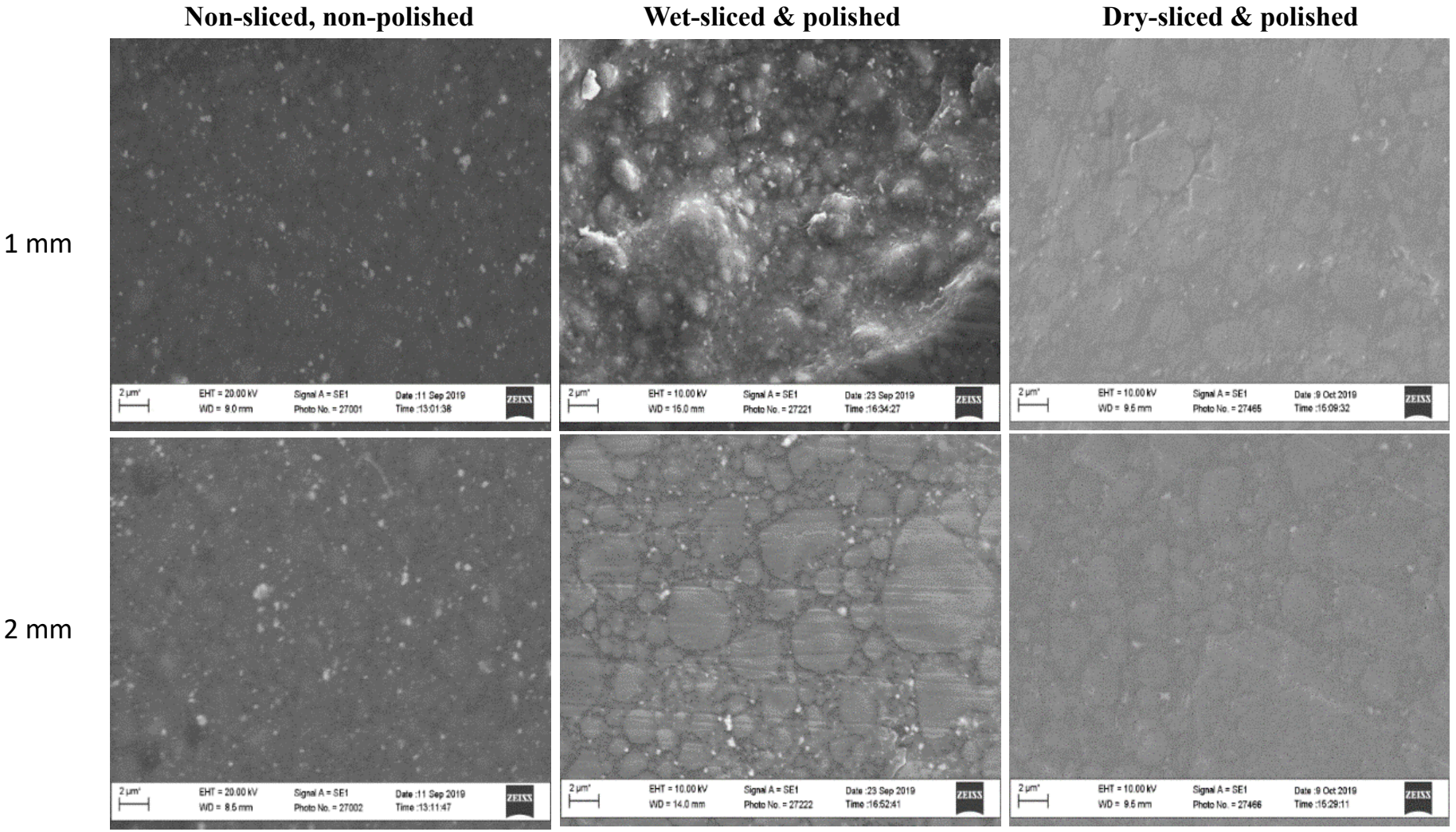

Figure 3.12a SEM images comparing non-sliced & non-polished, wet-sliced & polished specimens and dry-sliced & polished specimens against 1 - 2 mm thicknesses of Filtek^{TM} one bulk fill restorative material specimens viewed at 10K magnification.

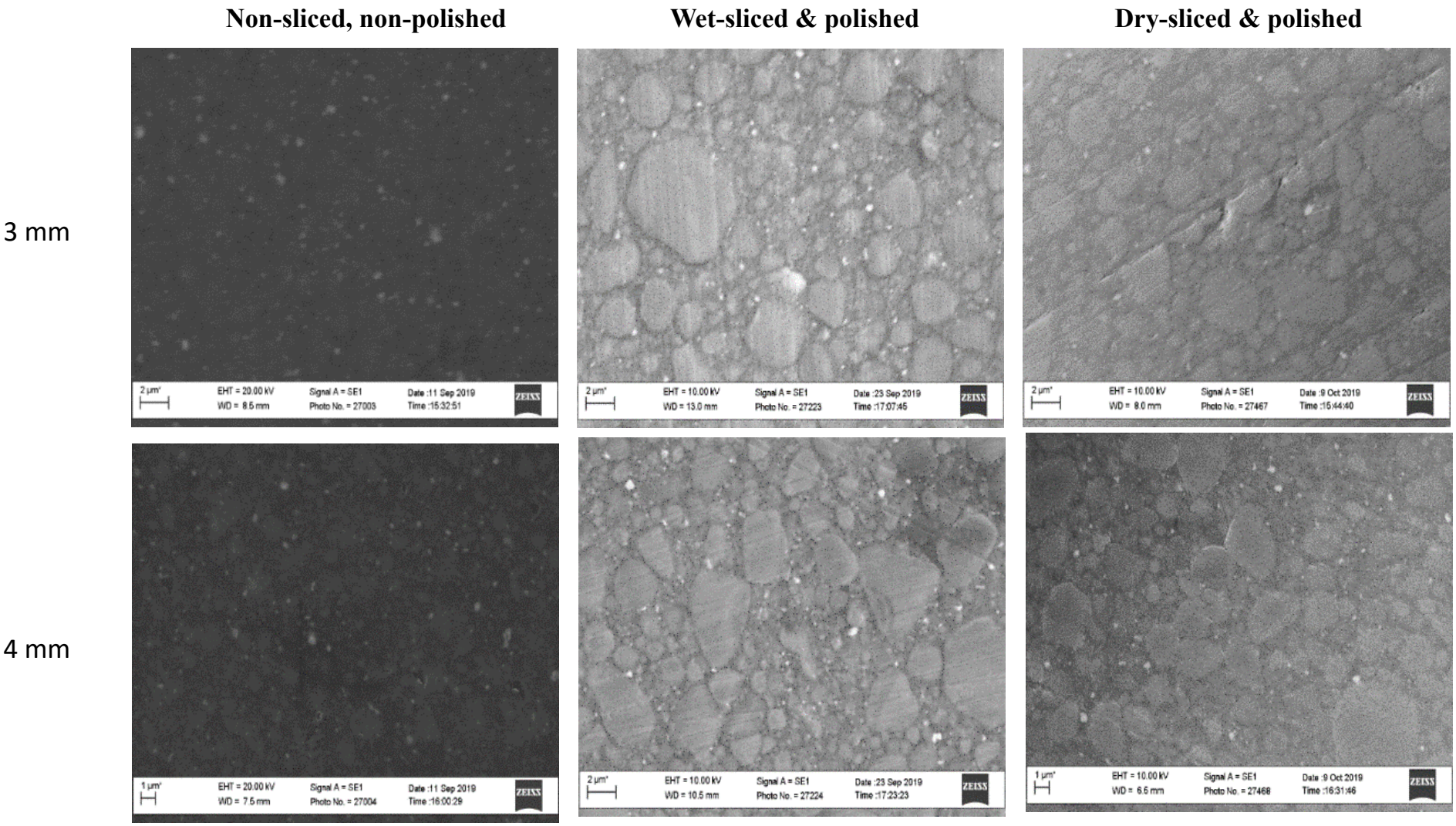

Figure 3.12b SEM images comparing non-sliced & non-polished, wet-sliced & polished specimens and dry-sliced & polished specimens against 3 - 4 mm thicknesses of Filtek^{TM} one bulk fill restorative material specimens viewed at 10K magnification.

3.7 Regression Analysis

3.7.1 6-H Central Single Point DC

Figure 3.13 revealed the fitted equation for the linear model that describes the relationship between Y and X is

$$Y = 81.23 – 6.952 X \qquad \text{Equation 3.1}$$

The relationship between 6 h non-sliced & non-polished (NSNP) DC (%) and depth (mm) is statistically significant ($p<0.05$) and the R squared value is 85.11%. Equation 3.1 can be used to predict the 6 h NSNP DC (%) for a value of depth (mm) or find the settings for depth (mm) that corresponds to a desired value or range of values for 6 h NSNP DC (%).

Figure 3.14 revealed the fitted equation for the linear model that describes the relationship between Y and X is

$$Y = 70.96 – 8.829 X \qquad \text{Equation 3.2}$$

The relationship between 6 h wet-sliced & polished (WSPS) DC (%) and depth (mm) is statistically significant ($p<0.05$) and the R squared value is 94.65%. Similarly, equation 3.2 can be used to predict the 6 h WSPS DC (%) for a value of depth (mm).

Figure 3.15 revealed the fitted equation for the linear model that describes the relationship between Y and X is

$$Y = 80.58 – 5.562 X \qquad \text{Equation 3.3}$$

The relationship between 6 h dry-sliced & polished (DSPS) DC (%) and depth (mm) is statistically significant ($p<0.05$) and the R squared value is 84.56%. Similarly, equation 3.3 can be used to predict the 6 h DSPS DC (%) for a value of depth (mm).

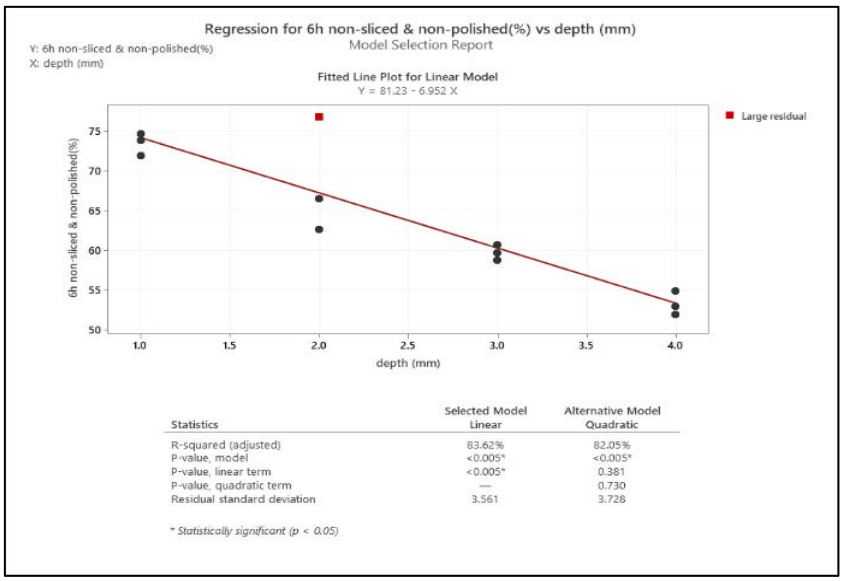

Figure 3.13: Fitted line plot for 6 h single non-sliced & non-polished DC vs depth.

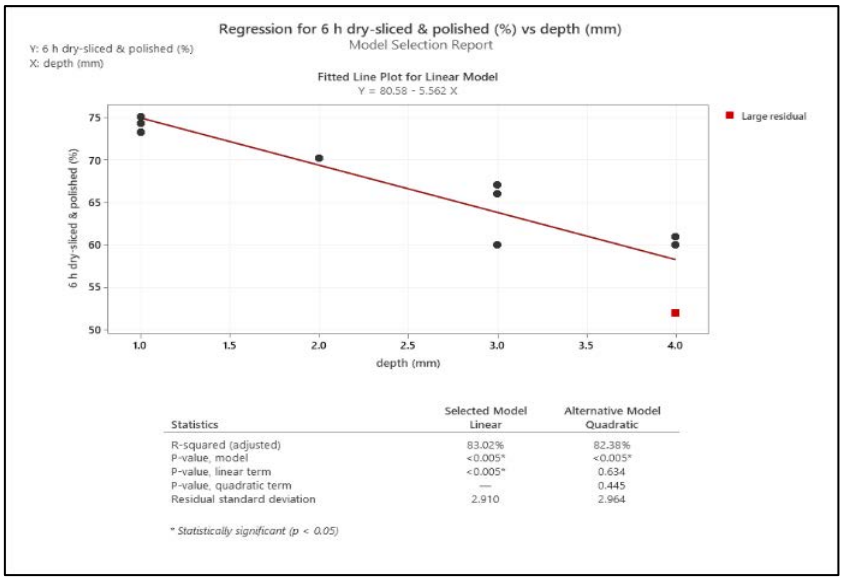

Figure 3.14: Fitted line plot for 6 h single wet-sliced & polished DC vs depth.

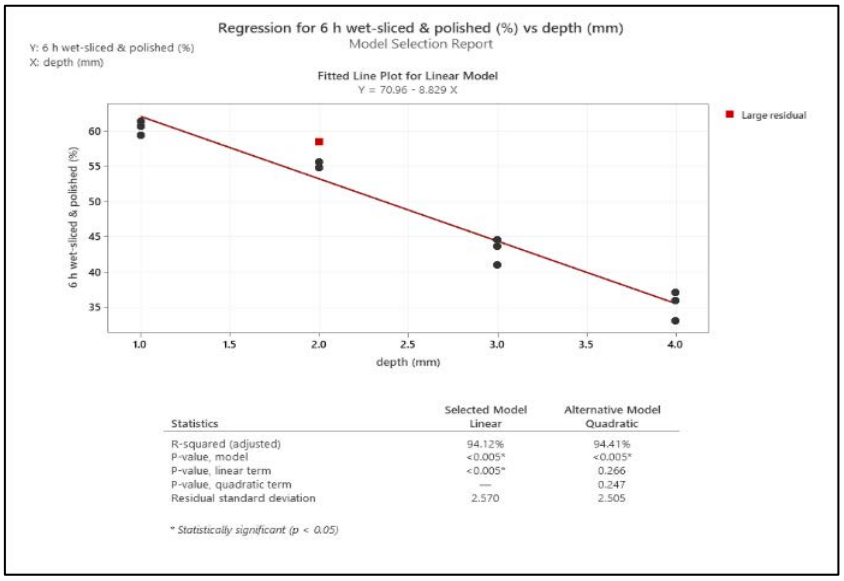

Figure 3.15: Fitted line plot for for 6 h single dry sliced & polished DC vs depth.

3.7.2 24-H Central Single Point DC

Figure 3.16 revealed the fitted equation for the linear model that describes the relationship between Y and X is

$$Y = 90.26 – 4.562\ X \qquad \text{Equation 3.4}$$

The relationship between 24 h non-sliced & non-polished (NSNP) DC (%) and depth (mm) is statistically significant ($p<0.05$) and the R squared value is 38.85%. Similarly, equation 3.4 can be used to predict the 24 h NSNP DC (%) for a value of depth (mm).

Figure 3.17 revealed the fitted equation for the linear model that describes the relationship between Y and X is

$$Y = 76.22 + 11.19\ X – 3.499\ X2 \qquad \text{Equation 3.5}$$

The relationship between 24 h wet-sliced & polished (WSPS) DC (%) and depth (mm) is statistically significant ($p<0.05$) and the R squared value is 82.31%. Similarly, equation 3.5 can be used to predict the 24 h WSPS DC (%) for a value of depth (mm).

Figure 3.18 revealed the fitted equation for the linear model that describes the relationship between Y and X is

$$Y = 95.02 – 15.86\ X \qquad \text{Equation 3.6}$$

The relationship between 24 h dry-sliced & polished (DSPS) DC (%) and depth (mm) is statistically significant ($p<0.05$) and the R squared value is 89.38%. Similarly, equation 3.6 can be used to predict the 24 h DSPS DC (%) for a value of depth (mm).

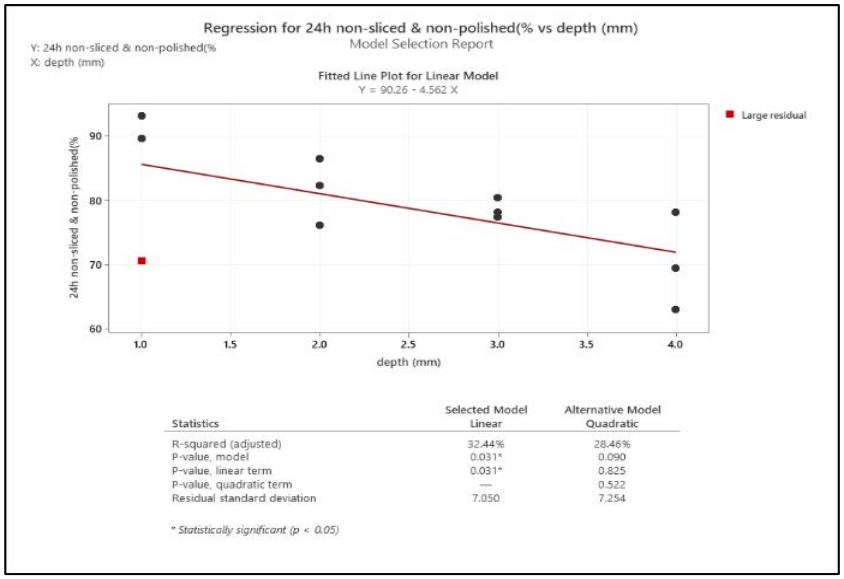

Figure 3.16: Fitted line plot for 24 h single non-sliced & non-polished DC vs depth.

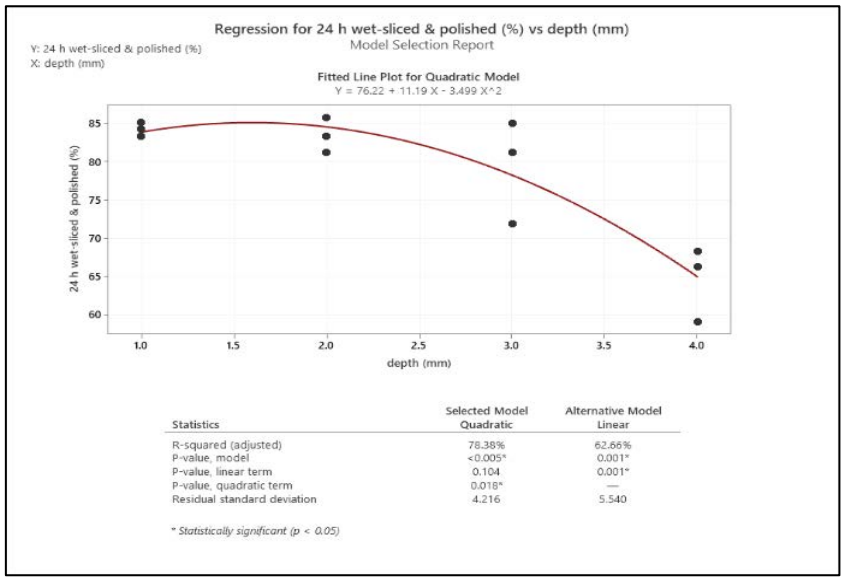

Figure 3.17: Fitted line plot for 24 h single wet-sliced & polished DC vs depth.

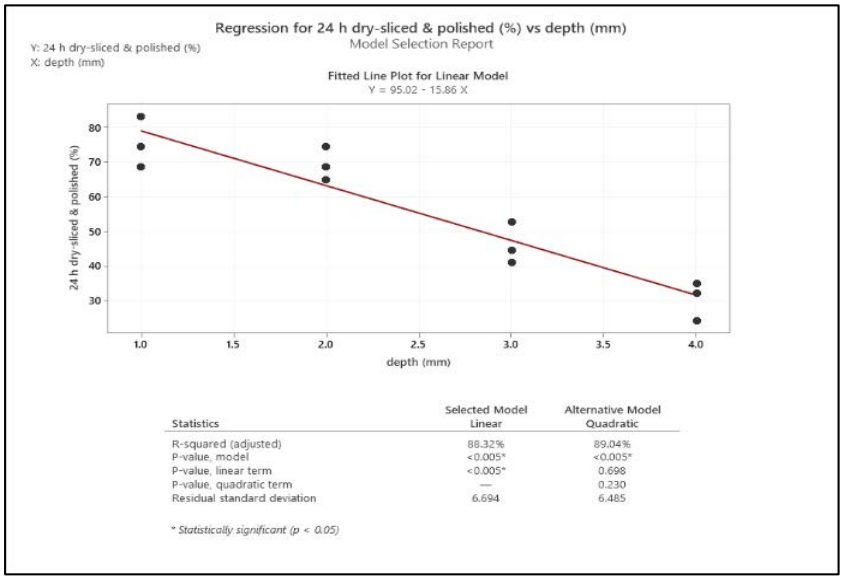

Figure 3.18: Fitted line plot for 24 h single dry-sliced & polished DC vs depth.

3.7.3 6-H Specimen Surface Mapped DC

Figure 3.19 revealed the fitted equation for the linear model that describes the relationship between Y and X is

$$Y = 111.9 - 52.05\ X + 8.992\ X^2 \qquad \text{Equation 3.7}$$

The relationship between 6 h non-sliced & non-polished (NSNP) DC (%) and depth (mm) is statistically significant ($p<0.05$) and the R squared value is 47.22%. Similarly, equation 3.7 can be used to predict the 6 h NSNP DC (%) for a value of depth (mm).

Figure 3.20 revealed the fitted equation for the linear model that describes the relationship between Y and X is

$$Y = 27.34 - 2.830\ X \qquad \text{Equation 3.8}$$

The relationship between 6 h wet-sliced & polished (WSPS) DC (%) and depth (mm) is not statistically significant ($p>0.05$) and the R squared value is 5.67%. Similarly, equation 3.8 can be used to predict the 6 h WSPS DC (%) for a value of depth (mm).

Figure 3.21 revealed the fitted equation for the linear model that describes the relationship between Y and X is

$$Y = 56.10 - 6.145\ X \qquad \text{Equation 3.9}$$

The relationship between 6 h dry-sliced & polished (DSPS) DC (%) and depth (mm) is statistically significant ($p<0.05$) and the R squared value is 28.16%. Similarly, equation 3.9 can be used to predict the 6 h DSPS DC (%) for a value of depth (mm).

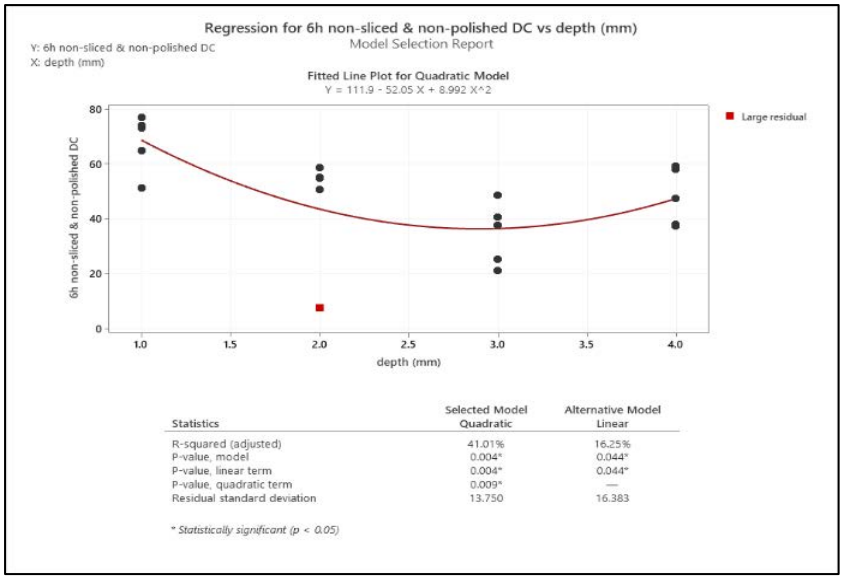

Figure 3.19: Fitted line plot for 6 h mapped non-sliced & non-polished DC vs depth.

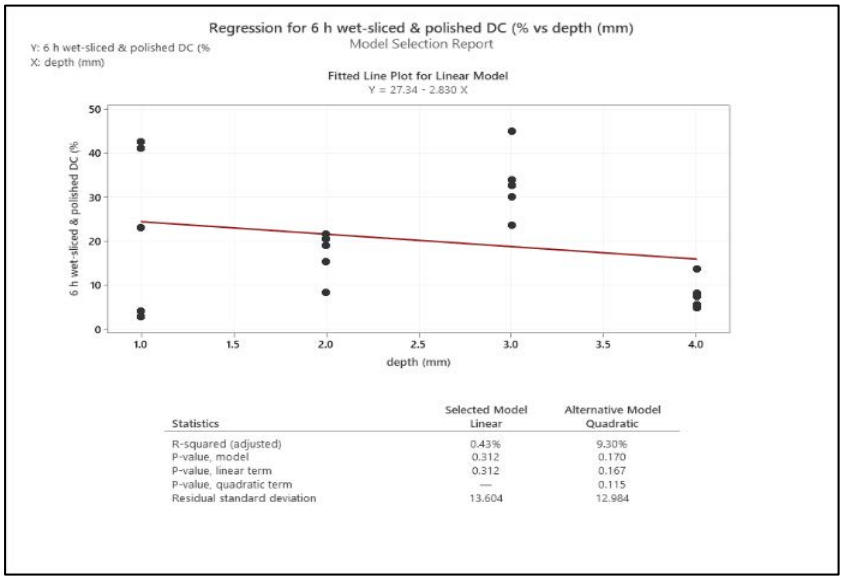

Figure 3.20: Fitted line plot for 6 h mapped wet-sliced & polished DC vs depth.

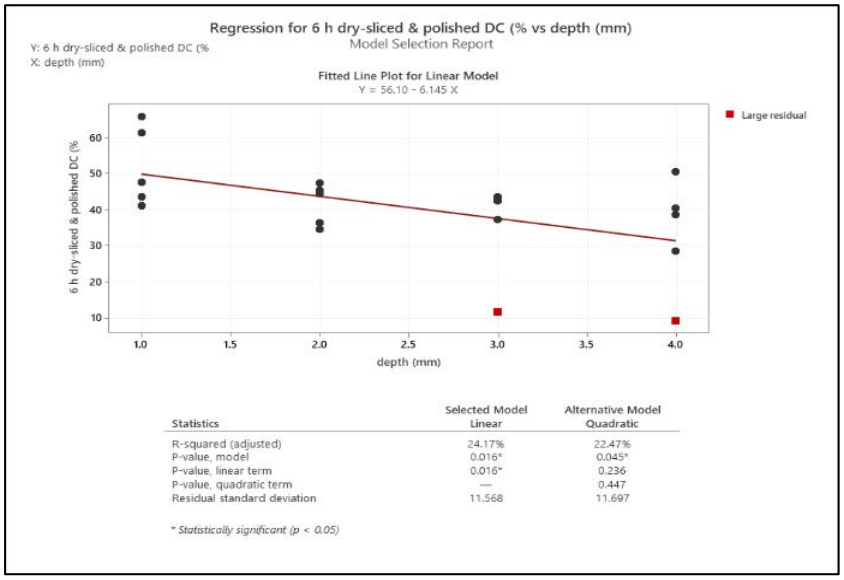

Figure 3.21:Fitted line plot for 6 h mapped dry-sliced & polished DC vs depth.

3.7.4 24-H Specimen Surface Mapped DC

Figure 3.22 revealed the fitted equation for the linear model that describes the relationship between Y and X is

$$Y = 57.38 – 2.549 X \qquad \text{Equation 3.10}$$

The relationship between 24 h non-sliced & non-polished (NSNP) DC (%) and depth (mm) is not statistically significant ($p>0.05$) and the R squared value is 5.66%. Similarly, equation 3.10 can be used to predict the 24 h NSNP DC (%) for a value of depth (mm).

Figure 3.23 revealed the fitted equation for the linear model that describes the relationship between Y and X is

$$Y = 75.06 - 33.43 X + 7.955 X^2 \qquad \text{Equation 3.11}$$

The relationship between 24 h wet-sliced & polished (WSPS) DC (%) and depth (mm) is statistically significant ($p<0.05$) and the R squared value is 49.11%. Similarly, equation 3.11 can be used to predict the 24 h WSPS DC (%) for a value of depth (mm).

Figure 3.24 revealed the fitted equation for the linear model that describes the relationship between Y and X is

$$Y = 51.15 + 0.476 X \qquad \text{Equation 3.12}$$

The relationship between 24 h dry-sliced & polished DSPS DC (%) and depth (mm) is not statistically significant ($p<0.05$) and the R squared value is 0.09%. Similarly, equation 3.12 can be used to predict the 24 h DSPS DC (%) for a value of depth (mm).

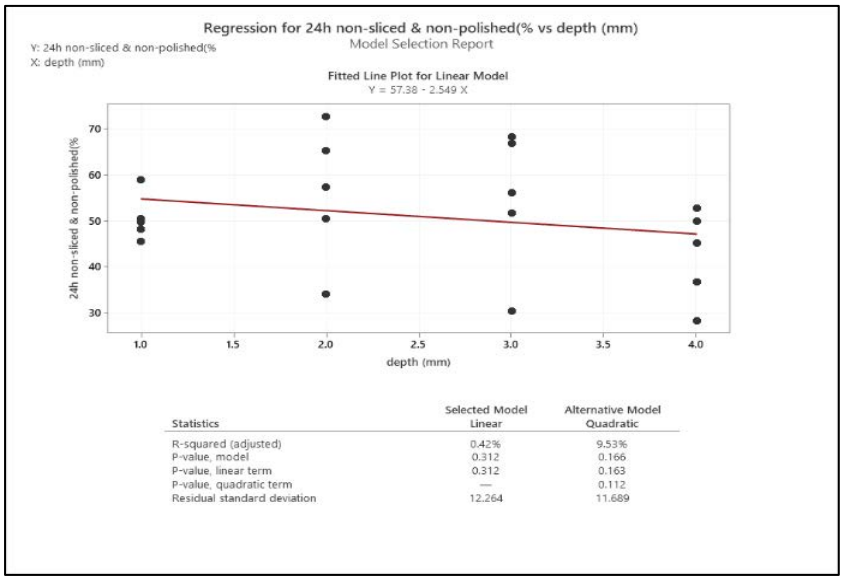

Figure 3.22: Fitted line plot for 24 h mapped non-sliced & non-polished DC vs depth.

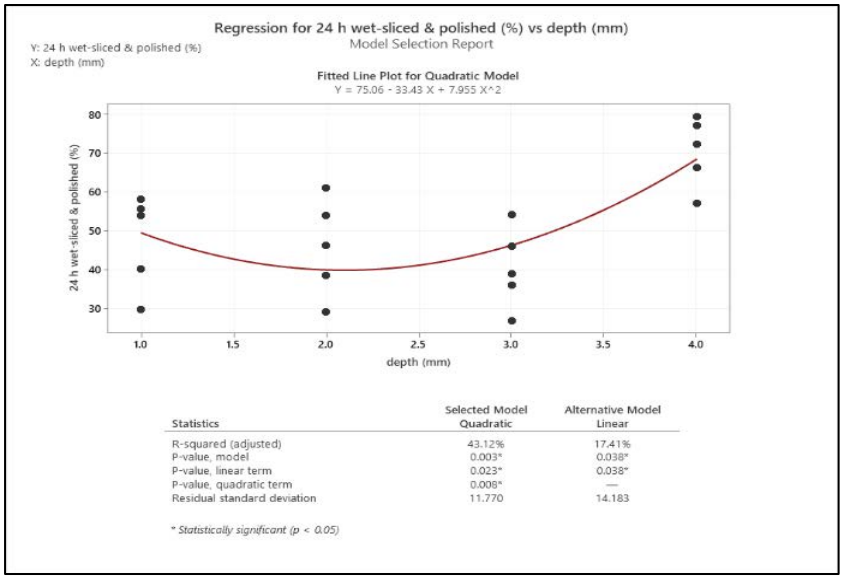

Figure 3.23: Fitted line plot for 24 h mapped wet-sliced & polished DC vs depth.

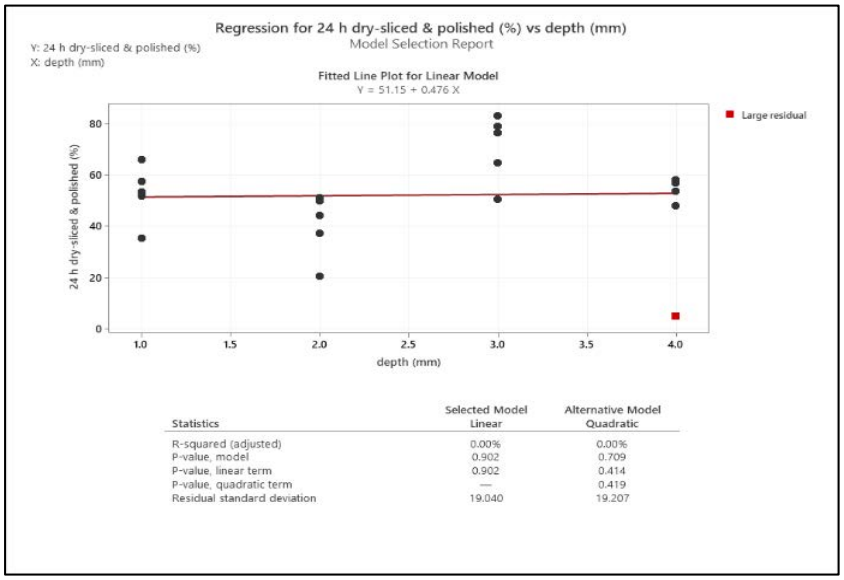

Figure 3.24: Fitted line plot for 24 h mapped dry-sliced & polished DC vs depth.

CHAPTER FOUR

DISCUSSION

Many researchers have used various techniques to investigate and analyse degree of conversion (DC) and hardness (VHN) values of resin based composite materials and these techiniques are indirect methods (Hadis, 2011). Moore, 2008 stated that dentist have no means of monitoring the cure of the resin surfaces that are not directly exposed to the curing light. The knowledge of the values of DC and VHN within and at the surface of the material are both important to ascertain the efficiency of polymerization process and the adequacy of irradiation. The scraping technique which is an internationally accepted technique for measuring how deep is the curing in an experimental material i.e., depth of cure according to the International Standard Organization (ISO), standard for dental resins 4049 (ISO Standard, 2000) is prone to error, yet, it has been the standard that many have used to measure the depth of cure in many research studies (Flury, 2012). One of the reasons for the error may be due to the measurement being estimated and the ratio of 0.8 or 0.85 used as benchmark is an arbitrary figure. Another reason can be traced to the scraping technique methodology, during which part of the cured layer of the material could be peeled off, thus introducing error into the accuracy of the measurement (Moore, 2008).

Apart from that, many of the techniques used to determine the DC and VHN are point based methods, during which researchers carried out random measurements about the centre area of the specimens and then determine the average values of the centre DC and VHN points measurement to represent the surface area and a conclusion is drawed based on the average values of the centrally measured DC and VHS values. Thus, in this current research, a recently developed mapping technique (Hadis et al., 2019) was used to analyse the DC values of the

entire surface area of sectioned specimens of all the group categories of specimens under investigation at incremental depth of 1 mm up to 4 mm. This technique involved sectioning of specimens and contact mapping over the sectioned surfaces using FTIR (Germanium Crystal ATR) spectroscopy and Vickers hardness, also, at incremental depth of 1 mm up to 4 mm. This technique was used to generate some maps which revealed how the DC values varied across the surfaces of the specimens at (1 – 4 mm) depths and post-polymerization assessment of spatial DC was also conducted. Furthermore, many experimental methods of specimen preparation to measure the DC and VHN involve one form of sectioning or grinding or polishing to prepare the surface where the reading will take place. Thus, the aim of this current research was to study and investigate the effect that specimen preparation will have on the DC and VHN of dental resin composite. Therefore, the hypothesis is specimen preparation will affect the degree of conversion and hardness of dental resin composite samples and the hypothesis was tested through the following objectives:

4.1 Effect of Thickness

The first objective of the hypothesis states that "the difference in the DC and VHN obtained depends on the depth at which measurements are taken was upheld. With increasing depth 1 - 4 mm, DC and VHN values significantly decreased ($p<0.05$); for *single point DC*, the values of DC decreased by 11 ± 1 % as the depth of the specimen increased for 6 h specimens in Figures 3.13 – 3.15 and the values of DC decreased by 12 ± 1 % as the depth of the specimens increased for 24 h specimens in Figures 3.16 - 3.18 at 1 - 4 mm depths, respectively; for *mapped DC* measurements, DC decreased by 21 ± 3 % at 6 h & 10 ± 3 % at 24 h in Figures 3.3, 3.6, 3.19 & 3.21. Similarly, for *VHN measurements*, VHN decreased by 8 ± 2 % at 6 h & 6 ± 1 % at 24 h in Table 3.2. These differences are likely due to in efficient light transmission caused

by light absorption by photo initiators, light attenuation by dyes and pigments, light scattering by fillers, and surface light reflection. (Arikawa, 2009). The result of single point DC, mapped DC and hardness values obtained in Figures 3.3 & 3.6 and Table 3.2 thus correlate with studies that investigated the effect of light transmission through depth (Musanje, and Darvell, 2006). Furthermore, Palin et al., 2018 explained that photochemical reaction commenced when photo initiators absorb light photons and its concentration affect photo-polymerization process through the depth. With higher concentration of photo initiators, there are increased rate of initiations, which also increases conversion and light transmission are reduced at depth of the composite (Ogunyinka, et al., 2007). The technical document of the materials did not indicate the type of photo initiator(s) used but the range of the emission of the curing light was 420 – 500 nm and showed the peak output λ_{max} = 449 nmsuggested that camphorquinone (CQ) was part of the photo initiators used in the material.

Another related point that may have affected the obtained values of DC and hardness in this study is light scattering. Rocha pointed out that the scattering of light occurs due to filler particle size being greater than or equal to the wavelength of the incident visible light 400 - 750 nm (Rocha, 2018). Shortall, et al., 2008; Palin, et al., 2018 explained that light scattering occurs at the interfaces because of refractive index mismatch which occurs between resin and filler particles, and the larger the difference in the refractive indexes between the components of the material the lower the light transmission (Shortall, et al., 2008). In the current research, the refractive indexes of the material used for 3M™ Filtek™ One bulk fill restorative composite are silica filler (1.540; size = 20nm), zirconia filler (1.520; size = 4 to 11nm), ytterbium trifluoride filler (1.530; size = 100nm), the sum total of inorganic filler particles is approx. 58.4% by volume (76.5% by weight), and UDMA (1.481) (O'Brien, et al., 2008; 3M ESPE, 2016) but it is difficult to understand what the exact reflective index of the resin matrix is as it is made up of different resins and the manufacturer does not divulge this information.

Consequently, in the current research, the material used is Filtek^{TM} One bulk fill restorative material utilized nanotechnology to change the translucency of the composite during cure (3M ESPE, 2016) which may have contributed significantly to the improvement seen in the DC and hardness values through the thickness of the bulk of the material. Furthermore, the composite material was designed so thatthe paste of the uncured appeared more translucent than the paste of the final cured composite, thereby, allowing the penetration of light into the lower part of the composite, therefore, exhibiting less change in translucency at the surface layer during polymerisation, Also, allowing enough light penetration and the generation of free radical at the lower part of the composite, thereby achieving considerable depth of cure by activating the cure chemistry throughout the composite (3M ESPE, 2016).

Some of the mapped DC in Figures 3.4 – 3.5 & 3.25 (Appendix 2) showed 'white' noise signals alongside some of the DC maps. The reason for the noise signal were traced to effect of diffused reflectance from the surface of the specimens. The FTIR microscope crystal used for the DC measurements, is inverted and the crystal comes down and applies a constant pressure which is pre-set. This happened at every point on the specimen. In the normal ATR measurements, the pressure is manually set, and that is what leads to the 'white' noise which occurred with the images. Al--shaali, 2013 explained that during his research using ATR crystal that noise was introduced to the specimens used for his research when the specimens were being removed from the crystal plate of the ATR with the view of re-assesses it later, thus generating poor spectra. In the current research, the ATR crystal made good contact with the specimens at every point of DC measurement, but some noise signals were discovered in the mapped images. In the current study, the reason why some of the DC images look 'noisy' is because of slicing and polishing procedure which exposed the fillers on the surface of the specimens. As a result of that, the ATR crystal picks up a signal from fillers, not the resin. The fillers do not have a string signal produced by the C=C groups and therefore a weak signal and 'noise is experienced'.

4.2 Effect of Post-Irradiation Time

The second objective of the hypothesis states that "the DC and VHN values for non-sliced & non-polished specimens (NSNP) will depend on time between curing and measurement was upheld. A significant difference was observed when the DC and VHN values of 24 h and 6 h NSNP specimens' measurements were compared, and it revealed; for *single point DC*, 24 h NSNP specimens increased by 24 ± 11 % than 6 h NSNP specimens; for *mapped DC* 24 h NSNP specimens increased by 2 ± 1 % than 6 h NSNP specimens, although it was not significant, but it should be noted; and for VHN values 24 h NSNP specimens increased by 19 ± 4 % than 6 h NSNP specimens, Figures 3.3 & 3.6 and Tables 3.1 – 3.2; $p<0.05$. The reason for these differences is likely to be due to further polymerisation through dark-cure process in 24 h specimens of all the group categories of specimens (Alrahlah et al., 2014). The dark-cure polymerization is a process in which the polymerization continues in a material even after the irradiation of the material has stopped. The availability of free radicals and other trapped active species during the polymerization process affect and aid the dark-cure polymerisation process. Al-Ahdal noted that the polymerization process will continue as long as there are availability of free radicals and other active species, but when there are decrease in the quantity of these active specices, the rate of polymerization will also decrease (Al-Ahdal, 2015). This was confirmed in the current research because 24 h NSNP specimens which were the control for no further preparation exhibited higher DC and VHN compared to 6 h measurements of the same group. In addition, previous research studies conducted on dark-cure polymerization established that at the initial stage of polymerization, the rate of free radical generation, mobility of free radicals and active monomers is high, but after some time, the mobility decreases because of the formation of network which obstructs the movement of active species (Hansen, 1983; Watts et al 1987; Alrahlah et al., 2014). The rate of mobility of active species

after irradiation remain significantly lower than during irradiation and thus able to polymerise into the existing network even after irradiation has ceased albeit at slower rates, thereby increasing DC (Alrahlah et al., 2014).

Meanwhile, Par et al, highlighted the factors that could affect the extent of the dark cure DC in resin-based material as: resin composition (Tarumi, et al., 1999; Mohamad, et al., 2007), the presence of free radicals (Burtscher, 1993), and specimen temperature (Ferracane, and Condon, 1992; Par et al., 2014). On the aspect of resin composition, Par et al 2014, established the presence of dark-cure polymerization using four different materials i.e., the study compared the results of different composite materials. Whereas, in the current research only one RBC bulk fill material was used but subjected to different preparation processes and comparing the differences in DC & VHN values at 1 – 4 mm depths in the material

4.3 Effect of Dry Slicing Procedure

4.3.1 6-Hour Specimens

The third objective of the hypothesis states that **"**dry-slicing and polishing within 6 hours after curing will lead to higher DC and VHN values due to heat generated by friction" was upheld. The result of DC and VHN values in Figures 3.3 & 3.6 and Table 3.2 revealed the DSPS had significantly higher DC and VHN values than NSNP. When 6 h DSPS were compared to 6 h NSNP specimens the results revealed; for *single point DC*, DSPS increased by 19 ± 2 % than NSNP for 6 h specimens; for *VHN values*, DSPS increased by 13 ± 4 % than NSNP for 6 h specimens, and for *mapped DC*, no significant difference between the 6 h & 24 h specimen groups ($p>0.05$) probably due to lack of active species.The reason for the differences in single point DC and VHN may be due to heat generated by friction, which increase diffusion and increase cross-linking density during dry-slicing process which correlate with the research

conducted by Nasoohi,et al.,2017 which revealed that dry finishing and polishing samples had higher hardness and surface roughness than samples subjected to wet finishing and polishing. In the current study, similar effects are likely under dry slicing/polishing which will increase DC as well as hardness.

Bausch, et al 1981, studied the influence of temperature on some physical properties of dental composition, when they discovered that the conversion and physical properties of resin based composite improved when they are exposed to temperature after light curing. Wu, et al 2016 & Peng, et al 2019, studies the characteristics and mechanisms of polymer interfacial friction heating in ultrasonic plasticization for micro injection molding. The mechanism of friction heat generation described in that research was similar and could be used to explain the dry sliced SEM images results. The rotation disc wheel blade cutting into the dry specimens and robbing against the cut surface of the specimens generated heat energy. In the current research, there was transformation of energies rotational energy from the disc and friction energy on the surface of the specimens both transforming into heat energy. Wu, et al 2016, discovered that the interfacial friction heating was for a short period of time and increase the interfacial temperature sharply to 160^0C, which is the flow temperature of poly-methyl methacrylate. In the current study, the temperature was not measured but the SEM images of dry-sliced specimens showed the matrix, and the filler were properly bonded together (Figure 3.12a & b). Furthermore, in another studies researchers showed the significant effect of temperature as it relates to the final DC and VHN values of commercial composites. It has been established that exist significant relationship between temperature and monomer conversion and that the rates of reaction of propagation and termination are influenced by temperature (Daronch, 2005). However, (Nasoohi, et al., 2017) explained further, that finishing without coolant and polishing generated heat which was significant enough to affect the matrix/filler bond/interface to the extend of causing a separation of the two. Also, this is an indication that some researchers

agreed that specimen preparation could have impact on the specimen but may not have linked the effect to the outcome of DC and VHN values.

4.3.2 24-Hour Specimens

The fourth objective of the hypothesis states that "the result of slicing and polishing process carried out at 24 h after curing will lead to non-significant differences in degree of conversion and hardness values obtained when compared with non-sliced and non-polished samples regardless of wet or dry conditions" was rejected.

The results obtained for 24 h specimens in the current research showed a significant difference between NSNP and DSPS specimens at 1 - 4 mm depths ($p<0.05$). The 24 h DSPS showed; for *single point DC,* 24 h DSPS increased by 5 ± 2 % than 24 h NSNP specimens; for *VHN values* 24 h DSPS increased by 27 ± 5 % than 24 h NSNP specimens and for *mapped DC*, no significant difference was observed between DSPS and NSNP specimens. With dry-sliced process, significant differences observed in DC and VHN results was attributed to specimen preparation processes. while with wet-sliced process, the water lubricant may have surpressed heat generated by friction, thus the DC and VHN values were affected accordingly.

Previous research highlighted that room when temperature rises 22^{o}C (room temperature) to 35^{o}C (mouth temperature), an increase of 6 - 10 % is observed in DC and VHN values and polymerization rate (Price, et al., 2011). The reason for that was because of improved monomer mobility, which allowed more reaction to occur before vitrification (Daronch, et al., 2006). Also, it should be noted that polymerization efficiency is affected by temperature during the polymerization reaction. (Leprince, et al., 2013). The current study confirmed the effect of heat generated by friction on the DC and hardness values of commercial dental composite material in Figures 3.3 & 3.6 and Table 3.2.

Bagis and Rueggeberg found out in the research that the composite cure was affected by post cured temperature during monomer conversionfurther showed. The reason given was because of the potentials of the trapped free radicals present in the resin matrix to react with the near neighbour was increased by temperature difference rather than the duration of heat applied (Bagis and Rueggeberg, 1997). Literature revealed, with elevation of temperature, polymerization rate causes the composite to reach glass transition temperature at an earlier stage (Leprince, et al., 2013). Trujillo, and Stansbury, 2004, revealed in their research that when a composite is pre-heated, it will result in increase of the monomer conversion and reduction of irradiation duration.

Lastly, previous researchers explained the kinetics behind the effect of temperature on the specimens during polymerization as follows; that immediately an active centre is formed, chain network start to form and grow depending on the nature of the polymer and this creates limitation for the movement of nearby free radicals to access the active centre thus creating increase in specimen modulus and glass transition temperature (T_g). Therefore, as the post-cure temperatureof specimens tend towards the resin glsaa transition temperature (T_g), the movement ofthe longer segment of the chain terminates at the end part, thereby permitting the active species close to that site to collide, and possibly react (Bagis and Rueggeberg, 1997). However, it should be noted that free radicals will not be diffused throughout the resin because they are covalently bonded on one end to the polymer chain. This is the reason any reaction that may occur would be limited to a very small local volume. (Bagis and Rueggeberg, 1997). This may also be used to explain the reasons for the varied DC and VHN values distribution across the surfaces of the specimens measured in Figures 3.4 – 3.5; 3.7 – 3.10; 3.25; 3.27 – 3.30.

4.4 Effect of Wet Slicing Procedure

The fifth objective of the hypothesis states that "slicing and polishing process carried out under wet conditions, within 6 h of curing will result in the lowest degree of conversion and hardness, which may be due to removal of free radicals was upheld.

When the DC and VHN values, for the group categories, measured within 6 hours were compared, the results revealed that the WSPS had the lowest DC values at each thickness in Figures 3.3 & 3.6 and Table 3.2. When the DC and VHN results of 6 h NSNP specimens were compared with 6 h WSPS, revealed; for *single point DC*, WSPS was 33 ± 11 % lower than NSNP for 6 h specimens, for *mapped DC*, WSPS was 50 ± 17 % lower than NSPS for 6 h specimens; for *VHN values*, WSPS was 5 ± 2 % lower than NSPS for 6 h specimens. This may have been due to removal of free radicals during wet-slicing process. Also, in section 4.5, the DC and hardness values for wet-sliced specimens were shown to have been significantly lower than dry-sliced specimens ($p<0.05$). Previous research pointed out that the polymerization progressed as soon as irradiation started to about 1 h after curing of the composite, and the polymerization then contined slowly to maximum at 24 h (Pilo, and Cardash, 1992), due to reduction in the number of active species trapped in polymer network during the reaction (Al-Ahdal, 2015). In the current research, the specimens were wet-sliced and polished within the 6 h at the stage where post-cure polymerisation was likely to have been significantly affect the result and the outcome was reduced DC and VHN. Therefore, the decrease observed for the wet sliced and polished specimens are likely because of both water and the absence of any heating effects during specimen preparation. It is likely that the lowest DC observed in this group of specimens is due to the abrasive removal of radicals under aquous conditions. Further research is required to confirm this hypothesis.

4.5 Effect of Slicing Procedure

The sixth objective of the hypothesis states that "the difference observed in DC and VHN values for specimens that are sliced (both wet & dry) and polished depend on process time between curing and preperation was upheld.

Figures 3.3 & 3.6 and Table 3.1- 3.2 revealed that when the dry-sliced & polished specimens (DSPS) at 6 & 24 h were compared to wet-sliced & polished specimens (WSPS) at 6 & 24 h for 1 - 4 mm thicknesses, a significant difference was observed in DC and VHN values; for *single point DC*, DSPS was 40 ± 13 % higher than WSPS for 6 h specimens and DSPS was 41 ± 14 % higher WSPS for 24 h specimens; for *mapped DC*, DSPS was 54 ± 6 % higher than WSPS for 6 h specimens and DSPS was 25 ± 11 % higher than WSPS for 24 h specimens; for *VHN values*, DSPS was 19 ± 3 % higher than WSPS for 6 h specimens and DSPS was 21 ± 5 % higher than WSPS for 24 h specimens. Thus, data suggests a significant effect of specimen preparation which has not been previously reported for DC. Research conducted by Nasoohi et al.2017, revealed the effect of dry and wet finishing on RBC materials. He studied effect of finishing on the surface roughness and hardness on the composite materials used. It was revealed that finishing techniques like slicing, grinding, and polishing without water coolant i.e., dry produced surfaces with increased hardness and roughness for micro hybrid was revealed i.e., dry. (Nasoohi, et al., 2017). The result obtained in the current research confirmed that dry slicing and polishing produced higher DC and VHN result in Figures 3.3 & 3.6 and Table 3.1-3.2.

The specimen surface area, when viewed under the SEM, revealed, clearly the state of the filler particles and the resin in Figure 3.12. Previous research pointed out that finishing procedure like slicing, grinding, and polishing removed matrix on top and around the filler particles which then left the filler particles exposed i.e., sticking out of the composite surface and this is what

resulted to the increased surface roughness and hardness result obtained (Gonçalves, et al., 2008) which was confirmed in the SEM images in Figure 3.12 of the current research. The effect of this surface structure was seen in the result of DC and VHN values obtained, which implies that specimen slicing i.e., specimen preparation, affected the DC and VHN result of the composite materials analysed. While the SEM images revealed the reason for the patchy effects obtained from the DC maps which point to the effect of diffused reflection on the specimens. Notwithstanding, Figures 3.4 – 3.5 showed the distribution of DC across the surface of the specimens, these maps obtained showed variation of DC values at various depths. The kinetic of polymerization is a complex phenomenon and the variation of DC and VHN values observed may be because of many factors which include a beam profile, transmission of light, scattering effects, the type of moulds used, and heat dissipation during irradiation and measurement. It has been established in other literature that polymerization process is a diffusion-controlled reaction, which involves the translational movement of the centres of gravity of active centres / species to a distance sufficiently small that reaction can be completed without further change in this distance (North and Benson, 1962). As a result of slicing and other finishing processes, the trapped active species present in the network moved slowly, thus resulting in the increase of DC and hardness values.

In addition, the low DC values obtained in Figures 3.4 – 3.5 may be due to initial temperature of the material. In this study, the monomer was not pre-heated and was used directly from the fridge. Daronch pointed out in a similar research that "when composite was polymerized at 3°C, system viscosity was apparently so great that maximum rate of polymerization occurred at less than 10% conversion, and final conversion was limited to values below 35%" (Daronch, 2006). This may be part of the reason for the low DC result obtained from some of the specimens, which is a confirmation of previous research study.

Appendix 2 showed the effect of Polishing Procedure

The result in Table 3.3 (Appendix 2.1) compared the DC and VHN values for non-sliced & non-polished and non-sliced & polished specimens. The processing difference between these two set of specimens was polishing and when non-sliced & non-polished specimens was compared to non-sliced & polished specimens, the effect of polishing revealed that the average mapped DC for non-sliced & non-polished specimens decreased by 16 ± 6 % than non-sliced & polished specimens at 1 – 4 mm depths, and there was no significant difference between the average hardness obtained for non-sliced & polished specimens and non-sliced & non-polished specimens at 1 – 4 mm depths.

CHAPTER FIVE

5.0 CONCLUSION

The following factors: post-irradiation time, thickness, slicing both wet and dry, and polishing which are elements of specimen preparation were studied during this project in respect to dental resin composite and the outcome revealed significant effect on the values of DC and hardness. This study has shown that experimental procedures during specimen measurements have a significant effect on the study outcomes. The study demonstrates the effect of slicing and polishing under wet and dry conditions where dry sliced specimens exhibited significantly higher DC and VHN values compared to wet non sliced specimens.

Better designed, controlled experiments that simulate clinical conditions will minimise these experimental artefacts and will improve reliability and reproducibilty to improve consistency between studies thatultimately may lead to clearer and better understanding of RBC cure characteristics, and performance. Evetually, these these may lead to the development of new novel RBC materials with better homogenous cure.

However, reserachers should be aware of the limitations of their study design and implement appropriate control measures to minimise experimental artefacts.

REFERENCE

3M, E., Filtek One, Filtek One Bulk Fill Technical Product 2016 Profile N.A.

Abouelnaga, M., A comparison of gingival marginal adaptation and surface microhardness of class II resin-based composites (conventional and bulk fill) placed in layering versus bulk fill techniques *Theses and Dissertations* 2014.

Adiguzel, O. & Cangul, S. The Latest Developments Related to Composite Resins. *International Dental Research*, 2017; 7:32-41.

Al-Ahdal, K., Ilie, N., Silikasa, N., and Watts, D. C. Polymerization kinetics and impact of post polymerization on the Degree of Conversion of bulk-fill resin-composite at clinically relevant depth. *Dental Materials*, 2015; 31:1207–1213.

Alrahlah, A., Silikas, N., & Watts, D. C.. Post-Cure Depth Of Cure Of Bulk Fill Dental Resin-Composites. *Dental Materials*, 2014; 30, 149-54.

Al-shaali, R., Salim, Z., Satterthwaite, J. D. and Silikasa, N. Post-irradiation hardness development, chemical softening, and thermal stability of bulk-fill and conventional resin-composites. *Journal of Dentistry*,2015; 43:209 – 218. 6.

Andrzejewska E. Photopolymerization kinetics of multifunctional monomers. *Progress in Polymer Science*, 2001; 26: 605–65.

Anseth, K.S, Anderson, K.J, Bowman, C.N. Radical concentration, environments, and reactivities during crosslinking polymerizations. *Macromolecular Chemistry Physics* 1996. 197:833-848.

Aravamudhan, K., Rakowski, D., and Fan P.L. Variation of depth of cure and intensity with distance using LED curing lights *Dental Materials* 2006 22 988-994

Arikawa, H., Takahashi, H. K., and Takahito, B., S. Effect of various visible light photoinitiators on the polymerization and colour of light-activated resins *Dental Materials Journal* 2009; 28 (4): 454–460.

Asmussen E. and Peutzfeldt A. Influence of UEDMA, Bis-GMA, and TEGDMA on selected mechanical properties of experimental resin composites. *Dental Materials* 1998; 14:51–6.

Atai, M. "Synthesis, characterization, shrinkage and curing kinetics of a new low-shrinkage

Ayub, K. V., Santos, G. C. Jr., Rizkalla, A. S., Bohay, R.; Pegoraro; L. F., José H. Rubo, M. Jacinta M. C., and Santos, D. Effect of Preheating on Microhardness and Viscosity of 4 Resin Composites. *Journal of the Canadian Dental Association* 2014;80: e12.

Azzopardi N., Moharamzadeh K., Wood D. J, Martin, NV.and Noort R. Effect of resin matrix composition on the translucency of experimental dental composite resins. *Dental Materials* 2009; 25:1564-1568.

Barszczewska-Rybarek, Izabela M."Characterization of urethane-dimethacrylate derivatives as alternative monomers for the restorative composite matrix", *Dental Materials*, 2014.

Barutcigil C., and Yildiz M. Intrinsic and extrinsic discoloration of dimethacrylate and silorane based composites. *Journal of Dentistry* 2012; 40: e57–63.

Barutcigil Ç., Barutcigil, K., €Ozarslan M. M, D€undar, A., and Yilmaz B. Color of bulk-fill composite resin restorative materials. *Journal of Esthetic Restorative Dentistry*; 2018; 30: E3–E8.

Bayne, S. et al., The evolution of dental materials over the past century: silver and gold to tooth colour and beyond. *Journal of Dental Research*, 2019. 98 (3), 257-265.

Beun S, Bailly C, Dabin A, Vreven J, Devaux J, and Leloup G. Rheological properties of experimental Bis-GMA/TEGDMA flowable resin composites with various macrofiller/microfiller ratio. *Dental Materials*, 2009; 25:198–205.

Bielawski, C. W.; Grubbs, R. H. "Living ring-opening metathesis polymerization". *Progress in Polymer Science*. 2007. 32 (1): 1–29.

Boaro L.C., Goncalves F., Guimaraes T.C., Ferracane J. L., Versluis A, & Braga R. R. Polymerization stress, shrinkage, and elastic modulus of current low-shrinkage restorative composites *Dental Materials*, 2010; 26(12) 1144-1150.

Boaro, L. et al., Clinical performance and chemical-physical properties of bulk fill composites resin—a systematic review and meta-analysis. Dental Materials Composite restorative materials: a review. *British Dental Journal*, 2019; 222(5), 337.

Bonilla, E.D., Hayashib, M., Pameijerc, C.H., Led, N.V., Morrowe, B.R., Garcia-Godoy, F. The effect of two composite placement techniques on fracture resistance of MOD restorations with various resin composites *Journal of Dentistry* 101 (2020) 103348

Bonsor, S J., and Pearson, G J. A clinical guide to applied dental materials. *Amsterdam: Elsevier/Churchill Livingstone*, 2013. 73–75.

Bouschlicher M.R., Rueggeberg F.A., & Wilson B.M. Correlation of bottom-to-top surface microhardness and conversion ratios for a variety of resin composite compositions *Operative Dentistry* 2004; 29 (6): 698-704.

Bowen R. L. Silica-resin direct filling material and method of preparation. *US Patents* 1965; 3.194.783 and 3.194.784.

Braga R.R., Boaro L.C., Kuroe T., Azevedo C.L., and Singer J.M. Influence of cavity dimensions and their derivatives (volume and 'C' factor) on shrinkage stress development and microleakage of composite restorations. *Dental Materials*, 2006; 22:818-823.

Braga, R.R. Yamamoto, T. Tyler, K. Boaro, L.C. Ferracane, J.L. andSwain, M.V. A comparative study between crack analysis and a mechanical test for assessing the polymerization stress of restorative composites, *Dental. Materials*. 2012; 28: 632–641.

Bucuta S. and Illie N. Light Transmittance and Micro-Mechanical Properties of Bulk Fill Vs Conventional Resin-Based Composite. *Clinical Oral Investigations*, 2014;18: 1991-2000.

Burrow M.F, Banomyong D, Harnirattisai C, Messer H.H. Effect of Glass-Ionomer Cement Lining on Postoperative Sensitivity in Occlusal Cavities Restored with Resin Composite—A Randomized Clinical Trial. *Operative Dentistry*, 2009; 34:648–55.

Burtscher P. Ivocerin in comparison to camphorquinone. *Ivoclar Vivadent Report*, No. 19; 2013;07: 13.

Burtscher, P. Stability of radicals in cured composite materials, *Dental Materials*. 1993; 9:218–221.

Chang, M., Dennison, J. & Yaman, P. Physical property evaluation of four composite materials *Operative Dentistry*, 2013, 38-5, E144-E153.

Chesterman, J.; Jowett, A.; Gallacher, A., and Nixon, P. Bulk-fill resin-based composite restorative materials: A review *British Dental Journal*, 2017; 222 (5): 337–344.

Clayden, J., Greeves, N. and Warren, S. Organic Chemistry, *Oxford University Press*, 2000; 1450–1466.

Clayden, Jonathan; Greeves, Nick; Warren, Stuart; Wothers, Peter. Organic Chemistry (1st ed.). *Oxford University Press*, 2001;.1450–1466.

Collares, F. M.; Fernando F. P., Vicente C., Branco L., Susana M., and Werner S. Discrepancies in degree of conversion measurements by FTIR; *Brazilian Oral Research* 2014; 02

Cook W.D. An Investigation of the Radiopacity of Composite Restorative Materials. *Australian Dental Journals*, 1981; 26(2):105-12.

Cowie, J.M.G. Polymers chemistry and physics of modern materials (3rd ed / J.M.G. Cowie and Valeria Arrighi ed.). *Boca Raton: Taylor & Francis*. 2007.

Daronch M, Rueggeberg F.A., and De Goes M.F. Monomer conversion of pre- heated composite. *Journal of Dental Research,* 2005; 84:663-667.

Daronch M, Rueggeberg F.A., De Goes M.F., and Giudici R. Polymerization kinetics of pre-heated composite. *Journal of Dental Research,* 2006; 85:38–43.

Daronch M., Rueggeberg F.A., De Goes M.F., and Giudici R. Polymerization kinetics of pre-heated composite. *Journal of Dental Research*, 2006; 85:38-43.

Darvell, B., Materials science for dentistry. Series in Biomaterials, *Woodhead publishing*. 2018; 3: 842.

Daugherty, M. et al., Effect of high-intensity curing lights on the polymerization of bulk-fill composites. *Dental Materials*, 2018; 34(10): 1531-1541.

Daugherty, M. M., Lien, W., Mansella, M. R., Risk, D. L.Savett, D. A., and Vandewalle, K. S. Effect of high-intensity curing lights on the polymerization of bulk-fill composites; *Dental Materials*, 2018.

Dewaele M., Asmussen E., Devaux J., and Leloup G. Class II restorations: influence of a liner with rubbery qualities on the occurrence and size of cervical gaps. *European Journal of Oral Sciences,* 2006; 114: 535 e41.

Dieckmann, P. et al., Light Transmittance and Polymerization of Bulk-Fill Composite Materials Doped with Bioactive Micro-Fillers. *Dental Materials*, 2019. 12(4), 4087.

Doerner MF, & Nix WD (1986) A method for interpreting the data from depth-sensing indentation instruments *Journal of Materials Research* 1(4) 601-609).

Dos Santos R.E., Lima A.F., Soares G.P., Ambrosano G.M., Marchi G.M, Lovadino J.R, et al. Effect of preheating resin composite and light-curing units on the microleakage of Class II restorations submitted to thermocycling. *Operative Dentistry*, 2011; 36(1):60-5.

Duarte, F. J. (1999). "Multiple-prism grating solid-state dye laser oscillator: optimized architecture". Applied Optics. 38 (30): 6347–6349.

Duda, A.; Kowalski, A., Thermodynamics and Kinetics of Ring Opening Polymerisation. In Handbook of Ring Opening Polymerisation; Dubois, P., Coulembier, O., Raquez, J-M., Eds.; *Wiley-VCH Verlag: Weinheim, Germany*, 2009; 1–51.

Durner J, Obermaier J, Draenert M, Ilie N. Correlation of the degree of conversion with the amount of elutable substances in nano-hybrid dental composites. *Dental Materials,* 2012; 28(11):1146–53.

Eibel, A. F., David E. and Gescheidt, G. Choosing the Ideal Photoinitiator for free radical photopolymerizations: predictions based on simulations using established data; *Polymer Chemistry*, 2018; 9:5107.

El-Saadany, A., El-Safty, S., Karim, U. & Kenawy, E. Reinforcing experimental resin-composites with synthesized zirconia and alumina nanofibers: evaluation of cuspal flexure, flexural strength, flexural modulus, and fracture toughness. *Tanta Dental Journal*, 2019; 16 (3): 149.

Eltaye, A. An in-vitro evaluation of the physical properties of a new bulk-fill composite. Magister Scientiae Dentium – *MSc (Dentistry) (Restorative Dentistry)*, 2017; 43.

Emami N., Sjodahl M., and Soderholm K. J. How filler properties, filler fraction, sample thickness and light source affect light attenuation in particulate filled resin composites. *Dental Materials* 2005; 21(8):721–730.

Ersen, K. A., Gürbüz, Ö. & Özcan, M., Evaluation of polymerization shrinkage of bulk-fill resin composites using microcomputed tomography. *Clinical oral investigations*, 2019;1-7.

Espelid I., Tveit A.B., Erickson R.L., Keck S.C, Glasspoole E.A. Radiopacity of Restorations and Detection of Secondary Caries. *Dental Materials,* 1991;7(2):114-7.

Evans, R. A., "The Rise of Azide–Alkyne 1,3-Dipolar 'Click' Cycloaddition and its Application to Polymer Science and Surface Modification". *Australian Journal of Chemistry*. 2007; 60 (6): 384–395.

Feilzer A.J, De Gee A.J., & Davidson C.L. Curing contraction of composites and glass-ionomer cements *Journal of Prosthetic Dentistry*, 1988; 59(3): 297-300.

Feilzer, A.J. Dooren, L.H. De Gee, A. J., and Davidson, C.L. "Influence of light intensity on polymerization shrinkage and integrity of restoration-cavity interface," *European Journal of Oral Sciences,* 1995; 5: 322–326.

Ferracane J.L., and Condon J.R. Post-cure heat treatments for composites: properties and fractography. *Dental Materials,* 1992; 8:290–5.

Ferracane JL, Condon JR. Post-cure heat treatments for composites: properties and fractography. Dent Mater 1992; 8:290–5.

Ferracane JL, Marker VA. Solvent degradation and reduced fracture toughness in aged composites. J Dent Res 1992; 71:13–9.

Ferracane, J. & Hilton, T., Polymerization stress–is it clinically meaningful? *Dental materials*, 2016; 32(1):1-10.

Fink, J. K. Acrylic Dental Fillers. Reactive Polymers: Fundamentals and Applications. (2018)

Flury, S., Hayoz, S., Peutzfeldt, A. Husler, Jand Lussia, A. Depth of cure of resin composites: Is the ISO 4049 method suitable for bulk fill materials? *Dental Materials* 2012; 28: 521–528.

Foreest A.W., Adhesive Dentistry with Direct Restorative Materials; *The Veterinary Quarterly*, Vol. 20, Supplement L, April 1998; S33-S34

Frauscher K.E, and Ilie N. Degree of conversion of nano-hybrid resin-based composites with novel and conventional matrix formulation. *Clinical Oral Investigations* 2013;17(2):635–42.

Fujita K, Ikemi T, and Nishiyama N. Effects of particle size of silica filler on polymerization conversion in a light-curing resin composite. *Dental Materials* 2011; 27(11):1079–1085.

Gajewski, V. E. S., Pfeifer, C. S. Fróes-Salgado, N. R. G. Boaro, L. C. C. and Braga, R. R. Monomers Used in Resin Composites: Degree of Conversion, Mechanical Properties and Water Sorption/Solubility *Brazil Dental Journal,* 2012; 23(5): 508-514.

Giachetti, L., Russo, D.S., Bambi, C., Grandini, R. A review of polymerization shrinkage stress: current techniques for posterior direct resin restorations, J. Contemp. Dent. Pract. 7 (2006) 1–13.

Gonçalves L, Filho J.D, Guimarães J.G, Poskus LT, Silva E.M. Solubility, salivary sorption, and degree of conversion of di-methacrylate-based polymeric matrixes. Applied Biomaterials *Journal of Biomedical Materials Research Part B,* 2008; 05: 85 (2):320-5.

Hadis et al., Inhomogenous curing wavelength distribution affects spatial photopolymerisation in multiple photoinitiator systems. European Conference, Brussels *Dental Materials* 2019; 6:1-22.

Hadis M, Tomlins P, Shortall A.C, and Palin W.M. Dynamic Monitoring of Refractive Index Changes Through Photoactive Resins. *Dental Materials*, 2010; 26: 1106-111.

Hadis M., Leprince J, Shortall A.C, Devaux J, Leloup G, and Palin W.M. High Irradiance Curing and Anomalies of Exposure Reciprocity Law in Resin-Based Materials. *Journal of Dentistry*, 2011. 39: 549-557.

Hadis M., Shortall A.C, Palin W.M. Competitive Light Absorbers in Photo-Active Dental Resin-Based Materials. *Dental Materials*, (2012). 28: 831-841.

Hageman, H. J. Photoinitiators For Free Radical Polymerization. *Progress in Organic Coatings*. 1985; 13 (2): 123–150.

Halasa, A. F. Recent Advances in Anionic Polymerization. *Rubber Chemistry and Technology,* 1981;54 (3): 627–640.

Hall, C., Polymer materials: an introduction for technologists and scientists. [s.l.] *Macmillan International Higher Education*. 2017.

Hamama, H. H. Recent advances in posterior resin composite restorations; Applications of Nanocomposite. *Materials in Dentistry*, 2019; 319-332.

Han, S. et al., Internal adaptation of composite restorations with or without an intermediate layer: effect of polymerization shrinkage parameters of the layer material. *Journal of Dentistry*, 2019;80: 41-48.

Hansen E. K. After-polymerization of visible light activated resins: surface hardness vs. light source. Scandinavia *Journal of Dental Research*, 1983;91(5):406–10.

Hein, C.D., Liu, X. & Wang, D. Click Chemistry, A Powerful Tool for Pharmaceutical Sciences. *Pharmaceutical Research*, 2008; 25, 2216–2230

Heshmat H, Hajian M, Hoorizad Ganjkar M, Emami Arjomand M. Effect of tea on color change of silorane and methacrylate based composite resins. *Journal Islam Dental Association Iran*. 2013;25(3):198–202.

Ilie, N. Impact of light transmittance mode on polymerization kinetics in bulk-fill resin-based composites. *Journal of dentistry*, 2017; 63: 51-59.

Instron-Corporation (2006) Operating Instructions: Instron Wilson-Wolpert Tukon 2100B Hardness Tester Instron Corp, Norwood, MA.

Islamova, R. M.; Puzin, Y. I.; Fatykhov, A. A.and Monakov, Y. B. A Ternary Initiating System for Free Radical Polymerization of Methyl Methacrylate. *Polymer Science, Series B*. 2006. 48 (3): 130–133.

ISO Standard 4049. Polymer-Based Filling, Restorative and Luting Materials. Technical Committee 106-Dentistry. *International Organization for Standardization*, 3rd edition Geneva, Switzerland; 2000: 1-27.

Jandt K.D, Mills R.W. A brief history of LED photopolymerization. *Dental Materials* 2013; 29:605–17.

Jestel, S., Marginal staining between pressed lithium disilicate ceramic crowns and direct restorative materials by various fluids: a microleakage study. *Electronic Theses and Dissertations*, 2019.

Johnston W.M, and Reisbick M.H. Colour and Translucency Changes During and After Curing of Esthetic Restorative Materials. *Dentistry Materials* 1997;13(2):89-97.

Joiner A. Tooth Colour: A Review of the Literature. *Journal of Dentistry*, 2004; 32:3-12.

Jung M, Sehr K, Klimek J. Surface texture of four nano-filled and one hybrid composite after finishing. *Operative Dentistry,.*2007;32(1):45-52.

Keaney, E., Shearer, J., Panwar, A. & Mead, J., Refractive index matching for high light transmission composite systems. *Journal of Composite Materials*, 2018. 52(24), pp. 3299-3307.

Khotbehsara M.M., et al. Polymer Degradation and Stability 170 (2019) 108-994.

Kim K.H, Park J.H, Imai Y, and Kishi T. Microfracture mechanisms of dental resin composites containing spherically shaped filler particles. *Journal of Dental Restoration*; 1994; 73:499–504.

Kim R.J, Kim Y.J, Choi N.S, & Lee I.B. Polymerization shrinkage, modulus, and shrinkage stress related to tooth-restoration interfacial debonding in bulk-fill composites *Journal of Dentistry,*2015; 43(4): 430-439.

Kiriy A., Stamm M., Polymer Science: A Comprehensive Reference Volume 1, 2012, Pages 367-386

Kleverlaan C.J., and Feilzer A.J., Polymerization shrinkage and contraction stress of dental resin composites. *Dental Material*; 2005, 21:1150–7.
Knock F.E, Glenn J.F. Dental Materials, *US Patent* No. 2,558,139, June 26, 1951; CA 46: 784f.

Kojic, D., The Efficacy of LED Light Polymerization Units in Private Dental Offices in Toronto. Canada: *Doctoral dissertation* 2018.

Kolb, H. C. Finn, M. G. and Sharpless, K. B. "Click Chemistry: Diverse Chemical Function from a Few Good Reactions". *Angewandte Chemie International Edition*. 2001; 40 (11): 2004 –2021.

Kroschwitz, Jacqueline I. (ed.), Encyclopedia of Polymer Science and Engineering, 2nd ed., 17 vol. (1985–90).

Kubisa, P.and Vairon, J.P. Cationic Ring Opening Polymerization of Cyclic Acetals. In Polymer Science: A Comprehensive Reference; Matyjaszewski, K., Möller, M., Eds.; *Elsevier BV: Amsterdam, the Netherlands*, 2012; 4:183–211.

Leach, M. R. "Radical Chemistry". *Chemo Genesis*. Retrieved 2 April 2010.

Lee S.Y. & Park S.H. Correlation between the amount of linear polymerization shrinkage and cuspal deflection. *Operative Dentistry*, 2006; 31(3): 364-370.

Lee Y.K. Influence of scattering/absorption characteristics on the colour of resin composites. *Dental Materials,* 2007; 23:124-131.

Lee Y.K., Influence of Filler on the Difference between the Transmitted and Reflected Colours of Experimental Resin Composites. Dental Materials; 2008, 24 (9):1243-7.

Lee Y.K., Lim B.S., Rhee S.H., Yang H.C., and Powers J.M. Colour and Translucency of A2 Shade Resin Composites after Curing, Polishing and Thermocycling. *Operative Dentistry*; 2005; 30 (4): 436-42.

Leon-Pineda, C. & Donly, K. Inhibition of Demineralization at Restoration Margins of Z100 and Tetric EvoCeram Bulk Fill in Dentin and Enamel. *Bioengineering*, 2019; 6(2):36.

Leprince J, Hadis M, Shortall A.C, Ferracane J. L, Devaux J, Leloup G, and Palin W.M. Photoinitiator Type and Applicability of Exposure Reciprocity in Filled and Unfilled Photoactive Resins. *Dental Materials*, 2011, 27: 157:164.

Leprince JG, Palin WM, Hadis MA, Devaux J, Leloup G Progress in dimethacrylate-based dental composite technology and curing efficiency. *Dental Material*, 2013; 29:139–156.

Leprince, J.G. Hadis, M. Shortall, A.C. Ferracane, J.L. J. Devaux, J. G. Leloup, J.G. and Palin W.M. Photoinitiator type and applicability of exposure reciprocity law in filled and unfilled photoactive resins; *Dental Materials,* 2011; 27 157–164.

Lins, R. et al., Polymerization Shrinkage Evaluation of Restorative Resin-Based Composites Using Fiber Bragg Grating Sensors. *Polymers*, 2019;11(5); 859.

Lopes G.C., Franke M, and Maia H.P. Effect of finishing time and techniques on marginal sealing ability of two composite restorative materials. *Journal Prosthetic Dentistry* 2002; 88(1):32-6.

Lowe, Andrew B. Thiol-Ene "Click" Reactions and Recent Applications in Polymer and Materials Synthesis. *Polymer Chemistry*, 2010; 1 (1):17–36.

Lundin S.A, and Koch G. Cure profiles of visible light-cured class II composite restorations in vivo and in vitro. *Dental Materials*; 1992, 8:7-9.

Maghaire, G. et al., Effect of thickness on light transmission and vickers hardness of five bulk-fill resin-based composites using polywave and single-peak light-emitting diode curing lights. *Operative dentistry*, 2019; 44(1), pp. 96-107.

Maghaireh, G.A., Taha, N.A. and Alzraikat, H., The Silorane-based Resin Composites: A Review; *Operative Dentistry*, 2017; 42-1, E24-E34.

Mahoney E, Holt A, Swain M, & Kilpatrick N (2000) The hardness and modulus of elasticity of primary molar teeth: an ultra-micro-indentation study *Journal of Dentistry* 28(8) 589-594.

Martos J, Osinaga P, Oliveira E, Castro L. Hydrolytic degradation of composite resins: effects on the microhardness. Mater Res 2003; 6:599–604.

Matsukawa S, Hayakawa T, Nemoto K. Development of high-toughness resin for dental applications. *Dental Materials,* 1994; 10, 343-346.

Moad, G. and Solomon, D. H. The Chemistry of Radical Polymerization. 2nd Edition. *Elsevier* 2006

Mohamad D, Young R.J, Mann A.B., and Watts DC. Post-polymerization of dental resin composite evaluated with nano-indentation and micro-Raman spectroscopy. *Archives of Orofacial Sciences*, 2007; 2:26–31.

Moloney, A.C., Kausch, H.H., Kaiser, T., Beer, H.R. Parameters determining the strength and toughness of particulate filled epoxide resins, J. Mater. Sci. 22 (2) (1987) 381-393.

Moore B.K, Platt J.A, Borges G, Chu T-M G., and Katsilieri I. Depth of Cure of Dental Resin Composites: ISO 4049 Depth and Microhardness of Types of Material and Shades, *Operative Dental,* 2008; 33-4, 408-412.

Moorthy, A. et al. Cuspal deflection and microleakage in premolar teeth restored with bulk-fill flowable resin-based composite base material. *Journal of Dentistry*, 2012; 40(6), 5.

Moraes R.R., Gonçalves L.S., Lancellotti A.C., Consani S., Correr-Sobrinho L, and Sinhoretti M.A. Nanohybrid Resin Composites: Nanofiller Loaded Materials of Traditional Micro-hybrid Resins. *Operative Dentistry*; 2009; 34: 551-557.

Moszner N, Fischer UK, Ganster B, Liska R, Rheinberger V. Benzoyl germanium derivatives as novel visible light photoinitiators for dental materials. *Dental Materials*, 2008; 24:901–7.

Moszner N, Volkel T, Fischer UK, Klester A, and Rheinberger V. Synthesis, and polymerization of new multifunctional Urethane methacrylates. *Die Angewandte Makromolekulare Chemie*, 1999; 265(1):31–5.

Musanje L, and Darvell B.W. Curing-light attenuation in filled resin restorative materials. *Dental Materials* 2006; 22(9):804–817.

Nasoohi, N. H., Maryam T., and Seyedeh F.. Effects of Wet and Dry Finishing and Polishing on Surface Roughness and Microhardness of Composite Resins. *Journal of Dentistry*, 2017; 14, 2.

Neumann M.G, Schmitt C.C, Ferreira G.C, and Correa I.C., The initiating radical yields and the efficiency of polymerisation for various dental photoinitiators excited by different light curing units. *Dental Materials*; 2006; 22: 576-584.

Neumann M.G., Miranda W.G. Jr, Schmitt C.C., Rueggeberg F.A., and Correa I.C. Molar Extinction Coefficients and The Photon Absorption Efficiency of Dental Photoinitiators and Light Curing Units. *Journal Dentistry*, 2005;33(6):525-32.

Neumann, M. G.. Molar Extinction Coefficients and the Photon Absorption Efficiency of Dental Photoinitiators and Light Curing Units. *Journal of Dentistry*, 2005; 33; 525-532.

Nikolaidis, A., Koulaouzidou, E., Gogos, C. & Achilias, D., Synthesis and characterization of dental nanocomposite resins filled with different clay nanoparticles. *Polymers*, 2019; 11(4): 730.

Nilsson, C., Simpson, N., Malkoch, M., Johansson, M., and Malmström, E. "Synthesis and thiol-ene photopolymerization of allyl-ether functionalized dendrimers". Polymer Chemistry *Journal of Polymer Science Part A*, 2008; 46 (4): 1339–1348.

Noort, R.N. (2007) Introduction to Dental Materials. 3rd Edition, Mosby Elsevier, London, UK.

Nuyken O. and Pask, S. D. Ring-Opening Polymerization—An Introductory Review. *Polymers* 2013; 5, 361-403.

O'Brien, et al., Dental Materials and Their Selection, Fourth Edition, *Quintessence Publishing company, Incorporation* 2008.

Odian, G. Principles of polymerization (4. ed.). Hoboken, New Jersey: *Wiley Inter-science.* 2004.

Ogunyinka, A. Palin, W.M. Shortall, A.C. and Marquis. P.M. Photoinitiation chemistry affects light transmission and degree of conversion of curing experimental dental resin composites. *Dental Materials,* 2007;23: 807-813.

Ottaviani, M.F. Fiorini, A. Mason, P.N. andCorvaja, C. Electron spin resonance studies of dental composites: effects of irradiation time decay over time, pulverization, and temperature variations, *Dental Materials*. 1992; 8: 118–124.

Palin W.M, Fleming G.J.P, Burke F.J.T, and Randall R.C. Monomer conversion versus flexure strength of a novel dental composite. *Journal of Dentistry*, 2003; 31: 341-351.

Palin W.M, Leprince J.G, and Hadis M.A. Shining a Light on High Volume Photocurable Materials. *Dental Materials*, 2018. 34: 695-710.

Papadopoulos, C. et al., Structural Integrity Evaluation of Large MOD Restorations Fabricated with a Bulk-Fill and a CAD/CAM Resin Composite Material. *Operative dentistry*, 2019. 44(3):312-321.

Par, M., Gamulin, O., Marovic, D., Klaric, E. & Tarle, Z.. Effect Of Temperature On Post-Cure Polymerization Of Bulk-Fill Composites. *Journal of Dentistry* 2014; 42, 1255-60.

Paravina R.D, Kimura M.and Powers J.M. Evaluation of Polymerization Dependent Changes in Colour and Translucency of Resin Composites Using Two Formulae. *Odontology* 2005;93(1):46-51.

Peutzfeldt, A. Resin composites in dentistry: the monomer systems. *European Journal of Oral Science*. 1997; 105(2):97-116.

Piccoli, Y. et al., Optical Stability of High-translucency Resin-based Composites. *Operative Dentistry*, 2019; 44(5): 536-544.

Pilo R, and Cardash H.S. Post-irradiation polymerization of different anterior and posterior visible light-activated resin composites. *Dental Materials* 1992; 8 (5):299–304.

Podgorski M., Becka E., Claudino M., Shah P.K., Stansbury J.W.and Bowman C.N. Ester-free thiol-ene dental restoratives-part A: resin development. *Dental Materials*; 2015, 31:1255–62.

Poggio C, Chiesa M, Scribante A, Mekler J, and Colombo M. Microleakage in Class II composite restorations with margins below the CEJ: In vitro evaluation of different restorative techniques. *Medicina Oral, Patologia Oral, Cirugia Bucal,* 2013; 18: 793-98.

Pojman, J. A.; Willis J.; Fortenberry D.; Ilyashenko V.; and Khan A. M. "Factors Affecting Propagating Fronts of Addition Polymerization: Velocity, Front Curvature, Temperature

Profile, Conversion, And Molecular Weight Distribution". Polymer Chemistry *Journal of Polymer Science Part A*: 1995; 33 (4): 643–652.

Polanský, R., Mentlík, V., Prosr, P., Susír, J. Influence of thermal treatment on the glass transition temperature of thermosetting epoxy laminate, *Polymer Test*. 28 (4) (2009) 428-436.

Posner, T. "Beiträge Zur Kenntniss Der Ungesättigten Verbindungen. II. Ueber Die Addition Von Mercaptanen An Ungesättigte Kohlenwasserstoffe" (PDF). *Berichte Der Deutschen Chemischen Gesellschaft*. 1905. 38 (1): 646–657.

Powers J.M., and Sakaguchi R.L. Restorative Dental Materials. 12th edition St. Louis: Mosby; 2006.

Price R.B, and Felix C.A. Effect of delivering light in specific narrow bandwidths from 394 to 515 nm on the microhardness of resin composites. *Dental Materials*, 2009; 25: 899–908.

Price R.B, Whalen J.M, Price T.B, Felix C.M, and Fahey J. The effect of specimen temperature on the polymerization of a resin-composite. *Dental Materials* 2011; 27: 983–9.

Price R.B.T, Rueggeberg F.A, Labrie D, and Felix C.M. Irradiance Uniformity and Distribution from Dental Light Curing Units *Journal of Esthetic and Restorative Dentistry,* 2010; 22: 86:103.

Price, R. B, and Felix, C. A. Effect of delivering light in specific narrow bandwidths from 394 to 515 nm on the micro-hardness of resin composites. *Dental Materials* 2009. 25:899-908.

Price, R. B. T., Corey A. F.and Pantelis A., Evaluation of a second- generation LED curing light. *Journal of the Canadian Dental Association* 2003; 11: 666a -666g.

Pulickel, M.A., Linda S.S and Paul V.B. Nanocomposite science and technology. Weinheim, FRG: *Wiley-VCH Verlag GmbH & Co. KGaA*, 2004.

Randolph et al., Filler characteristics of modern dental resin composites and their influence on physico-mechanical properties. *Dental Materials* 2016, 1586-1599.

Randolph L.D, Palin W.M, Bebelman S, Devaux J, Gallez B, and Leloup G, Ultra-fast light-curing resin composite with increased conversion and reduced monomer elution. *Dental Material*; 2014 30:594–604.

Reinelt S, Tabatabai M, Moszner N, Fischer UK, Utterodt A, and Ritter H. Synthesis and photopolymerization of thiol-modified triazine-based monomers and oligomers for the use in thiol–ene-based dental composites. *Macromolecular Chemistry Physics*; 2014, 215:1415–25.

Rivera-Torres, F. and Vera-Graziano, R Effects of Water on the Long-Term Properties of Bis-GMA and Silylated-(Bis-GMA) Polymers *Journal of Applied Polymer Science* 2008; 107: 1169–1178.

Robert G. C., Dieter W., Josef R., Klaus G. K., Klaus-Peter S., Klaus D., Hans-Joachim R., Gertraute F., Klaus M. L., and Matthias B. "Dental Materials". Weinheim: Wiley *Ullmann's Encyclopaedia of Industrial Chemistry,* 2006.

Rocha, R. M. Oliveira, D. D'Antonio, T. Qian, F and Skiff, F. Comparison of light-transmittance in dental tissues and dental composite restorations using incremental layering build-up with varying enamel resin layer thickness. *Restorative Dentistry & Endodontics*. 2018; 05; 43 (2): e22.

Rodd, H. D. Waterhouse, P. J. Fuks, A. B. Fayle S. A. & Moffat, M. A. Pulp Therapy for Primary Molar. *International Journal of Paediatric Dentistry* 2006; 8 (2): 113-117

Rueggeberg FA. State-of-the-art: dental photocuring – A review. *Dental Material* 2011; 27:39–52.

Rueggeberg, F. A., Giannini, M., Arrais, C. A. G. & Price, R. B. T. Light curing in dentistry and clinical implications: a literature review. *Brazil Oral Restorations*, 2017; 31, e 61.

Ruyter I.E., and Nilsen J Chemical characterization of six posterior composites (abstract). *Journal of Dental Research* 1993; 72::177.

Ruyter I.E., and Svendsen S.A. Remaining methacrylate groups in composite restorative materials. *Acta Odontologica Scandinavica*, 1978; 36: 75-82.

Santos J.N, Carrilho M.R, De Goes M.F, Zaia A.A, Gomes B.P, Souza-Filho F.J, et al. Effect of chemical irrigants on the bond strength of a self-etching adhesive to pulp chamber dentin. *Journal of Endodontics*,2006; 32:1088–90.

Sartori, N. et al., Effects of Light Attenuation through Dental Tissues on Cure Depth of Composite Resins. *Acta Stomatologica Croatica*, 2019;53(2), 95.

Satterthwaite, J. D. Maisuria, A. Vogel, K. and Watts, D. C. Effect of resin-composite filler particle size and shape on shrinkage-stress. *Dental Materials*.2012; 2 8: 609–614.

Schneider, L. Felipe J. Cavalcante, L. M. and Silikas N. Shrinkage Stresses Generated during Resin-Composite Applications: A Review *Journal of Dental Biomechanics* 2010; 131- 630:14.

Schwalm, R. Science and Technology *International Encyclopaedia of Materials:* , 2001 Scientific documentation Tetric EvoCeram Bulk Fill. Schaan, Liechtenstein: *Ivoclar Vivadent*; 2014;42.

Shah, M. B., Ferracane, J. L., Kruzic, J. J. R-curve behaviour and toughening mechanisms of resin-based dental composites: Effects of hydration and post-cure heat treatment dental materials 2 5 (2009) 760–770

Shah, P. K., Stansbury, J. W. & Bowman, C. N. Application of an addition–fragmentation-chain transfer monomer in di(meth)acrylate network formation to reduce polymerization shrinkage stress. *Polymer Chemistry*, 2017, 8, 4339-4351.

Shorthall A.C, Palin W.M, Burtscher P. (2008). Refractive index mismatch and monomer reactivity influence composite curing depth. Journal of Dental Research, 87: 84-88.

Shriver, D.F. Atkins, P. W.' Inorganic Chemistry, 4th edition, *Oxford University Press*, Oxford 2006, pp. 189-190.

Sideridou, I. Tserki, V. andPapanastasiou, G. Study of water sorption, solubility, and modulus of elasticity of light-cured dimethacrylate-based dental resins, *Biomaterials* 2003; 24 (4): 655–665.

Soares, C. J., Rodrigues, M. P., Oliveira, L. R. S., Braga, S. S. L., Barcelos, L. M., Silva, G. R. D., Giannini, M. & Price, R. B. An Evaluation of the Light Output from 22 Contemporary Light Curing Units. *Brazil Dentistry Journal*, 2017, 28, 362-371.

Sobhi, H. Synthesis and Characterization Acylphosphine Oxide Photoinitiators. *Electronic Thesis or Dissertation*, 2008.

Stannard J.G, Sornkul E, Collier R Mechanical properties of composite resin co-polymers (abstract) *Dental Restorations*,1993;.72 :135.

Stansbury, J. W. Dimethacrylate network formation and polymer property evolution as determined by the selection of monomers and curing conditions *Dental Materials* 2012;28(1): 13–22.

Stansbury, J.W. & Dickens, S.H. Determination of double bond conversion in dental resins by near infrared spectroscopy. *Dental Materials*, 2001, 17, 71-9.

Stansbury, J.W. and Bailey W.J., Evaluation of spiro orthocarbonate monomers capable of polymerization with expansion as ingredients in dental composite materials, in: C.G. Gebelein, R.L. Dunn (Eds.), *Progress in Biomedical Polymers*, Plenum Press, New York, 1990; 133–139.

Stevens M.P. Polymer Chemistry: An Introduction, Hartford, *Oxford University Press*. 2001.
Tarumi H, Imazato S, Ehara A, Kato S, Ebi N, Ebisu S. Post-Irradiation Polymerization of composites containing Bis-GMA and TEGDMA. *Dental Materials* 1999; 15:238–42.

Tauböck, T. et al., Genotoxic potential of dental bulk-fill resin composites. *Dental Materials*, 2017. 33(7):788-795.

Thomas, C. Comparison of Visual and Instrumental Shade Matching. s.l.: *Doctoral Dissertation*, 2019. The University of Texas School of Dentistry at Houston

Thomas, C. D., 2019 Comparison of Visual and Instrumental Shade Matching *Doctoral Dissertation*, The University of Texas School of Dentistry at Houston.

Trujillo M., and Stansbury J.W. Use of Near-IR to monitor the influence of external heating on dental composite photopolymerization. *Dental Materials* 2004; 20:766-777.

Tsai C.S.J., White D., Rodriguez H, et al. Exposure assessment and engineering control strategies for airborne nanoparticles: an application to emissions from nanocomposite compounding processes. *Journal of Nanoparticle Research*, 2012; 14: 989.

Turssi C.P, Ferracane J.L, and Vogal K. Filler Features and their effects on wear and degree of conversion of particulate dental resin composites. *Biomaterials*, 2005; 26: 4932-4937.
urethane dimethacrylate monomer for dental applications", *Dental Materials*, 2007; 08

Valizadeh, S., Asiaie, Z., Kiomarsi, N., Kharazifard, M. J., Color stability of self-adhering composite resins in different solutions, *Dental Medical Problems.* 2020;57(1):31–38

Van Dijken, J.W., Durability of resin composite restorations in high C-factor cavities: a 12-year follow-up, J. Dent. 38 (2010) 469–474.

Voigt, M., Legner, R., Haefner, S., Friesen, A., Wirtz, A. & Jaeger, M. Using fieldable spectrometers and chemometric methods to determine RON of gasoline from petrol stations: A comparison of low field 1H NMR@ 80 MHz, hand-held RAMAN, and benchtop NIR. *Fuel*, 2019; 236, 829-835.

Voit, B. New developments in hyperbranched polymers. Polymer Chemistry *Journal of Polymer Science*, 2000; 38, 2505–2525.

Voyiadjis, G. & Yaghoobi, M. Review of Nanoindentation Size Effect: Experiments and Atomistic Simulation. *Crystals*, 2017; 7.

Wang et al 'An In Vitro Screening assay for dental stain in cleaning' *BMC Oral Health* 2017; 9:17(1):37.

Watts D.C, Amer O.M, Combe E.C. Surface hardness development in light-cured composites. *Dental Materials,* 1987; 3(5):265–9.

Weinmann W, Thalacker C, & Guggenberger R Siloranes in dental composites *Dental Materials*, 2005; 21(1): 68-74.

Westland S. Review of the CIE System of Colorimetry and Its Use in Dentistry. *Journal Esthetic Restorative Dental* 2003;15: S5-12.

Wu, W. and Fanconi, B. M. Post-curing of dental restorative resin; *Society of Plastics Engineers, Inc.* 2009; 983.

Xu HHK. Long-term water-aging of whisker-reinforced polymer-matrix composites. J Dent Res 2003; 82:48–52.

Yamaguchi R, Powers J.M, and Dennison J.B Thermal expansion of visible-light-cured composite resins. *Operative Dentistry* 1989; 14: 64-67.

Yap A. U, Soh M.S and Siow K.S. Effectiveness of composite cure with pulse activation and soft-start polymerization *Operative Dentistry*, 2002; 27 (1): 44-49.

Yeli, M. Kidiyoor.K.H. Balaram, N. and Pradeep K.; Recent Advances in Composite Resins-A Review; *Annals and Essences of Dentistry*, 2010; 3 :7 – 9.134.

Yin, R., Suh, B. I,. Sharp, L. and Tiba, A. Low shrinkage dental composite. *US Patent* 6 709 271, assigned to Bisco, Inc., Schaumburgh, IL, Mar. 23, 2004.

Yu, B., and Lee Y.K. Translucency of Varied Brand and Shade of Resin Composites. *American Journal of Dentisry,* 2008; 21(4): 229-32.

Yu, Q. Nauman S., Santerre J.P., and Zhu S. U.V. Photopolymerization Behaviour of Dimethacrylate Oligomers with Camphorquinone/Amine Initiator System, *Journal of Applied Polymer Science*. 2001; 82:1107-1117.

Zhang, M., June, S.M. & Long, T.E. Principles of Step-Growth Polymerization (Polycondensation and Polyaddition) *Polymer Science: A Comprehensive Reference*, Volume 5, 2012, Pages 7-47.

Zhou, X., Huang, X., Li, M., Peng, X., Wang, S., Zhou, X., Lei Cheng, L. Development, and status of resin composite as dental restorative materials. *Journal of Applied Polymer Science*. 2019; 48180 (1) – 48180 (12).

APPENDIX 1

```
Sub ImportCSVsWithReferenceI()

' selectshe Macro
  Sheets("Sheet1").Select
  ActiveWindow.SmallScroll Down:=-3
  Range("A1").Select

'Import function_Updated byMH
   Dim xSht  As Worksheet
   Dim xWb As Workbook
   Dim xStrPath As String
   Dim xFileDialog As FileDialog
   Dim xFile As String
   Dim xCount As Long
   On Error GoTo ErrHandler
   Set xFileDialog = Application.FileDialog(msoFileDialogFolderPicker)
   xFileDialog.AllowMultiSelect = False
   xFileDialog.Title = "Select a folder [documents]"
   If xFileDialog.Show = -1 Then
   xStrPath = xFileDialog.SelectedItems(1)
   End If
   If xStrPath = "" Then Exit Sub
   Set xSht = ThisWorkbook.ActiveSheet
   If MsgBox("Clear the existing sheet before importing?", vbYesNo, "import") = vbYes
Then
    xSht.UsedRange.Clear
     xCount = 1
    Else
     xCount = xSht.Cells(3, Columns.Count).End(xlToLeft).Column + 1
    End If
```

```
Application.ScreenUpdating = False
 xFile = Dir(xStrPath & "\" & "*.csv")
 Do While xFile <> ""
 Set xWb = Workbooks.Open(xStrPath & "\" & xFile)
 Rows(1).Insert xlShiftDown
 Range("A1") = ActiveSheet.Name
 ActiveSheet.UsedRange.Copy xSht.Cells(1, xCount)
 xWb.Close False
 xFile = Dir
  xCount = xSht.Cells(3, Columns.Count).End(xlToLeft).Column + 1
  Loop
  Application.ScreenUpdating = True
  ErrHandler:

' full range select and convert to number and 5dp
    Cells.Select
    Selection.NumberFormat = "0.00000"
    Range("A1").Select
    Sheets("Sheet2").Select
    Range("A1").Select
    ActiveCell.FormulaR1C1 = "Wavenumber (cm-1)"
    Range("A2").Select
    ActiveCell.FormulaR1C1 = "=Sheet1!RC"
    Range("A2").Select
    Selection.AutoFill Destination:=Range("A2:A16"), Type:=xlFillDefault
    Range("A2:A16").Select
    Selection.AutoFill Destination:=Range("A2:A19"), Type:=xlFillDefault
    Range("A2:A19").Select
    Range("A19").Select
    Selection.ClearContents
    Columns("A:A").Select
    Selection.Font.Bold = True
Range("A19").Select
```

```
 Sheets("Sheet1").Select

'UPDATE range here depending on map dimensions
Range("A1:GK1").Select
Application.CutCopyMode = False
Selection.Cut
Range("B1").Select
ActiveSheet.Paste
Range("A1").Select
ActiveCell.FormulaR1C1 = "Wavenumber (cm-1)"
Range("A2").Select
Columns("A:A").Select
Selection.Font.Bold = True
Selection.Font.Bold = True

'Range select
Dim rng As Range
Dim InputRng As Range
Dim OutRng As Range
Dim xInterval As Integer
xTitleId = "Data Range Select from column B"
Set InputRng = Application.Selection
Set InputRng = Application.InputBox("Range :", xTitleId, InputRng.Address,
Type:=8)
xInterval = Application.InputBox("Enter column interval (always 1)", xTitleId,
Type:=1)
For i = 1 To InputRng.Columns.Count Step xInterval + 1
Set rng = InputRng.Cells(1, i)
 If OutRng Is Nothing Then
 Set OutRng = rng
 Else
 Set OutRng = Application.Union(OutRng, rng)
 End If
```

```
Next
OutRng.EntireColumn.Select

 Selection.Copy
 Sheets("Sheet2").Select
 Range("B1").Select
 ActiveSheet.Paste

End Sub
```

APPENDIX 2

THE COMPARISON OF NON-SLICED & NON-POLISHED SPECIMENS AND NON-SLICED & POLISHED SPECIMENS

APPENDIX 2.1 Degree of Conversion by FT-IR Microscopy

Figure 3.25 shows the mapped DC data of non-sliced & non-polished (NSNP) and non-sliced, & polished (NSP) specimens, measured within 6 h after curing using a FT-IR Microscope. The average DC data in Table 3.3 and Figure 3.26 revealed significant difference between the average DC against depths with 1 mm depth having the highest DC and 4 mm having the least DC and, there was significant difference between the means of NSPS and NSNP at 1 – 4 mm depths ($p<0.05$) in Table 3.3.

Thickness	Non-Sliced & Non-Polished	Non-Sliced but Polished
	Mean (DC)	Mean (DC)
1 mm	75 (1.89)^{a}	53 (8.6)^{ab}
2 mm	55 (4.0)^{b}	42 (4.1)^{bc}
3 mm	55 (6.5)^{b}	58 (10)^{ab}
4 mm	43 (5.5)^{c}	45 (7.6)^{bc}

Table 3.3: The average values of measured 16 points at the central part of the mapped DC of NSNP and NSPS. Significant difference existed between the means of both group categories of specimens at various depths ($p<0.05$). The numbers in bracket represents the standard deviation and the letters are the post-hoc Tukey comparison result. Significant difference determined by one-way ANOVA and post hoc Tukey comparisons ($p<0.05$) are represented in ascending alphaphetical order from high to low within each group.

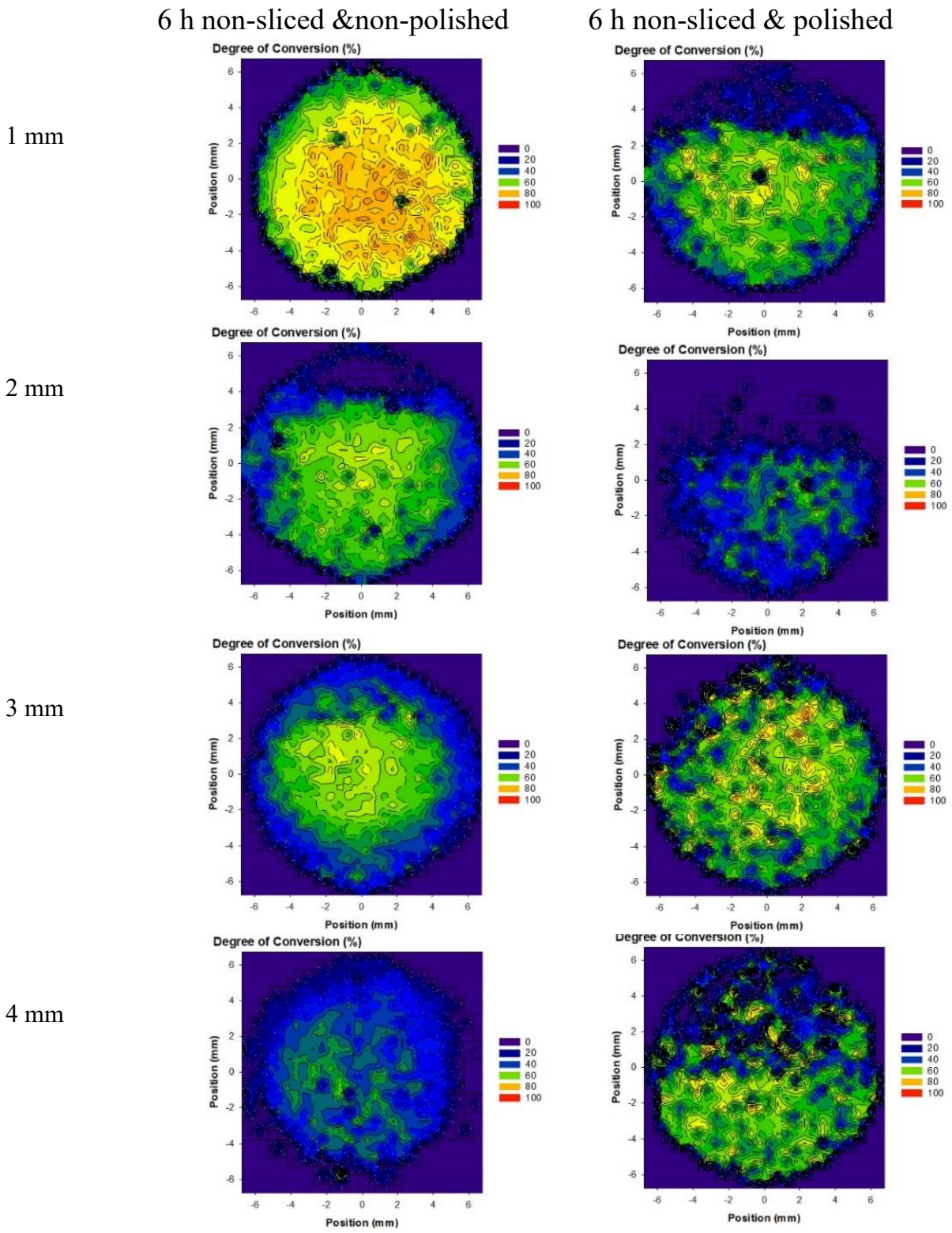

Figure3.25: NSNP specimens DC spread more on the surface area for 1 mm & 2 mm as compare to NSP specimens' counterpart. On the other hand, the non-sliced & polished specimens DC spread more on the surface area for 3 mm & 4 mm than DC for than for NSNP specimens. The colour scales represent DC.

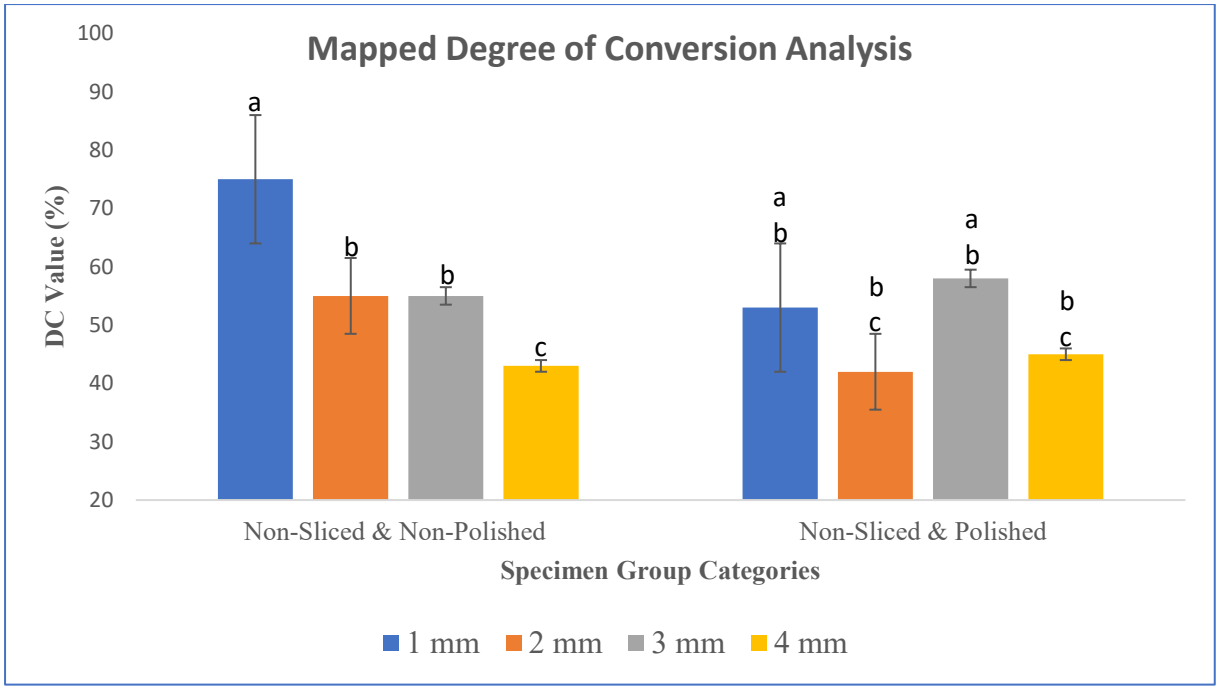

Figure 3.26: Average mapped DC values plot of Filtek^{TM}One bulk fill restorative (A2) shade material, measured within 6 h after irradiation. The plot shows clear trends of decreasing DC as the depth increases 1 - 4 mm. Significant difference determined by one-way ANOVA and post hoc Tukey comparisons ($p<0.05$) are represented in ascending alphaphetical order from high to low within each group.

APPENDIX 2.2 Longitudinal and Latitudinal Micro-Hardness Analysis

Figure 3.27-3.30 showed the results of micro-hardness plot for non-sliced & non-polished and non-sliced but polished specimens at 1 – 4 mm depths respectively, measured within 6 h of curing. The plot compared the values of the micro hardness across the surface of the specimen from one end to the other at various depths. The statistical analysis of the data shown in Table 3.4 revealed there was no significant difference between the means of the VHN values obtained for NSNP and NSP specimens at 1 - 2 mm depths. On the other hand, there was significant difference between the means of the VHN values at 3- and 4-mm depths ($p<0.05$) for both group category.

Average values of Micro-Hardness (VHN) for (1 - 4 mm) depths		
Specimen Depth	**non-sliced, non-polished**	**non-sliced, but polished**
1 mm	67 (4.0)[b]	68 (2.43)[a]
2 mm	67 (5.0)[b]	67 (2.64)[a]
3 mm	62 (4.4)[b]	62 (4.03)[b]
4 mm	53 (5.3)[b]	53 (3.8)[b]

Table 3.4: Average values of micro-hardness of NSNP and NSP specimens at 1 - 4 mm depths, measured within 6 h after irradiation. The numbers in bracket are the standard deviation and significant difference determined by one-way ANOVA and post hoc Tukey comparisons in ascending alphaphetical order from high to low within each group.

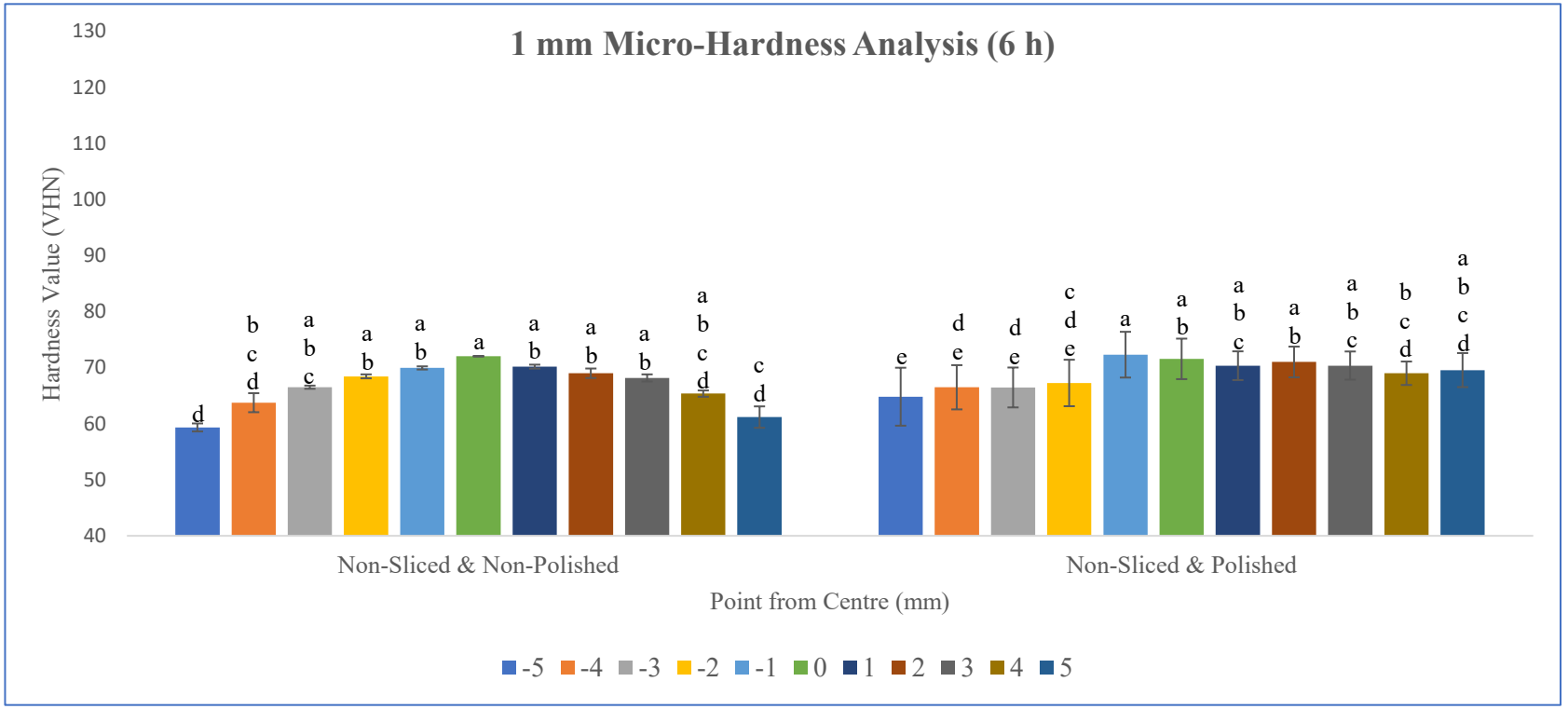

Figure 3.27: Non-sliced, non-polished hardness versus non-sliced but polished micro-hardness plots at 1 mm depths analysed within 6 h of irradiation. There was significant difference between the means of VHN within the group of specimens ($p<0.05$). The comparison among the group categories revealed there was no significant difference between the means of the groups at 1 mm depth ($p>0.05$). Significant difference determined by one-way ANOVA and post hoc Tukey comparisons in ascending alphaphetical order from high to low within each group.

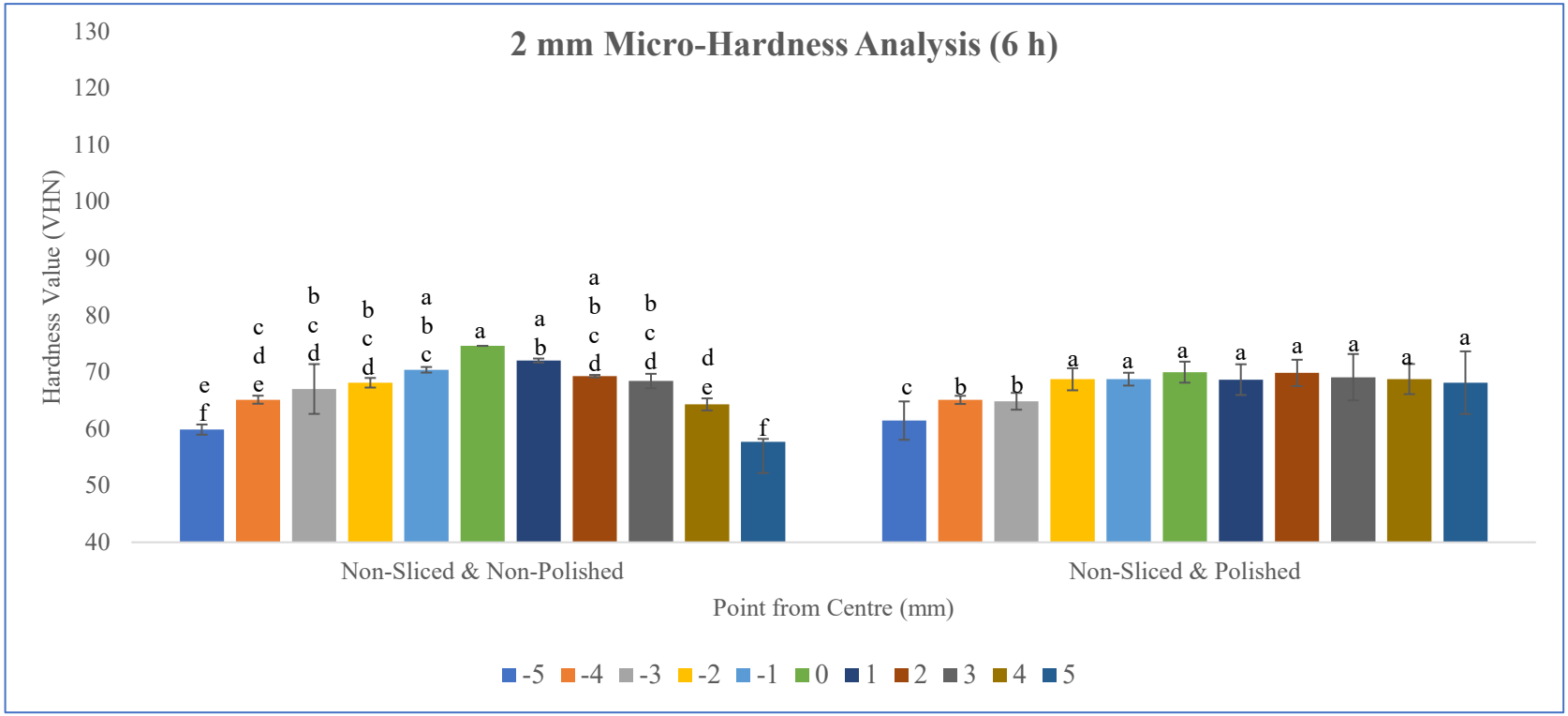

Figure 3.28: Non-sliced, non-polished hardness versus non-sliced but polished micro-hardness plots at (2 mm) depths, analysed within 6 h of irradiation. There was significant difference between the means of NSNP specimens ($p<0.05$), there was no significant difference between the means of NSP specimens ($p>0.05$). The comparison among the group categories revealed there was no significant difference between the means of hardness ($p>0.05$). Significant difference determined by one-way ANOVA and post hoc Tukey comparisons are represented in ascending alphaphetical order from high to low within each group.

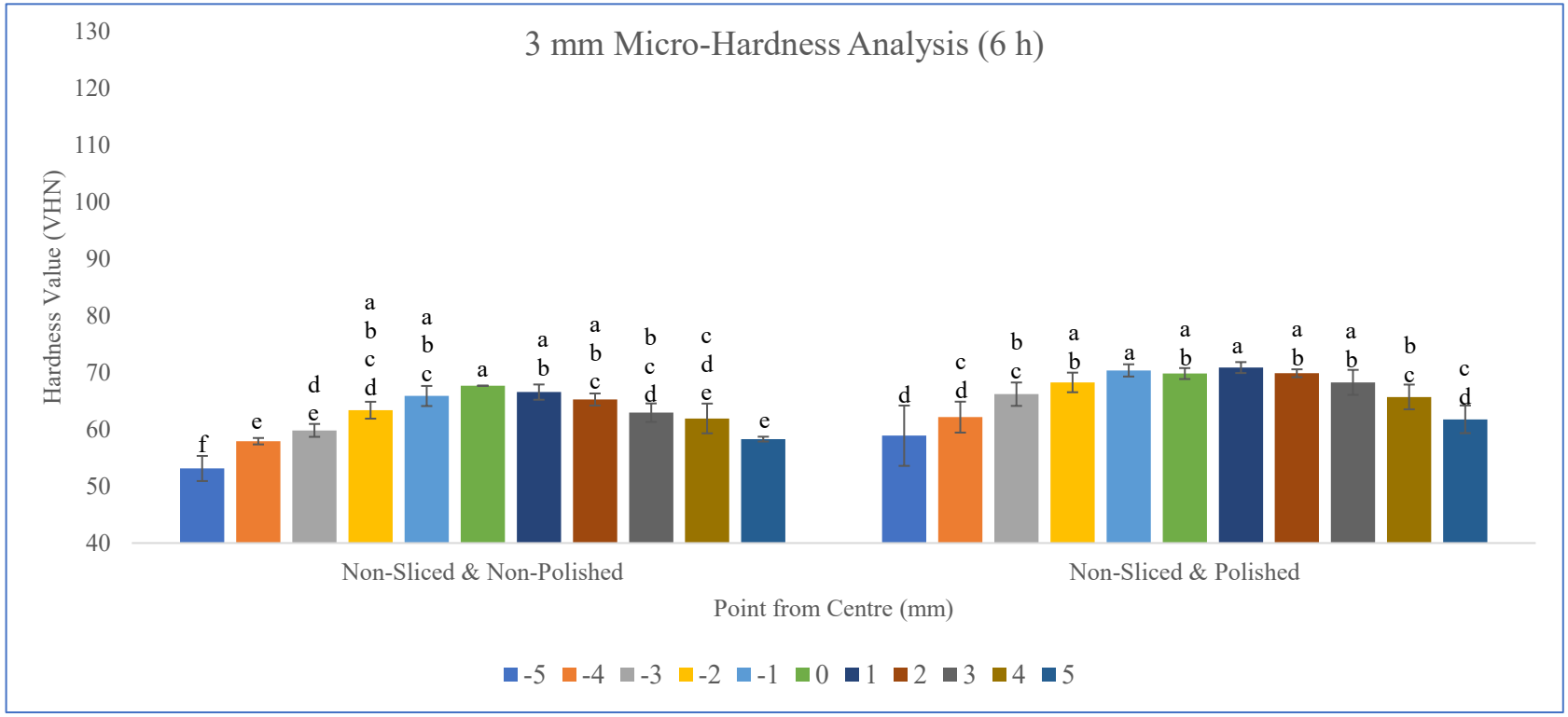

Figure 3.29: Non-sliced, non-polished hardness versus non-sliced but polished micro-hardness plots at 3 mm depths analysed within 6 h after irradiation. There was significant difference between the means at 3 mm depths ($p<0.05$) within these groups of specimens. The comparison among the group categories also revealed there was significant difference between the means of the group category at 3 mm depth ($p<0.05$). Significant difference determined by one-way ANOVA and post hoc Tukey comparisons ($p<0.05$) are represented in ascending alphaphetical order from high to low within each group.

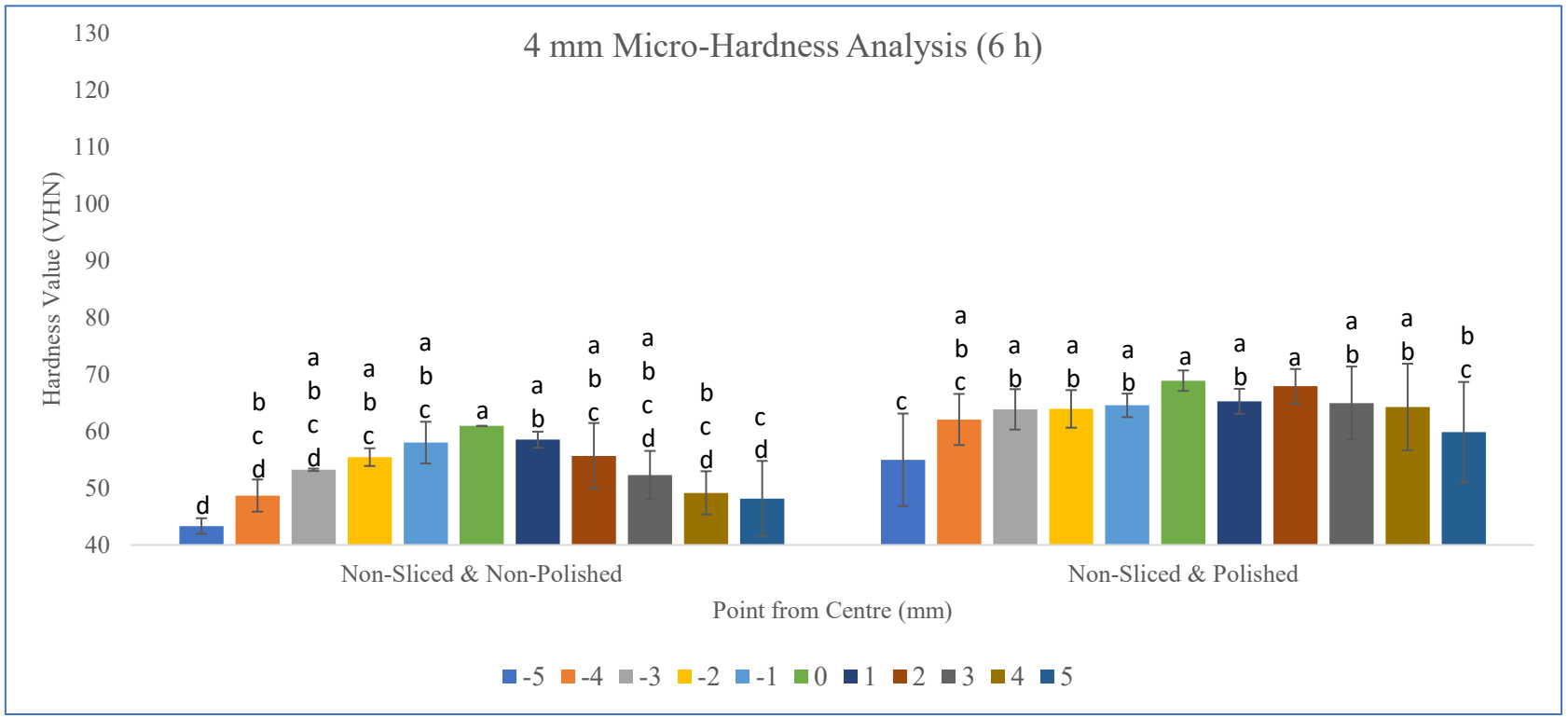

Figure 3.30: Non-**s**liced, non-polished hardness versus non-sliced but polished micro-hardness plots at 4 mm depths, analysed within 6 h after irradiation. There was significant difference between the means at 4 mm depths ($p<0.05$) within the groups. The comparison among the group categories also revealed there was significantdifference between the means of the groups at 4 mm depth ($p<0.05$). Significant difference determined by one-way ANOVA and post hoc Tukey comparisons ($p<0.05$) are represented in ascending alphaphetical order from high to low within each group.

APPENDIX 2.3 Surface Reflection Analysis

Figure 3.31 is a plot of the results of surface reflection test comparing non-sliced, non-polished specimen and non-sliced, but polished specimens against thickness (1 - 4 mm). The statistical analysis of the Rt values obtained for each thickness of non-sliced, but polished is below 95% when compare with non-sliced, non-polished specimens. Each of the group of specimens showed the same post-hoc Tukey indicator but when compared among the groups , there was significantdifference between the means of Rt betweenthe groups at 1 – 4 mm depths ($p < 0.05$).

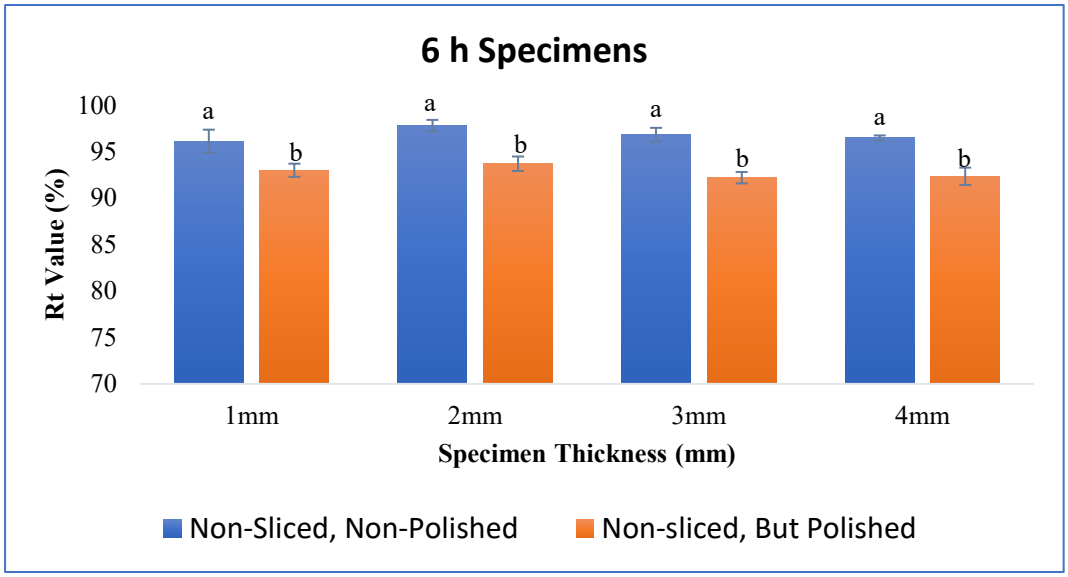

Figure 3.31: Post-Hoc Tukey of the lustrous surface of 6 h non-sliced, non-polished specimens, prepared using acetate as cover for the mould against non-sliced, but polished specimens at different depth. The statistical test of the result shows no significance difference between the means of reflection values (Rt; $p>0.05$) within the groups and significant difference between the means of Rt among the different groups ($p<0.05$). Significant difference was determined by one-way ANOVA and post hoc Tukey comparisons ($p<0.05$) are represented in ascending alphaphetical order from high to low within each group.

APPENDIX 2.4 Surface Analysis by Scanning Electron Microscopy

Figures 3.32a & 3.32b reveals the Scanning Electron Microscope images comparing non-sliced, non-polished specimens and non-sliced, but polished specimens of Filtek^{TM} One bulk fill restorative material, viewed at 10K magnification. The images of non-sliced, non-polished specimens reveals the cured resin matrix, mixed with clusters of the inorganic fillers evenly distributed in the body of the composite material while the images of non-sliced, but polished images show the exposed inorganic particles of bulk-fill composite material created due to polishing process.

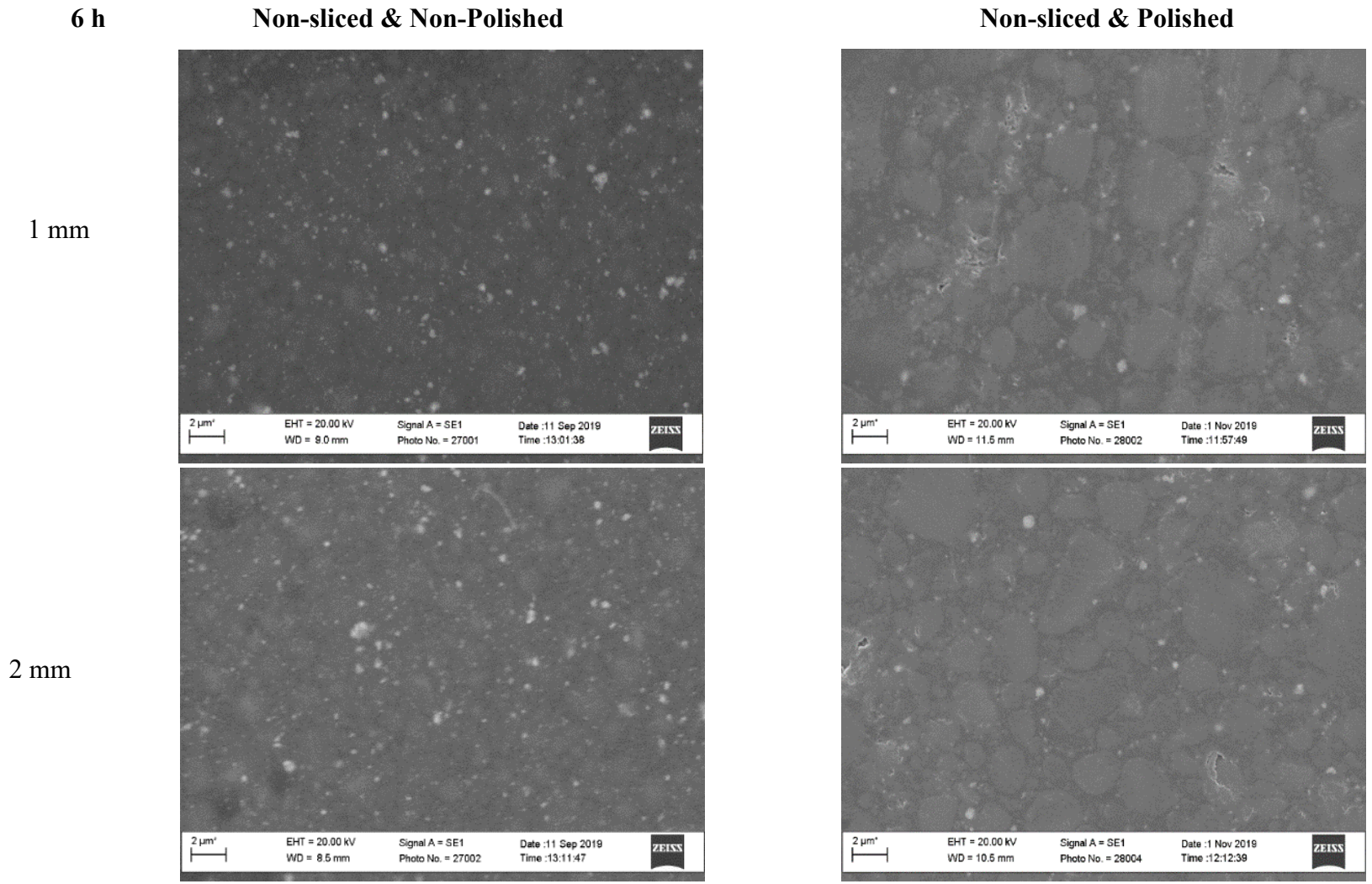

Figure 3.32a: SEM images comparing non-sliced &non-polished and non-sliced & polished specimens at 1-2 mm depth of Filtek^{TM} one bulk fill restorative composites, processed within 6 h after curing and viewed at 10K magnification, revealing the exposed fillers.

6 h	Non-sliced & Non-Polished	Non-sliced & Polished
3 mm	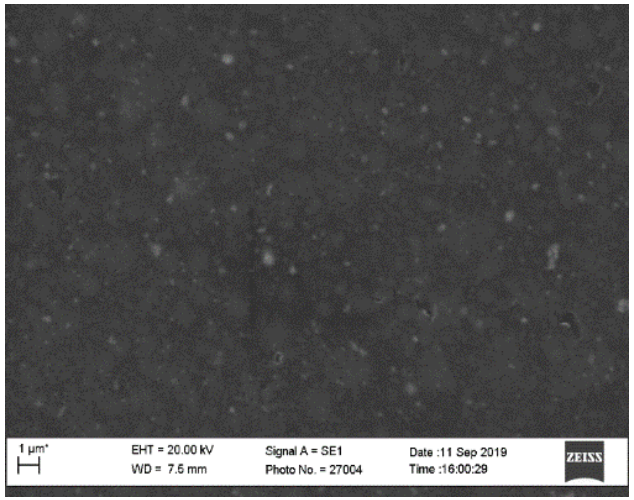	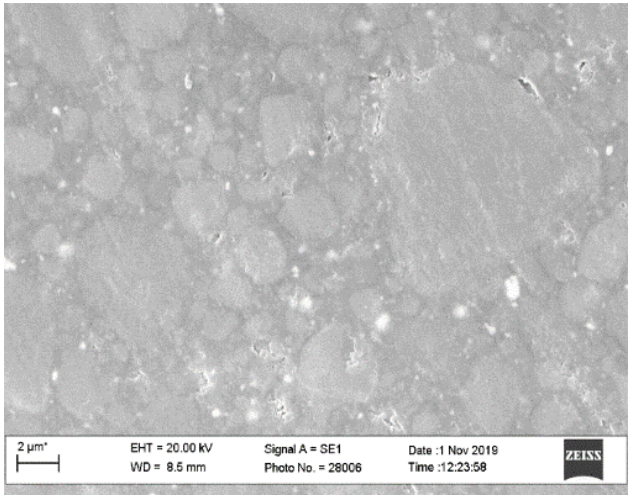
4 mm	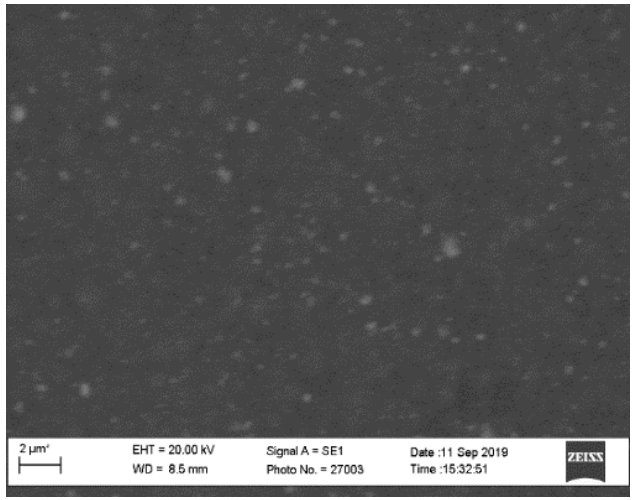	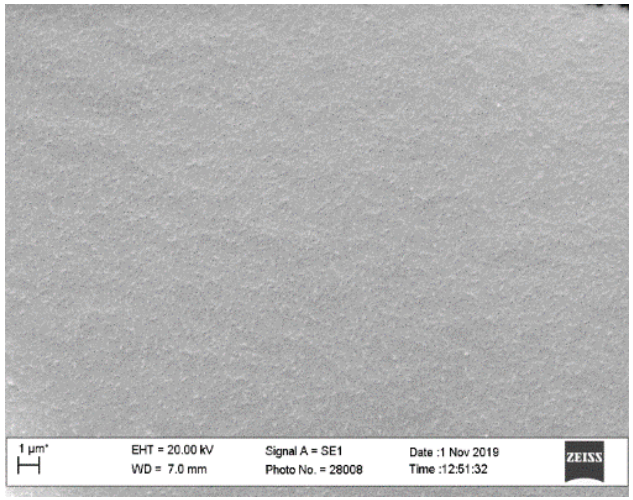

Figure 3.32b: SEM images comparing non-sliced &non-polished and non-sliced & polished specimens at 3-4 mm depth of Filtek^{TM} one bulk fill restorative composites, processed within 6 h after curing and viewed at 10K magnification, revealing the exposed filler